The Synthesis, Characterization and Study of Transition Metal Complexes for the Oxidation and Activation of Hydrocarbons

Thesis by

Robert E. Blake Jr.

In Partial Fulfillment of the
Requirements for the Degree of
Doctor of Philosophy

Division of Chemistry
and Chemical Engineering

California Institute of Technology
Pasadena, California

1996

(Submitted July 27, 1995)

For Mom and Dad

Upon my arrival at Caltech I had ideas regarding the personality, skills and commitment of the ideal advisor. Suffice it to say that Professor John Bercaw has met or exceeded that vision in every way. Any difficulties that I have encountered during the course of my work have been due to my limitations or other technical difficulties. My sincerest thanks go to John for giving me freedom when I wanted it and guidance when I needed it.

The people whom I have worked with are exceptional, too numerous to mention and continue to make Caltech a very special place. The Bercaw group in particular has been an excellent group of colleagues, personally and professionally. The staff at Caltech has also been extraordinarily helpful, patient and a pleasure to work with. Nobody could have provided me with more inspiration to me than my students. I continue to learn from them.

I especially wish to thank all the people who I have spent my extracurricular time with. My dinner guests at 556, Resbit Früm Hel, The Unofficial golf club, climbers, The Hogs and everyone else who I have gotten to know well will continue to be very special to me. Thank you so very much.

So as you read this know my friends
I'd love to stay with you all
Please smile when you think of me
I had to go, that's all

Paraphrased from Megadeth

"A Tout le Monde"

P.S. The NSF is acknowledged for a predoctoral fellowship

Abstract. The reaction of previously characterized ruthenium oxo complex, $[L_{OEt}Ru^{V}(O)(\mu\text{-}O)]_2$ with alcohol substrates was undertaken to elucidate the mechanism of the oxidation reaction. Unfortunately, an autocatalytic reaction between the organometallic product, $[L_{OEt}Ru^{IV}(OH)(\mu\text{-}O)]_2$ and the reactant alcohol, as well as catalyst decomposition made exact determinations of rate constants impossible. During the course of this investigation, the free acid form of the ligand, $L_{OEt}H$, was isolated as a viscous oil. Subsequent investigation of the reactions of $[L_{OEt}Ru^{V}(O)(\mu\text{-}O)]_2$ with other species such as acids, salts and bases demonstrated the inherent instability of the complex. In several cases, initial products were spectroscopically characterized, but isolation of pure compounds was not achieved.

Given the problems with the decomposition of ruthenium complexes which utilized the Klaui ligand, trimetaphosphate was studied as a potentially oxidation-resistant alternative for the development of oxidation catalysts. Attempts were made to prepare salts of the trimetaphosphate ligand which are soluble in nonpolar media and free of water of hydration. Coordination complexes of the trimetaphosphate anion and transition elements were synthesized. The mode of coordination and stability of the ligand was examined by infrared and visible spectroscopy. In all cases, the very weakly coordinating trimetaphosphate anion failed to displace other weakly associated ligands from the metal, failed to adopt the proper coordination geometry or was easily removed from the metal center by water.

Hexabenzyloxycyclotriphosphatriene was synthesized and thermally rearranged to 1,3,5 - tribenzyl - 2,4,6 tribenzyloxy - 2,4,6 trioxocyclotriphosphazane as per published procedures. Characterization of the rearranged product by NMR techniques revealed the previously undetermined stereochemistry of the product. This ligand precursor has been shown to react with trialkyl silyl chlorides, although the products have not been characterized.

$Cp^*_2Ta(=N^tBu)(THF)[B(C_6F_5)_4]$ (**1**) was synthesized according to the method developed previously in our group. A cationic analog to Bergman's $Cp_2Zr(=N^tBu)$, the reactivity of this complex to hydrocarbon substrates was studied. Contrary to previous reports, this complex does not react with methane, but C-H activation reactions were observed for propyne and phenyl acetylene. In the propyne case, an initial mixture of the [2+2] and C-H activation products was driven to exclusively the C-H activation product thermally. An interesting intramolecular activation of a Cp* methyl group precludes much of the desired C-H activation chemistry. The steric demands of the active site was demonstrated by the observed reaction with ethylene, but the lack of reactivity towards propene. A very interesting dealkylation of the imido group was observed upon reaction with carbon dioxide, which is proposed to involve the intermediacy of a coordinated isocyanate. $Cp^*_2Ta(=N^tBu)(THF)[B(C_6F_5)_4]$ reacts as expected with water, HCl and dihydrogen, and reacts cleanly with methylene chloride to give $Cp^*_2Ta(NH^tBu)Cl[B(C_6F_5)_4]$. Many of the new compounds have been crystallographically and spectroscopically characterized. The reactivity of this complex can be rationalized in terms of the presence of both electrophilic and nucleophilic sites in the same molecule.

Table of Contents

List of Figures

Chapter 1

Appendix 1:

Appendix 2:

List of Tables

Chapter 1:

Appendix 1:

Chapter 4:

Appendix 2:

Chapter 1

Oxidation of Alcohols and Other Reactions of the Ruthenium Oxo Complex $[L_{OEt}Ru^{V}(O)(\mu\text{-}O)]_2$

Abstract

The reaction of previously characterized ruthenium oxo complex, $[L_{OEt}Ru^{V}(O)(\mu\text{-}O)]_2$ with alcohol substrates was undertaken to elucidate the mechanism of the oxidation reaction. Unfortunately, an autocatalytic reaction between the organometallic product, $[L_{OEt}Ru^{IV}(OH)(\mu\text{-}O)]_2$ and the reactant alcohol, as well as catalyst decomposition made exact determinations of rate constants impossible. During the course of this investigation, the free acid form of the ligand, $L_{OEt}H$, was isolated as a viscous oil. Subsequent investigation of the reactions of $[L_{OEt}Ru^{V}(O)(\mu\text{-}O)]_2$ with other species such as acids, salts and bases demonstrated the inherent instability of the complex. In several cases, initial products were spectroscopically characterized, but isolation of pure compounds was not achieved.

Introduction

A general interest in oxidation chemistry is obvious, as can be demonstrated by the large number of papers, reviews and books that are written on the subject each year. The basic feedstocks for all organic chemistry are the vast deposits of crude hydrocarbons that are sequestered in the earth's crust. For this material to be useful, much of it must be oxidized. Many high valent metal compounds are capable of oxidizing hydrocarbons under very forcing conditions, but then the reactions tend to be nonspecific and are driven toward the thermodynamic minimum of the system, carbon dioxide and water. Thus, the design of a system for very selective oxidations remains a great challenge to chemists, and requires fundamental understanding of the chemistry behind these transformations.

A variety of reagents have been utilized in both stoichiometric and catalytic oxidation reactions, and in almost every case, there has been a longstanding debate as to the mechanism(s) of the transformations. Many of the active systems are not clean enough to be amenable to detailed study. Despite the great deal of effort put forth to understand the chemistry of this field, there is still a need for fully-documented, conclusive mechanistic work.

Many nonspecific reagents like permanganate are thought to react via a radical mechanism, and evidence to support this hypothesis has been provided by Wiberg.[1]

$$R_3CH + MnO_3^+ \longrightarrow R_3C\bullet + HMnO_3^+ \longrightarrow R_3COMnO_2H^+ \longrightarrow R_3COH + "MnO_2^+"$$

The relative reactivity of alkanes with permanganate was found to follow the trend tertiary>secondary>primary. The result parallels the reactivity ordering

of alkanes in hydrogen abstraction reactions with radicals. One reason for uncertainty in this conclusion is that the expected reactivity ordering is exactly what one would predict for a mechanism in which the first step is hydride abstraction. In general, these two mechanisms can be difficult to distinguish, unless the presence of radicals or hydrides can be clearly demonstrated. Since either of these species will be short lived in the reaction medium, they are frequently not detectable.

Sharpless and coworkers, who first worked on the mechanism of selenium oxidations, proposed that hydrocarbons could be activated by high valent metal dioxo species by 1,2 addition across the metal oxo double bond.[2] Subsequent migration of the alkyl group to the unreacted oxygen followed by elimination of the product alcohol would complete the reaction.

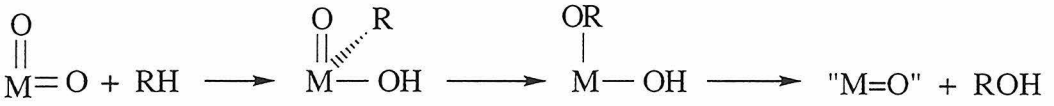

Evidence of the proposed intermediates has not been observed for any of the polyoxo systems studied.

Somewhat analogous to the activation of alkanes by high valent transition metal oxo complexes is the reaction of olefins with metal oxo complexes. In this case, the actual reactions and the possible mechanisms for each are numerous. Depending on the reagent and conditions utilized, the reaction can give epoxides, simple alcohols, cis diols or allylic alcohols. Molybdenum(VI) complexes tend to give epoxides, osmium tetroxide produces cis diols and selenium reagents give allylic alcohols.[3]

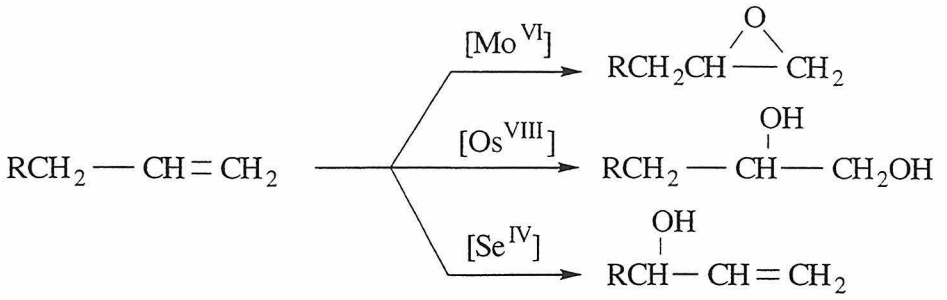

Each reagent may be operating by a completely different mechanism, but it is hoped that some fundamental principles remain consistent between these systems. Some of the proposed routes involve direct attack of the olefin by metal-bound oxygen.[4] This would yield a three-centered intermediate, which could be substituted for at the metal to give epoxide or attacked at the olefin to give 1,2 disubstituted products.

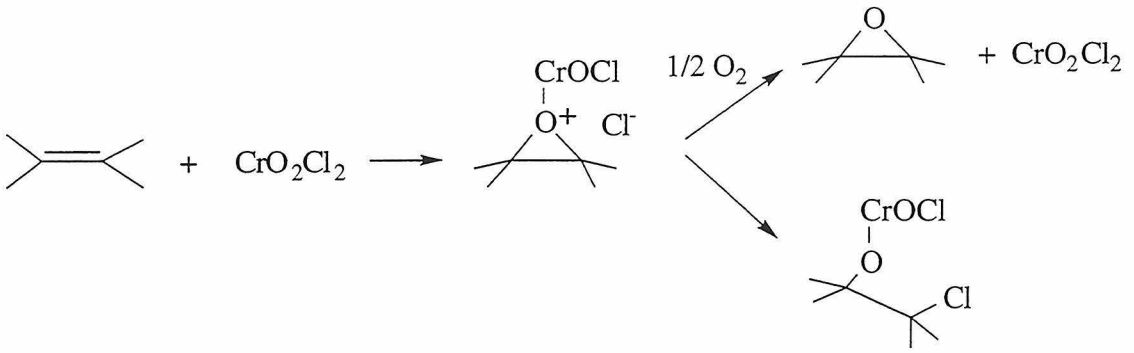

Sharpless argues against this type of mechanism because the polarity of the metal oxygen bond in oxos should be reminiscent of the carbon oxygen bonds in carbonyls, with the greater electron density located on the oxygen. The nucleophillic olefin would be more likely to interact with the metal center. In general, in any reactions with oxidants, one would expect the oxidant to be electrophillic, since it is lacking electron density relative to the reductant. Mechanisms resembling Diels-Alder cyclizations or containing four-centered

transition states have also been proposed, but the experimental evidence supporting any of these mechanisms is inconclusive.[4] A cis-dioxo osmium(VI) ester has been characterized crystallographically and is proposed to be on the reaction path for these oxidations.[5]

One of the major concerns underlying much of this work is the question of which oxo complexes would be expected to be more reactive than others. Work in this area has generated a large number of oxo complexes, but many of them seem to be remarkably unreactive toward potential substrates. A striking example is trioxo pentamethyl cyclopentadienyl rhenium(VII)[6], which has been proven to be a valuable starting material for other rhenium complexes, but does not undergo any stoichiometric or catalytic oxidations of organic materials. Recently, Mayer searched through the structural libraries in order to find statistical information about metal oxos to help understand the observed reactivity trends[7]. He found that monooxo complexes demonstrate clearly shorter bond lengths than dioxo complexes and that early-metal oxo bonds are shorter than late-metal oxo bonds. This trend is supported by calculations done by Goddard, which give considerable insight into the bond length trends[8]. The early metals generally have vacant π orbitals, which can be used to form stabilizing multiple metal-oxygen bonds by accepting electron density from the oxo ligand.

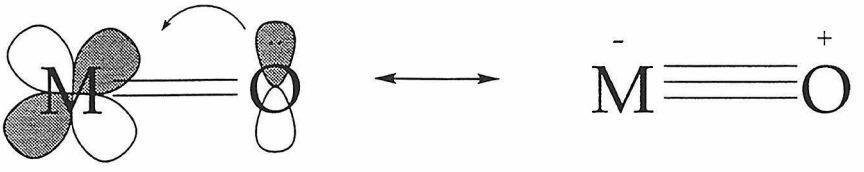

In dioxo complexes, the two oxo ligands will be in competition for the vacant orbital, thus preventing either from forming a second stabilizing π bond.

Work by Bercaw suggests that tantalum[9] and tungsten[10] are sufficiently oxophillic that formation of a terminal metal oxo bond is a prevalent theme.

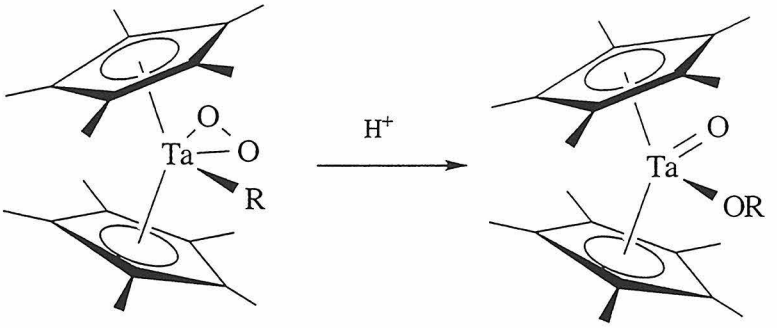

In fact, recent reports describe a tungsten compound as a convenient deoxygenation reagent for transforming epoxides into olefins, the reverse of the useful oxidation reaction.[11] The clear indication of this work is that the early transition metals seem to be poor choices for oxidation catalysts.

A common belief is that among dioxo complexes, the relative geometry of the oxo ligands has direct consequence on the reactivity of the complex. In particular, for d^2 systems, the cis isomer is predicted to be more reactive than the trans isomer[12]. Thus, ligands which will facially coordinate to a metal center have been preferred. The traditional workhorses of organometallic chemistry the cyclopentadienyl(Cp) and pentamethyl cyclopentadienyl(Cp*) ligands have been shown to be troublesome as ancillary ligands for high valent complexes. The cyclopentadienyl ligand is less electron donating than most others, thus it helps stabilize the lower oxidation states of most metals, and prevents them from being oxidized. Pentamethyl cyclopentadienyl is not robust enough to resist oxidation in some cases, and slips from η^5 to η^3 or η^1 when trans to an oxo in several compounds of rhenium or tungsten.[10]

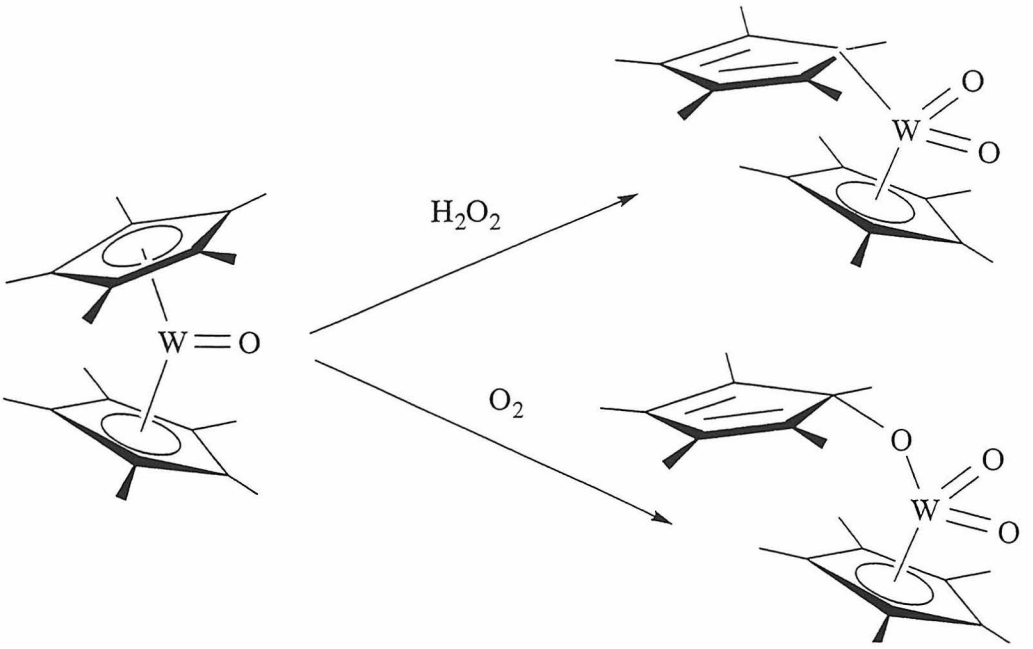

In the last ten years, many groups have been trying to prepare good oxidants for organic materials, and as expected from the above observations, much of this work has been directed at the later transition metals. Ruthenium in particular has received a great deal of attention, and a number of groups have achieved the preparation of monooxo or dioxo complexes which effect interesting transformations. Drago has synthesized the *cis*-diaquo complex[Ru(II)(2,9-dimethyl-1,10-phenanthroline)$_2$(H_2O)$_2$]$^{2+}$, which is an effective catalyst for the epoxidation of alkenes by O_2.[13] Takeuchi reported the catalytic aerobic oxidation of cyclohexene[14] with [(bpy)$_2$(PPh_3)Ru^{II}(OH_2)]$^{2+}$ and the oxidation of alcohols by the the Ru(IV) oxo version of the complex.[15] A rate law was determined for the alcohol case, but no linear free energy plots, which could give useful insight to the mechanism, were attempted. Takeuchi could not identify the detailed mechanism of that reaction, although a very large isotope effect was seen for the alcohol oxidations, implying that C-H bond breakage is important in the transition state. A

reasonably detailed kinetic study was done on a catalytic system for the oxidation of alcohols by Beattie and coworkers, and they present good evidence for a Ru(II)/Ru(III) couple in the catalytic cycle.[16] Unfortunately, they were unable to find conclusive evidence to determine the rate limiting step in the alcohol oxidation portion of the cycle. They saw a definite pH dependence on reaction rates and the lifetime of the catalyst, but due to the unknown nature of the active catalyst, they could not even speculate about the cause of this phenomenon. Meyer and coworkers have concentrated on complexes which contain polypyridyl ligands, which have proven compatible with high valent systems. Typically, proton coupled oxidation/reduction reactions were reported, which are quite amenable to electrochemical examination. These systems have been observed to effect reactions including the oxidations of olefins to epoxides, alcohols to ketones, sulfides to sulfoxides, phosphines to phosphine oxides and water to oxygen. They also transform phenols to quinones and cyclohexene to cyclohexenone. In the last two cases, the mechanism of the reactions have been investigated by isotopic labelling and stopped-flow kinetics. Again, a very large isotope effect implies that C-H bond cleavage is important in the rate limiting step. Meyer invokes mechanisms in which the first step is direct insertion of the oxo ligand into a C-H bond in the substrate.

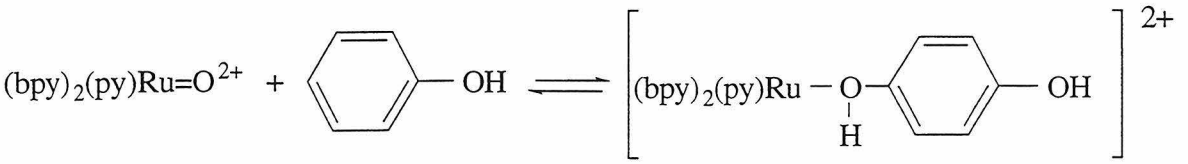

He discounts prior coordination because he believes the system to be substitutionally inert, but work by his own group[17] and Anson's[18] has shown

substitution to be a factor in these systems, especially in basic solution. His mechanism suffers from the requirement for oxygen to behave as an electrophile, because it should be negatively charged when bonded to a metal. In short, mechanistic studies have been plagued in this area by i) a lack of characterization data for the active catalyst and ii) ambiguity in the nature of the transition state due to a pronounced lack of information. Unless a properly conducted Hammett study is done on a series of substrates, the hydrogen atom abstraction and hydride transfer mechanisms may be indistinguishable.

Previous work in our group[19] has taken advantage of the properties of a cyclopentadienyl tris(phosphito) cobalt(III) complex anion L_{OEt}^-, prepared by Klaui and coworkers[20]. to prepare new complexes of ruthenium.

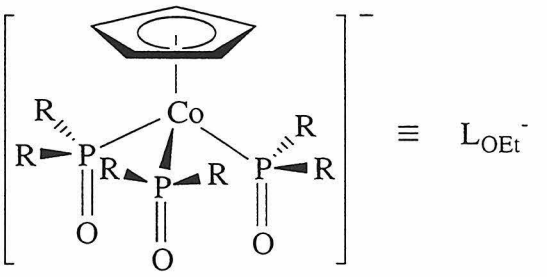

(R = OCH_2CH_3)

The anion acts as a tridentate ligand, binding exclusively through the oxygen atoms, and coordinating facially. The robustness of the ligand in oxidizing environments was demonstrated by the fact that it forms stable complexes with cerium(IV). Electron donation from the oxygen ligands should be conducive to the preparation of high valent complexes, and the required facial coordination of the ligand should enforce *cis*-dioxo geometry. Kaspar Evertz and John Power were successful in preparing and characterizing several complexes of ruthenium in oxidation states +3, +4 and +5. The structures of some of these materials have been determined by X-ray

crystallography. The complexes which are of greatest interest for this study are $[L_{OEt}Ru(O)(\mu\text{-}O)]_2$(V-V) and $[L_{OEt}Ru(OH)(\mu\text{-}O)]_2$ (IV-IV), which have both been fully characterized.

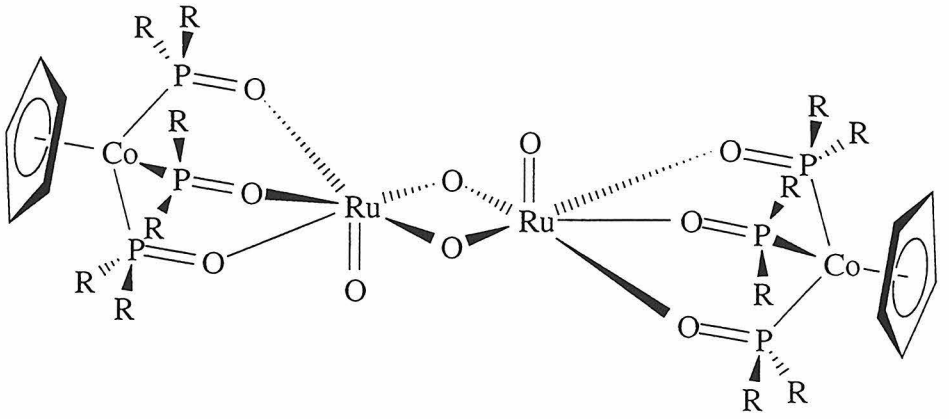

$[L_{OEt}Ru(O)(\mu\text{-}O)]_2$

The reaction chemistry of V-V with isopropyl alcohol had been preliminarily studied by NMR, and seems to be clean and quantitative. The organic product of the reaction was acetone, as expected. The visible spectra of the two ruthenium complexes are quite different, both exhibiting strong characteristic absorptions. Thus, it appeared that this system is well suited for a detailed examination of the mechanism by spectroscopic techniques.

Results and Discussion

The synthesis of IV-IV and V-V had been previously worked out by Power, et. al., but there was some difficulty in getting consistent yields for the preparation of IV-IV and the preparation of V-V frequently yielded impure material. Since rigorously pure materials are required for valid kinetic measurements, optimization of the synthetic procedures was attempted. Particularly distressing was an obvious difference in the visible characteristics of IV-IV from batch to batch, despite the clean NMR signals and elemental analyses for the material. Since the reactions were to be monitored by visible spectroscopy, reliable extinction constants were necessary for this work.

The reaction scheme for the preparation of IV-IV is shown below:

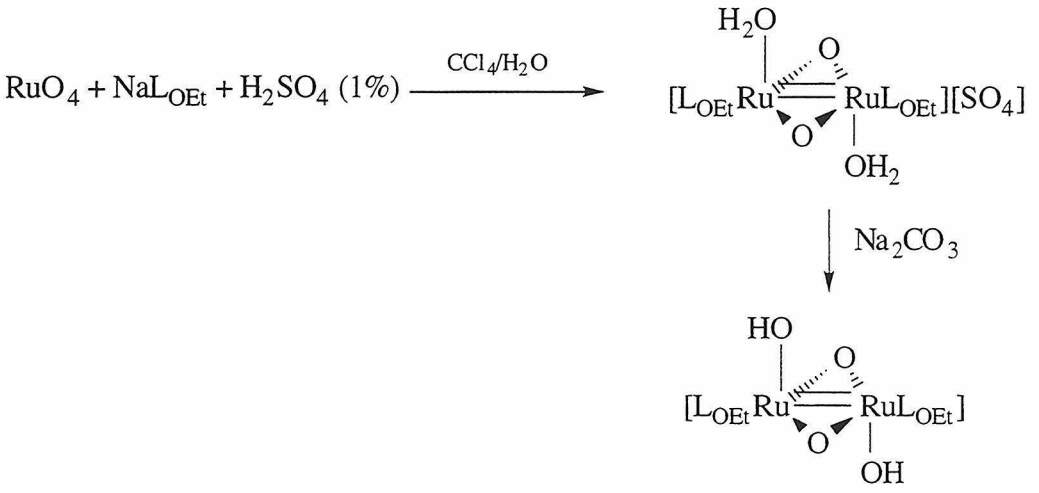

The amount and concentration of acid has been shown to be essential to the isolation of the product. Use of a large excess of acid gives an uncharacterized red solid after neutralization, while a slight excess of acid results in a brown-green material which has the same NMR spectrum as

IV-IV. Use of less than a 1:1 H_2SO_4 to ruthenium ratio causes a decrease in the yield and the production of a black insoluble precipitate, which is presumed to be RuO_2. This strong dependence on the concentration and amount of acid used prompted an attempt at preparing the protonated form of the ligand from the sodium salt. This would allow more exact control of the stoichiometry of added acid in the reaction, plus would eliminate possibly non-innocent counterions. Treatment of an aqueous slurry of insoluble NaL_{OEt} with 1M HCl showed the dissolution of the ligand at pH 1.7. Thus, preparation of the neutral $L_{OEt}H$ was attempted by dissolution of the complex in 0.1 M HCl and extraction into ether. Removal of the solvent gave a viscous orange oil which was dried over $MgSO_4$ to give a yellow solid. The NMR of the compound was characteristic of a highly symmetric L_{OEt} environment, but no resonance was visible for the acidic proton. An IR spectrum showed the presence of L_{OEt}, but no stretch for an OH bond was present. Preparation of IV-IV was attempted with this material, but only the unchanged starting material and RuO_2 were isolated. It was confirmed by elemental analysis and comparison to an authentic sample that the yellow solid was $(L_{OEt})_2Mg$, from reaction of the free acid with magnesium sulfate.

$$2L_{OEt}H + MgSO_4 \longrightarrow (L_{OEt})_2Mg + H_2SO_4$$

The orange oil was resynthesized, dried in vacuo overnight and subsequent analysis was consistent with the formulation $L_{OEt}H$. A broad peak for the acidic proton was observed at 14.5 ppm in the ^1H NMR spectrum of the material in benzene-d_6, which was observed to move upfield and increase in relative intensity upon the addition of water to the sample. Unfortunately, use of this compound did not improve the synthesis of IV-IV. $L_{OEt}H$ does

not contain enough protons to neutralize the excess oxide from RuO_4, so H_2SO_4 still had to be added, but in reduced amount. At this point, the optimization of the synthesis was abandoned.

To assist in the purification of IV-IV for spectroscopic purposes, the stability of the compound in a variety of solvents was investigated. Separate small amounts of IV-IV was placed in contact with C_6H_6, CCl_4, petroleum ether, isopropanol, water and acetonitrile and left to stir overnight. The supernatant was pumped down and an NMR was taken of the resulting solid. The dimer is almost insoluble in petroleum ether, but substantial decomposition was seen by NMR. Minimal decomposition was seen in benzene and acetonitrile, significant decomposition was seen in carbon tetrachloride, and total decomposition was observed in isopropanol. In these reactions no products were isolable except in the cases in which unreacted starting material was recovered. The reaction with alcohol was unfortunate in terms of the overall goal of the project, since this would complicate the kinetic analysis of the reaction of V-V with alcohols (*vide infra*).

Reliable purification of IV-IV was effected via formation of the dication with dilute sulfuric acid which allowed extraction of the dark brown impurities into benzene. Reprecipitation of the neutral species with sodium carbonate gave material of consistent quality. It is essential that the concentration of acid for the neutralization be between 0.5 and 1.0%. Higher acid concentrations result in the decomposition of the material, while insufficient acid gives lower yields of product (some gets extracted into the benzene).

While working on the synthesis and purification of IV-IV, a yellow material of limited solubility in acetone was noticed on several occasions. To identify this product, the carbon tetrachloride extracts from a IV-IV

preparation were evaporated in vacuo and washed with cold acetone to yield a yellow powder. Large orange crystals of this material were grown by slow evaporation of a benzene solution of the compound. A lack of NMR signal indicated that the material was paramagnetic, and IR spectrometry confirmed the existence of the Klaui ligand (L_{OEt}). The solubility properties, IR and nmr of the material were identical to that of the 19e$^-$ complex $(L_{OEt})_2Co$, so a crystal structure determination was not attempted. Neither solid melted up to 265°C, so a mixed melting point was not determinable. The apparent production of $(L_{OEt})_2Co$ during these reactions suggests that some Klaui ligand is being decomposed by an unknown mechanism to provide cobalt for the formation of the sandwich complex. This was suprising, since up till this point it was believed that L_{OEt} was quite robust.

Difficulties in preparing completely pure V-V were also encountered in the course of this work. As reported in the literature, V-V is obtained by treatment of IV-IV with either ruthenium tetroxide or iodosobenzene. Typically, the isolated material contained 15-20% of unoxidized starting material when iodosobenzene was used, even after crystallization from pentane/CCl_4. After unsuccessful attempts at obtaining pure material by recrystallizations, washing with other solvents, multiple additions of iodosobenzene, and preparation with alternate oxidants, exclusion of air and moisture was incorporated into the synthetic scheme. Powdered molecular sieves were added to the reaction to remove water which was formed by the oxidation, and only dry, distilled solvents were used in all preparation and crystallization steps. This procedure reliably gives microcrystalline material in excess of 80% yield when freshly prepared IV-IV is used in the synthesis.

This result suggested that V-V might react with water, possibly by an oxidative pathway to give peroxide or oxygen. An NMR experiment was

performed in which V-V was dissolved in d^6-benzene, then an excess of water was added. A complete conversion of V-V to IV-IV was observed over several hours. The oxo dimer is also converted to the hydroxo dimer in neat benzene over days as observed by Power, but the oxidized products of this reaction were not identified. The two obvious possibilities at this stage were that i) V-V reacts with water or ii) water accelerates a reaction of the dimer with solvent or itself. To distinguish between these possibilities, a Toepler pump experiment was conducted. Pure V-V was degassed, then benzene and a large excess of water were vacuum transferred into the flask. The reaction was allowed to run until the solution was green. At that time, the headspace of the reaction was Toepler pumped, but no gases were detected. To test for the possibility that peroxide was the product of the oxidation of water, H_2O_2 was reacted with IV-IV and V-V. The hydroxo dimer catalyzed the disproportionation of peroxide, and the oxo dimer oxidized peroxide to oxygen, with the formation of the hydroxo dimer. This result strongly suggests that water does not directly react with the oxo dimer, but may be involved in promoting decomposition reactions for the complex.

Preliminary kinetics experiments have been conducted for the reaction of V-V with +/- *sec*-phenethyl alcohol. Extinction coefficients for the two characterized complexes have been determined at λ=558 nm and λ=688 nm, the λ_{max} for V-V and IV-IV respectively. Both complexes exhibit good Beer's Law behavior at the concentrations studied, as depicted in the plots below (Figure 1). For the reaction of V-V and sec-phenethyl alcohol, loss of isobestic points was observed within 2 or 3 half lives of the reaction (Figure 2). The pseudo-first order rate constant for the reaction between V-V and *sec*-phenethyl alcohol was determined based on initial rates of reaction (Figure 3) and compared to the observed rates for the decomposition of V-V and IV-IV

in solvent alone. Based upon the approximate values for these rate constants, the decomposition of the complexes is seen to be competitive with the reaction of substrate (see Table 1).

One concern in the kinetic runs was that the ruthenium IV-IV product was a potent enough oxidant to react with the alcohol starting material, complicating the analysis of the target reaction. A spectrophotometric study of the reaction of IV-IV with sec-phenethyl alcohol revealed that the reaction proceeded autocatalytically. Overlay spectra which clearly indicate this phenomenon are provided in Figure 4. Spectra were recorded in 20 minute intervals.

Since the desired kinetic investigation was problematic, a survey was conducted to determine empirically if an added catalyst or co-reactant would modify the system in a useful way. In particular, due to the observed stability of the protonated form of IV-IV, it was hoped that a weak acid might either accelerate the reaction of V-V with alcohols and/or stabilize IV-IV under the reaction conditions. Kinetic runs were conducted in either benzene or acetonitrile with benzoic acid, sodium perchlorate, sodium triflate, water and pyridine as possibly beneficial additives. The salts, water and benzoic acid all provided modest rate enhancement as studied spectrophotometrically by looking at the disappearance of IV-IV. Pyridine rapidly reacted with V-V to give an uncharacterized species which did not oxidize secondary alcohols. Unfortunately, control reactions in the absence of alcohol revealed that even in the absence of the substrate alcohol, V-V was converted to IV-IV. The observed rate enhancements were due to increased rate of autodecomposition of the complex and did not indicate increased activity for the oxidation of alcohols.

Table 1: Observed rate constants for the reactions of IV-IV and V-V with and without *sec*-phenethyl alcohol present

Reference	complex	reagent/[ ]	solvent	kobs (min^{-1})
REB-I-117	V-V	$PhCHOHCH_3$/0.0112 M	C_6H_6	$2x10^{-3}$
REB-I-121	V-V	$PhCHOHCH_3$/0.0166 M	C_6H_6	$2.4x10^{-3}$
REB-I-131	IV-IV	solvent	C_6H_6	$1x10^{-5}$
REB-I-132	V-V	solvent	C_6H_6	$1.4x10^{-4}$

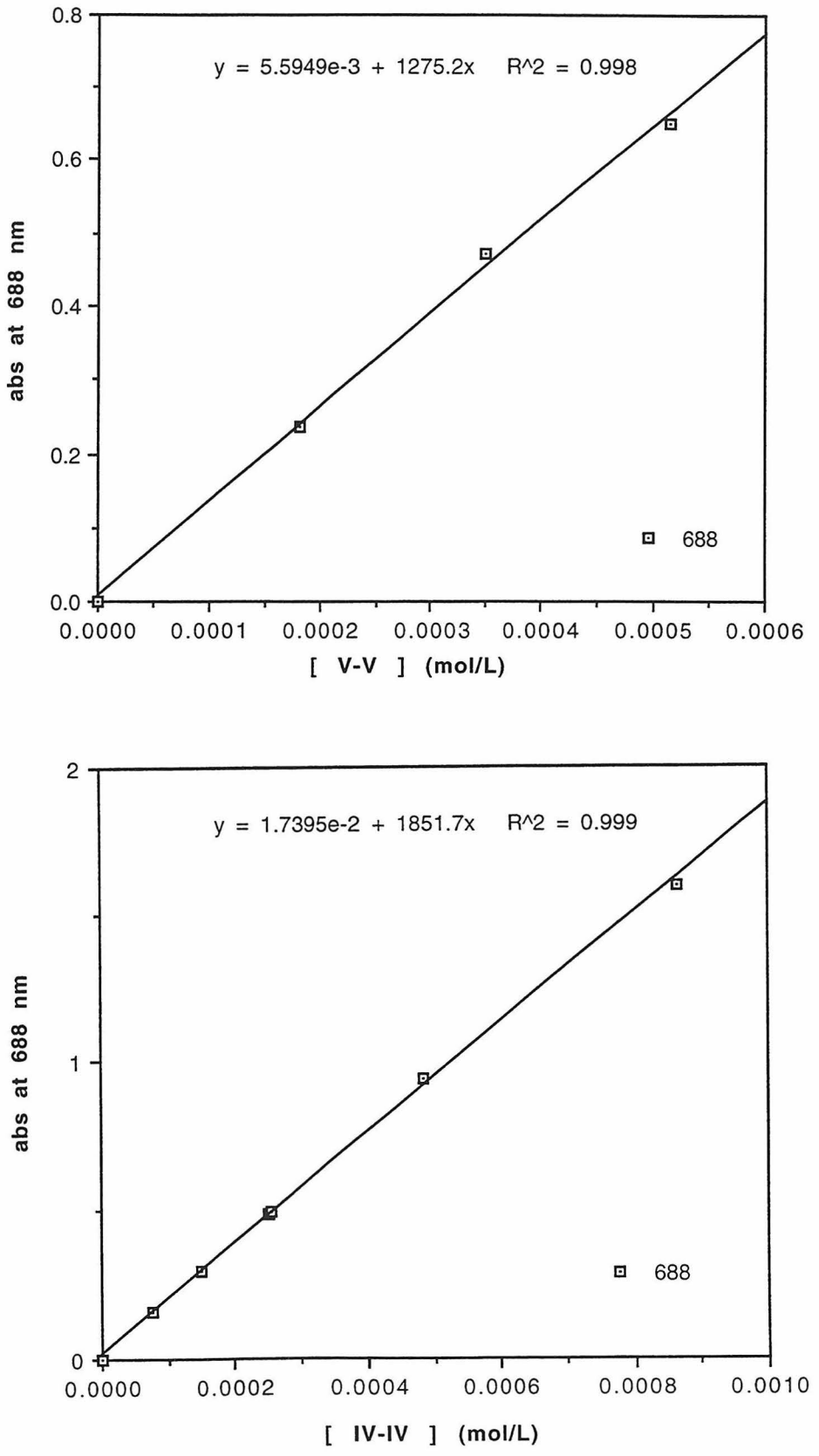

Figure 1: Sample Plots Showing Beer's Law Behavior for IV-IV and V-V

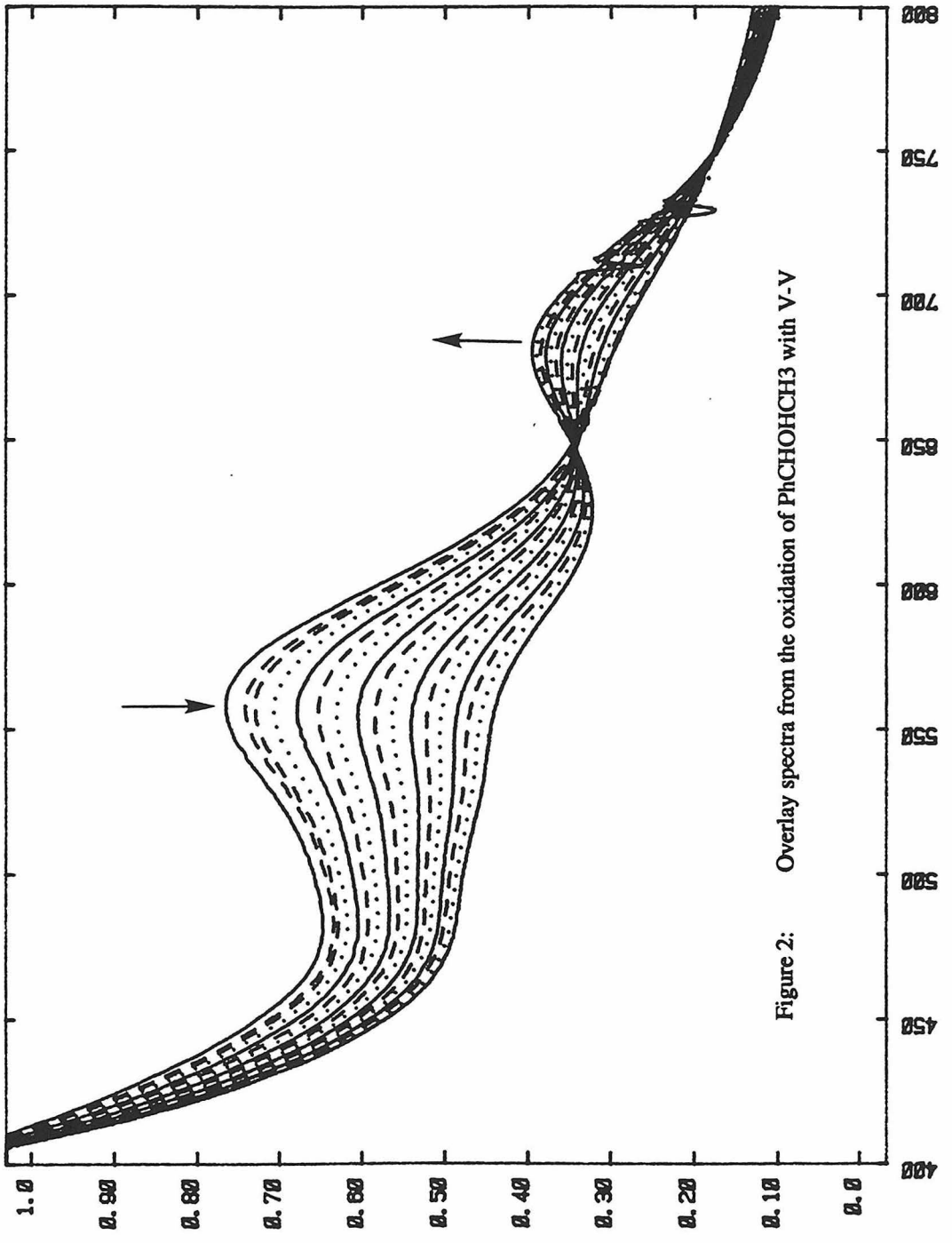

Figure 2: Overlay spectra from the oxidation of PhCHOHCH3 with V-V

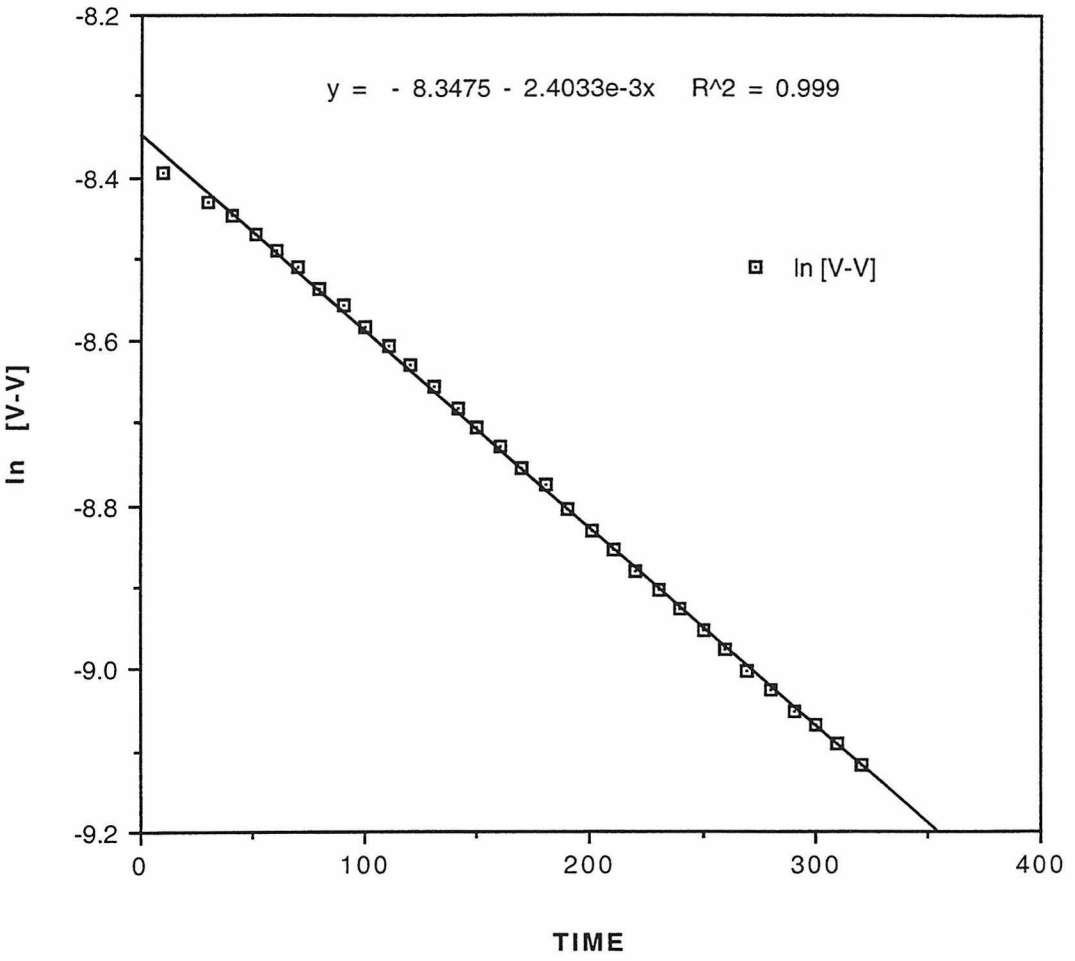

Figure 3: Plot of [V-V] vs time for determination of k_{obs} for the reaction of V-V with $PhCHOHCH_3$

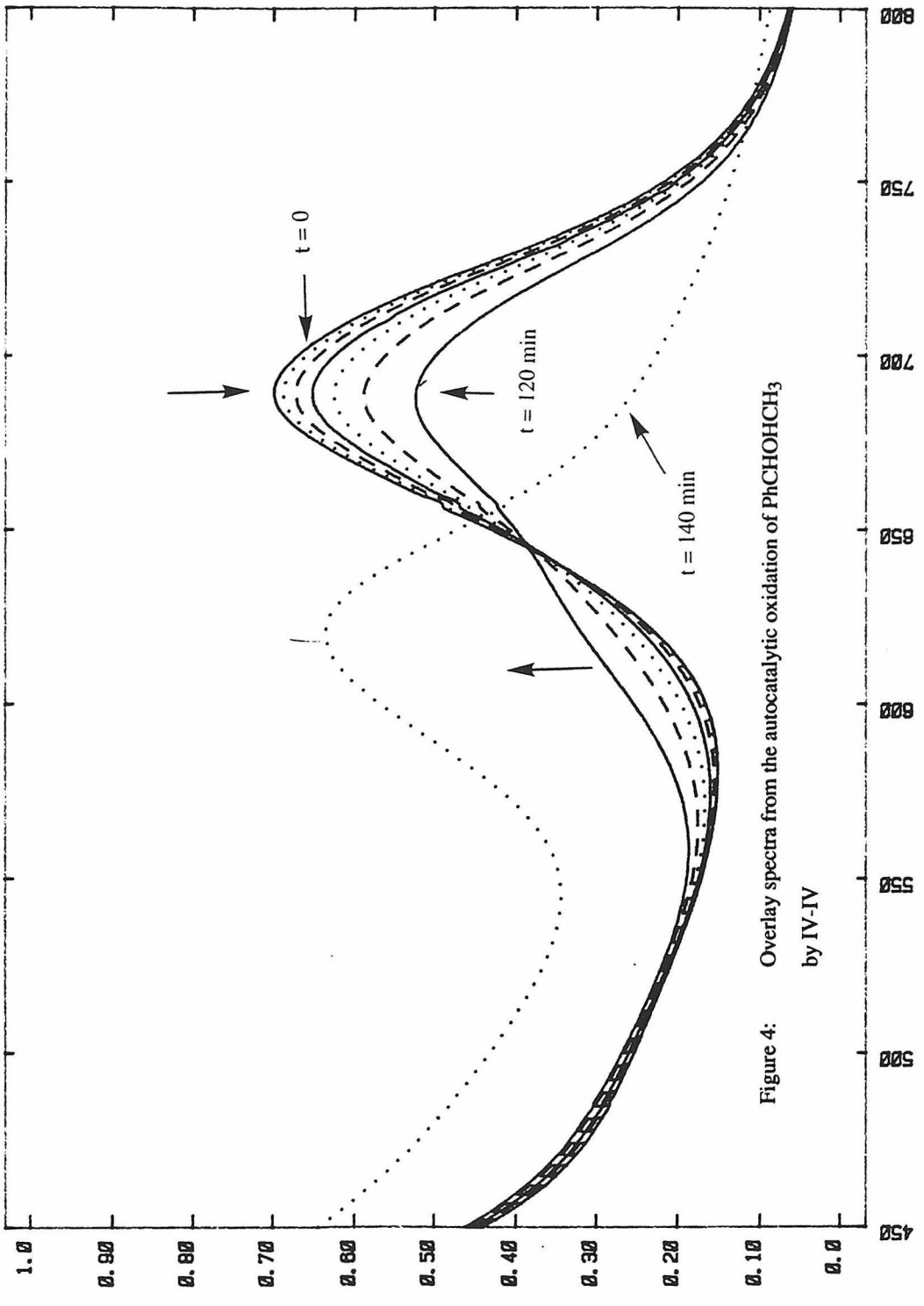

Figure 4: Overlay spectra from the autocatalytic oxidation of $PhCHOHCH_3$ by IV-IV

During these kinetic studies, NMR reactions between V-V and sodium triflate, pyridine and triflic acid were conducted. A reasonably clean reaction was observed for the pyridine case by NMR, but no clean product was isolable. Two products were isolated for the reaction of sodium triflate and V-V, but a control reaction revealed that they were the identical products that were obtained from the reaction of IV-IV with sodium triflate, not higher valent products. Both products decomposed quite rapidly, so were not studied further.

Conclusions

Reliable syntheses and purifications for IV-IV and V-V were worked out to facililitate the mechanistic study of alcohol oxidation by the high valent species. Unfortunately, it is quite clear that this system was far too problematic for the proposed study. Oxidations of *sec*-phenethyl alcohol by V-V was complicated by the subsequent reaction of the alcohol with IV-IV as well as the decomposition of both IV-IV and V-V, which proceeded in the absence of substrate. The formation of $(L_{OEt})_2Co$ in the preparation of IV-IV strongly suggested that the Klaui ligand was not robust enough to support high valent catalysts, and that ligand degradation was a likely source of the instability of the complexes. Additional components added to the reaction mixture afforded no additional insight into the system, they merely accelerated the decomposition of the organometallic oxidant. It was decided that our catalyst design needed to incorporate ligands which were more resistant to oxidation, so work was discontinued on this project.

Experimental Section

Starting materials. IV-IV, V-V, L_{OEt}, and $(L_{OEt})_2Co$ were synthesized via published procedures.[19] Sec-phenethyl alcohol, acetonitrile, pyridine and carbon tetrachloride were dried over CaH_2 and distilled before use. Pentane and benzene were distilled from sodium benzophenone ketyl. Anhydrous sodium triflate was prepared by the action of triflic acid on an aqueous solution of sodium carbonate, followed by heating in vacuum to remove the water of hydration. All other reagents were used as received.

Ultraviolet-Visible spectra. Solvents and solutions were syringed or cannula transferred to cells for measurement. Spectra for Beer's law verification were recorded on a Hewlett Packard HP8452 diode array spectrophotometer and extinction coefficients were determined by least squares analysis. Kinetic measurements were made in a closed cell under argon. Constant temperature was maintained by use of a Hewlett-Packard Peltier principle heater-cooler. Approximate rate constants were determined by least squares analysis.

Other Spectra. ^1H NMR spectra were recorded with a JEOL GX400(400MHz) spectrophotometer in benzene-d_6, solution and referenced to tetramethyl silane by residual ^1H signal from C_6D_5H. IR spectra were obtained on a Perkin Elmer 1600 series FTIR spectrometer from nujol mull if solids or neat if liquid. Chemical Analyses were performed by Fenton Harvey at Caltech.

Procedure for Kinetic Runs. In all cases, a known mass of the ruthenium containing material was weighed into a volumetric flask covered with a septum in a Vac Atmospheres glovebox under a dry dinitrogen atmosphere. Solvent was cannula transfered to the flask after argon flush, then sec-phenethyl alcohol was syringed in against argon counterflow.

$(L_{OEt})_2Mg$. 10.3 g of NaL_{OEt} was weighed out and dissolved in 100 mL of 0.1 N HCl. This solution was extracted with 2x100 mL diethyl ether. The combined fractions were rotovapped to give a viscous orange oil. This was redisolved in 100 mL diethyl ether and shaken over 15 g of MgSO4. Removal of the solid gave 6.44 g of a yellow solid.(61%).

^1H NMR δ 1.34 ppm 18H(t), 4.31 ppm 12H (d of m), 5.149

IR ν = 596, 721, 767, 834, 925, 1038, 1140, and 1253 cm^{-1}

Elemental analysis:	Calculated	C 37.30%, H 6.40%
	Found	C 36.82%, H 6.24%

$L_{OEt}H$. The above procedure was followed with 5.0 g NaL_{OEt} except the viscous oil obtained was dried in vacuo.to yield 3.82 g (76%)

^1H NMR: δ 1.71 ppm 18H (t), 4.15 ppm 12H (d of m), 5.07 ppm 5H (s), 14.67 ppm 1H(s)

IR ν = 573, 720, 761, 832, 932, 1049 1167, and 1567 cm^{-1}

Elemental analysis:	Calculated	C 38.10%, H 6.72%
	Found	C 37.44%, H 6.81%

Purification of $[L_{OEt}Ru^{IV}(OH)(\mu\text{-}O)]_2$. 3.1g $[L_{OEt}Ru^{IV}(OH)(\mu\text{-}O)]_2$ (0.0023 mol) was dissolved in 100mL of a 1% aqueous sulfuric acid solution. This solution was washed with 3x50 mL of benzene. The brown benzene washings were

discarded and the acid solution treated with a saturated sodium carbonate solution until CO_2 evolution ceased. The resulting green solid was collected by filtration and dried *in vacuo*. Yield = 2.23g of product (72% recovered).

Toepler Pump Experiment of $[L_{OEt}Ru^{V}(O)(\mu\text{-}O)]_2$ decomposition. $[L_{OEt}Ru^{V}(O)(\mu\text{-}O)]_2$ (0.2g,1.5×10^{-4} mol) was dissolved in 50 mL of benzene containing 5 mL water and degassed. After 2 days, the solution was green. Toepler pumping through a -78°C trap collected 0.02 mm of gas in a 25mL volume (2×10^{-8} mol). Apparently the oxidation product is non-volatile.

Isolation of $(L_{OEt})_2Co$ from IV-IV preparation. A IV-IV preparation was run on a 0.017 mol scale (11.53g theoretical yield). 4.3g of IV-IV was isolated (37%). The carbon tetrachloride extracts were evaporated and the resulting solid washed with acetone to yield 1.23g of yellow powder (20% based on L_{OEt} and formulation as $(L_{OEt})_2Co$). Solubilities, melting point (>265°C) and NMR (no signals seen, paramagnetic) were all identical to $(L_{OEt})_2Co$.

Elemental analysis:	Calculated:	C 36.16%, H 6.24%
	Found	C 35.78%, H 6.18%.

Treatment of IV-IV and V-V with H_2O_2. In air, small quantities of IV-IV and V-V were added to test tubes containing 30% aqueous hydrogen peroxide. In both cases, substantial gas evolution was seen, almost certainly due to the disproportionation of the hydrogen peroxide. The sample of V-V immediately turned green during the experiment, indicating oxidation of the peroxide.

References

[1]Wiberg, K. B.; Foster, G. *J. Amer. Chem. Soc.* **1961**, *83*, 422

[2] Sharpless, K. B. ; Teranishi, A. Y. ; Backvall, J. *J. Amer. Chem. Soc.* **1972**, *99*, 3120

[3] Kochi, J. K. ; Sheldon, R. A. *Metal Catalyzed Oxidations of Organic Compounds*, Academic Press **1981**, New York

[4] Cristol, S. J. ; Eilar, K. R. *J. Amer. Chem. Soc.* **1950**, *72*, 4353

[5] Pearlstein, R. M.; Blackburn, B. K. ; Davis, W. M. ; Sharpless, K. B. *Angew. Chem. Int. Ed. Engl.* **1990**, *29*, 639

[6] Herrmann, W. A.; Angew. *Chem. Int. Ed. Engl.* **1988**, *27*, 1297

[7] Mayer, J. M. *Inorg. Chem.* **1988**, *27*, 3899

[8] Rappe, A. K. ; Goddard, W. A. III, *J. Amer. Chem. Soc.* **1982**, *104*, 3287

[9] van Asselt, A.; Trimmer, M. S. ; Henling, L. M. ; Bercaw, J. E.

J. Amer. Chem. Soc. **1988**, *110*, 8254

[10] Parkin, G. ; Bercaw, J. E. *J. Amer. Chem. Soc.* **1989**, *111*, 391

[11] Sharpless, K. B. ; Umbreit, M. A. ; Nieh, M. T. ; Flood, T. C. *J. Amer. Chem. Soc.* **1972**, *94*, 6538

[12] a) Atovmyan, L. O. ; Koshits, M. A. ; *Zh. Strukt. Khim.* **1969**, *10*, 853
b) Mingos, D. M. P. *J. Organomet. Chem.* **1979**, *179*, C29

[13] Bailey, C. L. ; Drago, R. S. *J. Chem. Soc., Chem. Comm.* **1987**, 179

[14] Leising, R. A. ; Takeuchi, K. *J. Inorg. Chem.* **1987**, *26*, 4391

[15] Marmion, M. E. ; Takeuchi, K. J. *J. Chem. Soc., Dalton Trans.* **1988**, 2385

[16] Kaziro, R. W. ; Beattie, J. K. *Australian J. Chem.*, **1989**, *42*, 1273

[17] Doppelt, P. ; Meyer, T. J. *Inorg. Chem.* **1987**, *26*, 2027

[18] McHatton, R. C. ; Anson, F. C. *Inorg. Chem.* **1984**, *23*, 3935

[19]Power, J. M. *et. al. Inorg. Chem.* **1990**, *29*, 5058

[20] Klaui, W. ; Eberspach, W. ; Schwarz, R. *J. Organomet. Chem.* **1983**, *252*, 347

Chapter 2

The Preparation and Stability Study of Complexes Containing the Oxidation-Resistant Trimetaphosphate Anion

Abstract

Given the problems with the decomposition of ruthenium complexes which utilized the Klaui ligand, trimetaphosphate was studied as a potentially oxidation-resistant alternative for the development of oxidation catalysts. Attempts were made to prepare salts of the trimetaphosphate ligand which are soluble in nonpolar media and free of water of hydration. Coordination complexes of the trimetaphosphate anion and transition elements were synthesized. The mode of coordination and stability of the ligand was examined by infrared and visible spectroscopy. In all cases, the very weakly coordinating trimetaphosphate anion failed to displace other weakly associated ligands from the metal, failed to adopt the proper coordination geometry or was easily removed from the metal center by water.

Introduction

Metals and metal complexes have shown great general utility as catalysts for a variety of important chemical transformations. As the understanding of the fundamental principles underlying the industrial systems increases, the rational design of catalysts is becoming possible, and in a few cases, realized.(1) Frequently, solid oxide supports are used in the development of catalysts for a number of important industrial processes. Many solid supports have the attractive property of being quite inert to most reaction conditions, reactants and products. Many oxides are in particular, completely inert with respect to oxidation, in contrast to the Klaui ligand studied in the previous chapter (*vide supra*). Unfortunately, many common techniques for studying chemical systems are ineffective for the study of solid or heterogenous systems. It is thus desirable to study homogeneous model systems which may provide insight to the heterogeneous systems.

Trimetaphosphate as a supporting ligand has the attractive feature of being completely resistant to oxidation, thus a good ancillary for the study of oxidation reactions. The synthesis of the ligand is simple and inexpensive, involving pyrolysis of the monosodium salt of phosphoric acid, NaH_2PO_4.

$$3\ NaH_2PO_4 \xrightarrow{550^\circ C} Na_3P_3O_9 + 3\ H_2O$$

Sodium trimetaphosphate is also available commercially. Work with this potential ligand has been slow due to its trianionic nature and its instability in the presence of water.(2) Due to its highly ionic character, it is only soluble in water, and even when derivatives which are soluble in organic solvents are prepared, they retain water of hydration. Attempts to drive off the water

of hydration by heating the salts results in hydrolysis of the cyclic phosphate to the linear version. Trimetaphosphate anion is not stable in pure water for long, being hydrolyzed in several days even at room temperature. This decomposition is accelerated by the presence of metal ions

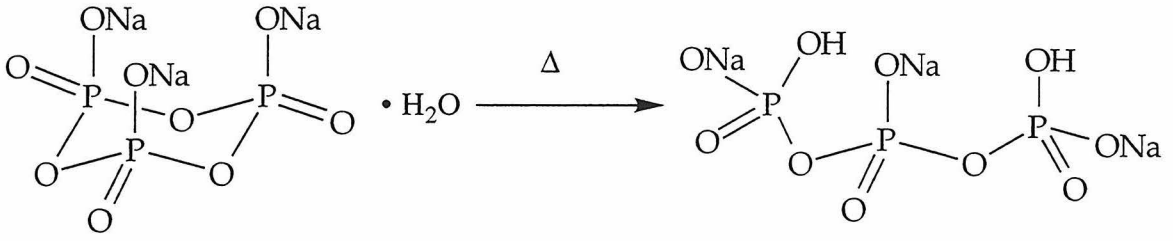

To understand these systems, Klemperer and others have attempted to model the properties of solid supports by developing homogeneous analogs to the heterogeneous catalysts[3-8]. Klemperer's group has succeeded in utilizing the trimetaphosphate trianion (cyclo-$P_3O_9^{3-}$) as a model ligand. During their work, they have been quite tenacious in overcoming the difficulties associated with that ligand, and synthesized several trimetaphophate-metal complexes. In particular, to assist in their syntheses they have made derivatives of the trimetaphosphate anion which are soluble in organic solvents. Unfortunately, they have not succeeded in eliminating the associated water of hydration which would interfere with many common troues to organometallic complexes. A picture of an idealized trimetaphoshate metal complex is shown below .

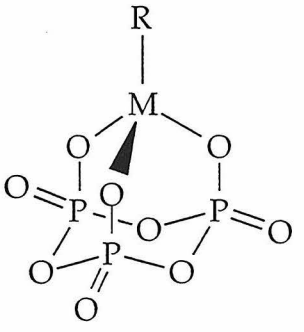

Klemperer has observed an interesting solid state structure for an iridium cyclooctadiene complex, $[TBA]_2[(P_3O_9)Ir(C_8H_{12})]$ which consists of a tridentate-coordinated trimetaphosphate. One of the metal-oxygen bonds is particularly weak, and probably fluxionally decoordinated in solution. It is proposed that the decoordination of the oxygen site is important for the observed chemistry of the complex. In contrast to the inactivity of the analogous cyclopentadienyl derivative, this complex inserts an oxygen atom to form a characterizable oxametallacycle which in turn rearranges to an alcohol[9]. In a particularly elegant study, both the intermediate and final product have been crystallographically characterized. Comparisons between this work and the heterogeneous epoxidation of ethylene have been drawn, and the activity of the trimetaphosphate complex over the Cp analog is significant.

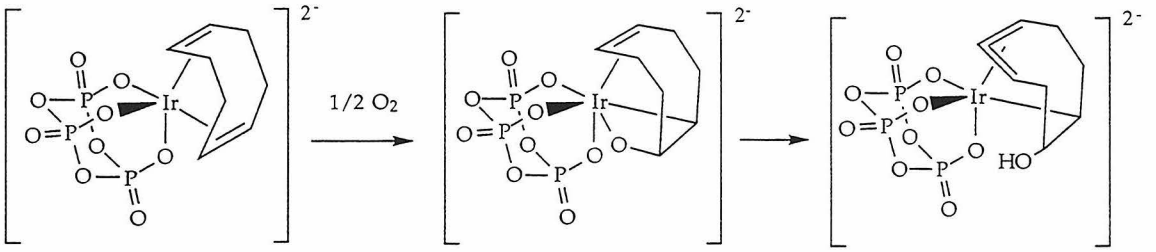

The study of reactions involving the trimetaphosphate anion is facilitated by several convenient spectroscopic techniques. ^{31}P NMR can easily be used to distinguish the free anion from the coordinated anion in solution. Infrared spectroscopy is diagnostic of the coordination mode adopted by the ligand. In typical salts, extensive coupling between the various ν(P-O)'s results in a small number of broad IR absorptions. In the desired mode of coordination for the ligand, the symmetry of the complex is reduced

and distinct P-O stretching frequencies are distinguishable. This behavior is illustrated in the literature.[6]

Several forms of the trimetaphosphate anion are readily available via published procedures, which allow for several synthetic strategies for new complexes. The sodium salt can easily be converted to silver or tetrabutylammonium salts.

$$Na_3P_3O_9 + 3\ AgNO_3 \xrightarrow{H_2O} Ag_3P_3O_{9(s)} + 3\ NaNO_3$$

$$Ag_3P_3O_9 + 3\ TBABr \xrightarrow{H_2O} (TBA)_3P_3O_9 + 3\ AgBr_{(s)}$$

The silver reagent is convenient for reaction with metal halides, while the tetrabutyl ammonium salt is soluble in nonpolar solvents. Unfortunately, water of hydration is persistent in these salts, which eliminates the possibility of using very water sensitive reagents in the syntheses.

Results and Discussion

The initial goal of the work was to make new complexes in which trimetaphosphate was coordinated to the metal in a tridentate fashion. Toward this end, many cations containing labile ligands were made according to literature reports. The study was directed toward metals that could potentially be oxidized and in turn used to oxidize organic substrates. Due to Klemperer's success with late metals and the many reports of ruthenium catalysts for oxidations, ruthenium complexes were an early target. Solutions of "ruthenium blue", $RuCl_3 \cdot nH_2O$, $[Cp^*RuCl_2]_2$, $[Cp^*RuCl]_4$, $Ru(DMSO)_4Cl_2$, $Ru(DMSO)_4(OTf)_2$, $Cp^*Ru(CH_3CN)_3OTf$ and $(C_6H_6)RuCl_2$ were all reacted with either silver or tetrabutylammonium trimetaphosphate in a variety of solvents. In all cases except that of $(C_6H_6)RuCl_2$, ^{31}P NMR showed that the ligand was not coordinated to the metal. $(Bu_4N)_2(C_6H_6)Ru(P_3O_9)$ was prepared and subsequently studied in some detail by Andy Kiely. In the presence of water, the trimetaphosphate was displaced from the metal center. Analogous to phosphate, from these studies, it is believed that the trimetaphosphate ligand is a very poor ligand, held to the metal primarily by electrostatics.

Concurrent with attempts to make ruthenium complexes of trimetaphosphate, attempts to eliminate the water of hydration in tetrabutylammonium trimetaphosphate were made as well. Diisopropylcarbodiimide was used as a drying agent. In an NMR tube experiment, the signals for water disappeared over a 12 hour period, and signals for diisopropyl urea were apparent. After scaling up this reaction, it was discovered that the diisopropylcarbodiimide was similar enough in

physical properties to $TBA_3(P_3O_9)$ that the residual drying agent was not separable from the reagent.

The binary compounds $Co_3(P_3O_9)_2$, $Mn_3(P_3O_9)_2$ and $Fe_3(P_3O_9)_2$ were prepared by straightforward routes such as the one shown below:

$$2\ Ag_3P_3O_{9(s)} + 3\ MCl_2 \xrightarrow{H_2O} M_3(P_3O_9)_{2(s)} + 6\ AgCl$$

After evaporation of the solvent and drying *in vacuo*, the IR spectra for these complexes showed no evidence for the desired mode of coordination of the $P_3O_9^{3-}$ ligand. The higher valent $CrCl_3(THF)_3$ was used to make a complex which showed the desired IR spectrum in the P-O region. Unfortunately, contact with moist air displaced the ligand as shown by visible changes in the material. Unfortunately, it seemed that the chelate effect was insufficient to give the complex the desired stability. This was also the case for a cobalt complex which was formed from $Co(CH_3CN)_6(BF_4)_2$ and $TBA_3(P_3O_9)$ Since the complexes were unstable, full characterization was not attempted. It may have been possible to make higher valent derivatives which would have the advantage of greater electrostatic stability, but this was not pursued. This strategy was unsuccessfully applied by Andy Kiely for $(Bu_4N)_2(C_6H_6)Ru(P_3O_9)$ and $(Bu_4N)_2Re(CO)_3(P_3O_9)$. Several oxidants were tried, but no tractable materials were isolated. He proposed that the tetrabutylammonium counterion, which was necessary to solubilize the complexes, was interfering with the oxidations. He also encountered difficulties keeping the ligand on the metal in any solvent with reasonably large dielectric constants (for instance, water).

A final effort to get a stable trimetaphosphate complex was made prior to abandonment of the project. A high valent, oxophilic, sterically protected

early metal complex with labile ligands was desired. To this end, $Cp^*Ta(OTf)_3Cl$ was synthesized in high yield by reacting Cp^*TaCl_4 with 3 equivalents of silver triflate. The compound was recrystallized as large orange needles which were suitable for structure determination by X-ray diffraction. All three triflate ligands are coordinated to tantalum, one as a bidentate ligand.

$Cp^*Ta(OTf)_3Cl$ and tetrabutylammonium trimetaphosphate were independently dissolved in methylene chloride and the two solutions mixed, resulting in the immediate precipitation of a yellow insoluble material. Due to its insolubility in common organic solvents and lack of the characteristic IR spectrum for $P_3O_9^{3-}$ complexes of the desired structure, it was assumed to be a polymeric material and not pursued futher.

Conclusions

The initial hopes were that trimetaphosphate could be utilized as a non-oxidizable supporting ligand for the study of hydrocarbon oxidations or activations. Due to the lability of the ligand, few complexes were formed with the desired mode of coordination. Those which were formed were not stable in the presence of weak field ligands such as water. Based upon these observations, the use of this ligand was abandoned as an ancillary for the design of transition metal complexes. These studies suggest that $(P_3O_9)^{3-}$ salts may make good starting materials for the introduction of other ligands due to the lability of the ligand which was problematic for this work.

Experimental Section

General Considerations. All air and/or moisture sensitive compounds were manipulated using standard Schlenk techniques or in a dry box under a dinitrogen atmosphere. Phosphorus NMR spectra were recorded on a JEOL FX90Q (36.28 MHz for ^{31}P) spectrometer and referenced to an external 85% H_3PO_4(aq) standard (δ=0 ppm). Hydrogen NMR spectra were recorded on a General Electric QE 300 (300.152 MHz for ^{1}H) spectrometer.

Drying of $(TBA)_3P_3O_9 \cdot H_2O$ In an NMR tube, 0.1g ($1x10^{-4}$ mol) of $(TBA)_3P_3O_9 \cdot H_2O$ was dissolved in a suitable amount of CD_3CN. 0.08mL of diisopropylcarbodiimide was added to this. After 12 hours the resonance for water was not observable and new peaks corresponding to diisopropyl urea were present.

^{1}H NMR: Assignments for sample after drying: For (TBA): δ = 0.915 ppm (t, 12H); 1.32 ppm (m, 8H); 1.58 ppm (m, 8H); 3.15 ppm (m, 8H). For diisopropyl carbodiimide: δ = 1.11 ppm (d, 18H); 3.46 ppm (m, 3H). For diisopropyl urea: δ = 0.99 ppm (d, 2H); 3.65 ppm (m, 0.5 H).

Preparation of the uncharacterized $Cr(P_3O_9)$ compound. 1.48g of $CrCl_3 \cdot 3$ THF and 4g of $(TBA)_3P_3O_9$ were weighed into a schlenk flask in the glovebox. 80 mL of dry THF was transferred into the flask resulting in a purple solution. Warming to 50°C caused the precipitation of a pink solid, which was isolated by filtration and dried *in vacuo*. The deliquescent compound turned green slowly upon contact with the air.

IR spectrum: ν = 3422.2 (br), 2962.0 (s), 2875.3 (m), 1488.0 (m), 1383.7 (w), 1318.7 (s), 1288.1 (s), 1135.4 (s), 937.2 (s), 884.2 (w), 775.2 (m), 718.0 (m), 557.9 (m)

Preparation of the uncharacterized $Co(P_3O_9)$ compound. 2.0g (0.004 mol) of $Co(CH_3CN)_6(BF_4)_2$ and 4.0g of $(TBA)_3P_3O_9$ (0.004 mol) were loaded into a schlenk flask in the glovebox. 60 mL of dry acetonitrile was tranferred onto them, which resulted in a bright blue solution. After drying in vacuo, the product was washed with ether to yield a 1.87g of bright blue solid. The ether washings were pumped down to give 2.67g of a light blue solid. Both fractions turn pink when exposed to air.

Preparation of $Cp^*Ta(OTf)_3Cl$. 2.0g (0.00437 mol) of Cp^*TaCl_4 and 3.37g (0.00437 mol) of AgOTf were weighed into a 100 mL flask and attached to a filter frit in the glovebox. 60 mL of dry methylene chloride was vacuum transferred onto the solids at -78°C and the reaction mixture allowed to warm to room temperature. A white precipitate formed as the solids dissolved and the solution turned orange rapidly. The solution was filtered and both sides pumped to dryness in vacuo. The orange product was dissolved in a minimum amount of methylene chloride, layered with 50 mL ether and cooled to -55°C. The resulting orange powder was isolated by filtration (2.7g, 77.6% yield). Crystals suitable for X-ray analysis were isolated from vapor diffusion of ether into a concentrated methylene chloride solution of the product. A large needle was cleaved to an appropriate size and sealed in a thin-walled capillary under a dinitrogen atmosphere.

^1H NMR: δ = 2.868 ppm (CH_3 of Cp^*)

Elemental analysis:	Calculated	C 19.54%, H 1.89%
	Found	C 19.53%, H 1.97%

Preparation of the uncharacterized $Cp^*Ta(P_3O_9)$ compound.

1.0g ($1.25x10^{-3}$ mol) of $Cp^*Ta(OTf)_3Cl$ and 1.21g of $(TBA)_3P_3O_9$ ($1.25x10^{-3}$ mol) were loaded into a roundbottom flask in the glovebox and attached to a flip frit assembly. 30 mL of dry methylene chloride was vacuum transferred onto the solids at -78°C and the mixture stirred at room temperature overnight. As the solution warmed, it changed from orange to yellow as a yellow precipitate formed. The solid was collected by filtration and dried in vacuo. 40.73g (quantitative yield based upon formulation as $Cp^*TaP_3O_9Cl$) was isolated and found to be quite insoluble in all common solvents studied (methylene chloride, acetonitrile, THF, toluene, petroleum ether and ethyl ether). Satisfactory elemental analysis of the compound was not obtained.

References

1) Coughlin, E. B.; Bercaw, J. E. *Journal of the American Chemical Society* **1992**, *114*, 7606.

2) Kalliney, S. Y. *Topics in Phosphorus Chemistry* **1970**, *7*, 255-309.

3) Day, V. W.; Klemperer, W. G.; Main, D. J. *Inorganic Chemistry* **1990**, *29*, 2345-2355.

4) Day, V. W.; Eberspacher, T. A.; Klemperer, W. G.; Planalp, R. P.; Schiller, P. W.; Yagasaki, A.; Zhong, B. *Inorganic Chemistry* **1993**, *32*, 1629-1637.

5) Day, V. W.; Eberspacher, T. A.; Klemperer, W. G.; Zhong, B. *Journal of the American Chemical Society* **1994**, *116*, 3119-3120.

6) Klemperer, W. G.; Main, D. J. *Inorganic Chemistry* **1990**, *29*, 2355-2360.

7) Klemperer, W. G.; Zhong, B. X. *Inorganic Chemistry* **1993**, *32*, 5821-5826.

8) Besecker, C. J.; Day, V. W.; Klemperer, W. G. *Organometallics* **1985**, *4*, 564-570.

9) Day, V. W.; Klemperer, W. G.; Lockledge, S. P.; Main, D. J. *Journal of the American Chemical Society* **1990**, *112*, 2031-2033.

Appendix 1: X-Ray Structure Data for $Cp^*Ta(OTf)_3Cl$

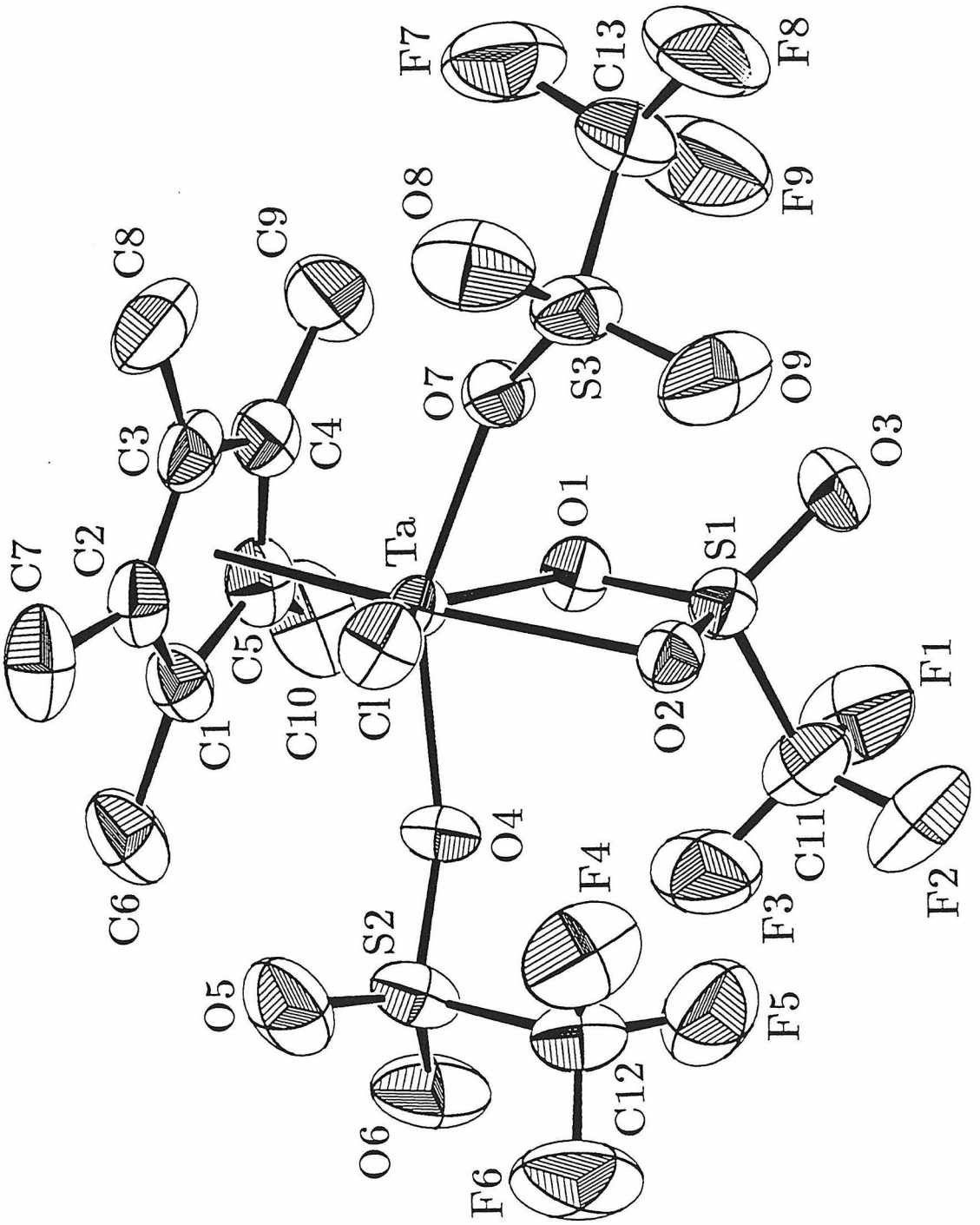

Figure 1: ORTEP diagram of the structure of $Cp^*Ta(OTf)_3Cl$

Table 1: Crystal and Intensity Data for $Cp^*Ta(OTf)_3Cl$

chemical formula	$C_{13}H_{15}ClF_9S_3O_9Ta$
crystal dimension, mm	0.33 x 0.43 x 0.59
crystal system	monoclinic
space group	$P2_1/c$
a, Å	11.513(3)
b, Å	13.999(4)
c, Å	15.718(4)
β, deg	103.69
V, $Å^3$	2461.3
Z	4
λ, Å	0.71073
μ, cm^{-1}	48.74
temp, °K	296
2θ range, deg	2 to 45
no. of reflections measured, total	7025
R	0.025
GOF	1.68

Table 2: Final Heavy Atom Parameters for $Cp^*Ta(OTf)_3Cl$

x, y, z and $U_{eq}{}^a \times 10^4$

Atom	x	y	z	U_{eq}
Ta	2431(.1)	1881(.1)	2196(.1)	300(.3)
C1	1845(4)	1836(3)	578(3)	437(11)
C2	2136(4)	2793(3)	831(3)	449(12)
C3	3367(4)	2818(3)	1256(3)	475(12)
C4	3824(4)	1880(4)	1282(3)	460(12)
C5	2878(4)	1269(3)	864(3)	467(11)
C6	703(5)	1501(4)	−15(3)	664(16)
C7	1341(6)	3633(4)	577(4)	720(16)
C8	4058(6)	3709(4)	1531(4)	756(16)
C9	5090(5)	1564(4)	1598(4)	699(16)
C10	2964(5)	233(4)	661(4)	722(16)
Cl	1593(1)	3242(1)	2622(1)	497(3)
O1	3204(2)	499(2)	2545(2)	410(7)
S1	2981(1)	396(1)	3442(1)	432(3)
O2	2235(3)	1228(2)	3503(2)	406(7)
O3	3979(3)	210(2)	4131(2)	614(9)
C11	2058(5)	−682(4)	3361(4)	604(14)
F1	2737(3)	−1424(2)	3335(3)	882(10)
F2	1612(3)	−734(2)	4052(3)	937(10)
F3	1182(3)	−675(2)	2658(2)	832(10)

Atom	x	y	z	U_{eq}
O4	790(2)	1251(2)	1916(2)	422(8)
S2	−543(1)	1284(1)	1687(1)	520(3)
O5	−963(3)	2172(3)	1306(3)	755(11)
O6	−1009(3)	414(3)	1299(3)	781(11)
C12	−913(4)	1295(4)	2748(4)	597(15)
F4	−532(3)	2067(2)	3197(2)	935(10)
F5	−446(3)	559(3)	3238(2)	905(10)
F6	−2074(3)	1248(3)	2635(3)	1083(14)
O7	4007(3)	2301(2)	3043(2)	423(7)
S3	4481(1)	2852(1)	3874(1)	565(3)
O8	4478(3)	3845(3)	3723(3)	847(12)
O9	4040(4)	2500(4)	4571(2)	984(14)
C13	6048(5)	2490(5)	4095(4)	749(18)
F7	6564(3)	2817(3)	3495(3)	993(12)
F8	6621(3)	2854(3)	4846(3)	1192(14)
F9	6155(3)	1563(3)	4115(3)	1273(16)

U(eq) is defined as one third of the trace of the orthogonalized Uij tensor.

Table 3: Assigned Hydrogen Atom Parameters for $Cp^*Ta(OTf)_3Cl$

	x, y and $z \times 10^4$			
Atom	x	y	z	B
H6 A	91	1960	−72	5.6
H6 B	432	919	239	5.6
H6 C	816	1325	−576	5.6
H7 A	1637	4176	957	5.8
H7 B	542	3499	652	5.8
H7 C	1277	3824	−12	5.8
H8 A	4319	4007	1082	6.5
H8 B	4749	3578	2019	6.5
H8 C	3565	4164	1773	6.5
H9 A	5421	1395	1110	5.9
H9 B	5138	1001	1966	5.9
H9 C	5563	2054	1928	5.9
H10A	3104	147	77	5.9
H10B	2236	−107	670	5.9
H10C	3612	−78	1067	5.9

Table 4: Anisotropic Displacement Parameters for $Cp^*Ta(OTf)_3Cl$

Atom	U_{11}	U_{22}	U_{33}	U_{12}	U_{13}	U_{23}
Ta	309(1)	322(1)	280(1)	6(1)	93(1)	−20(1)
C1	462(27)	533(28)	307(24)	83(24)	76(21)	−6(22)
C2	555(31)	480(28)	336(25)	113(22)	151(23)	74(21)
C3	601(32)	537(30)	348(26)	−71(24)	231(25)	21(21)
C4	430(26)	704(32)	294(24)	68(27)	180(21)	−2(24)
C5	572(31)	517(28)	358(26)	147(25)	204(25)	−16(22)
C6	683(36)	870(38)	371(29)	110(31)	−13(27)	−51(27)
C7	1017(46)	621(33)	562(35)	263(33)	269(34)	174(28)
C8	948(45)	755(38)	652(39)	−336(34)	362(35)	15(31)
C9	475(31)	1172(47)	487(32)	165(31)	188(26)	42(31)
C10	996(45)	608(33)	542(34)	274(32)	145(33)	−122(27)
Cl	602(7)	403(6)	546(7)	76(5)	255(6)	−51(5)
O1	431(18)	392(16)	431(18)	56(14)	151(15)	17(14)
S1	404(7)	441(6)	457(7)	11(5)	113(6)	92(5)
O2	424(17)	439(17)	374(17)	1(14)	131(14)	35(14)
O3	512(21)	735(23)	539(22)	100(17)	15(18)	197(18)
C11	553(33)	484(31)	851(42)	22(28)	315(33)	96(30)
F1	785(22)	446(16)	1495(34)	100(17)	427(22)	128(20)
F2	1040(27)	808(23)	1158(29)	−183(20)	649(24)	162(21)
F3	682(21)	612(19)	1112(28)	−183(17)	35(21)	7(20)
O4	257(15)	471(17)	515(20)	−25(13)	44(14)	−43(15)
S2	341(7)	635(8)	545(8)	22(6)	26(6)	−104(7)
O5	628(24)	892(28)	699(26)	296(20)	65(20)	117(21)
O6	548(22)	903(27)	846(28)	−230(20)	76(21)	−384(23)
C12	416(31)	667(36)	727(39)	−45(27)	171(28)	−72(32)
F4	1097(29)	955(26)	875(25)	−274(21)	475(23)	−374(20)
F5	899(25)	980(25)	954(26)	65(21)	457(22)	203(22)
F6	420(19)	1743(39)	1163(31)	−31(22)	338(20)	−181(28)
O7	412(17)	518(17)	343(17)	−81(14)	95(14)	−52(14)
S3	505(8)	748(9)	455(8)	−210(6)	141(6)	−220(6)
O8	796(28)	609(24)	1069(34)	−153(20)	85(25)	−336(23)

Atom	U_{11}	U_{22}	U_{33}	U_{12}	U_{13}	U_{23}
O9	994(31)	1597(40)	473(23)	−598(32)	396(23)	−369(26)
C13	590(37)	872(46)	678(41)	−157(35)	−66(34)	−76(36)
F7	561(20)	1432(34)	1050(30)	−190(21)	317(21)	−184(25)
F8	799(25)	1787(42)	793(27)	−324(26)	−204(22)	−255(27)
F9	809(27)	991(30)	1754(47)	79(23)	−225(28)	132(29)

U_{ij} values have been multiplied by 10^4
The anisotropic displacement factor exponent takes the form:
$-2\pi^2 [h^2 a^{*2} U_{11} + ... + 2 h k a^* b^* U_{12}]$

Table 5: Complete Distances and Angles for $Cp^*Ta(OTf)_3Cl$

	Distance(Å)		Distance(Å)
Ta –C1	2.473(4)	C9 –H9 C	0.950
Ta –C2	2.450(5)	C10 –H10A	0.977
Ta –C3	2.412(5)	C10 –H10B	0.966
Ta –C4	2.393(5)	C10 –H10C	0.962
Ta –C5	2.428(5)	O1 –S1	1.498(3)
Ta –Cp*	2.112	S1 –O2	1.465(3)
Ta –Cl	2.305(1)	S1 –O3	1.404(3)
Ta –O1	2.146(3)	S1 –C11	1.832(6)
Ta –O2	2.309(3)	C11 –F1	1.306(6)
Ta –O4	2.036(3)	C11 –F2	1.309(7)
Ta –O7	2.066(3)	C11 –F3	1.309(6)
S1 –C11	1.832(6)	O4 –S2	1.491(3)
S2 –C12	1.815(6)	S2 –O5	1.414(4)
S3 –C13	1.826(7)	S2 –O6	1.411(4)
C1 –C2	1.415(6)	S2 –C12	1.815(6)
C1 –C5	1.411(6)	C12 –F4	1.309(7)
C1 –C6	1.495(7)	C12 –F5	1.322(7)
C2 –C3	1.417(7)	C12 –F6	1.308(7)
C2 –C7	1.486(7)	O7 –S3	1.504(3)
C3 –C4	1.412(7)	S3 –O8	1.410(4)
C3 –C8	1.488(8)	S3 –O9	1.401(4)
C4 –C5	1.418(7)	S3 –C13	1.826(7)
C4 –C9	1.491(7)	C13 –F7	1.311(7)
C5 –C10	1.494(7)	C13 –F8	1.311(8)
C6 –H6 A	0.943	C13 –F9	1.303(8)
C6 –H6 B	0.990		
C6 –H6 C	0.955		
C7 –H7 A	0.976		
C7 –H7 B	0.973		
C7 –H7 C	0.949		
C8 –H8 A	0.928		
C8 –H8 B	0.983		
C8 –H8 C	0.987		
C9 –H9 A	0.964		
C9 –H9 B	0.972		

			Angle(°)				Angle(°)
Cp*	-Ta	-Cl	109.3	H6 B	-C6	-C1	108.8
Cp*	-Ta	-O1	102.2	H6 C	-C6	-C1	111.4
Cp*	-Ta	-O2	164.6	H6 B	-C6	-H6 A	107.5
Cp*	-Ta	-O4	104.8	H6 C	-C6	-H6 A	110.5
Cp*	-Ta	-O7	101.8	H6 C	-C6	-H6 B	106.5
Cl	-Ta	-O1	147.9(1)	H7 A	-C7	-C2	110.4
Cl	-Ta	-O2	86.2(1)	H7 B	-C7	-C2	110.7
Cl	-Ta	-O4	89.4(1)	H7 C	-C7	-C2	112.7
Cl	-Ta	-O7	86.7(1)	H7 B	-C7	-H7 A	106.3
O1	-Ta	-O2	62.4(1)	H7 C	-C7	-H7 A	108.2
O1	-Ta	-O4	88.4(1)	H7 C	-C7	-H7 B	108.3
O1	-Ta	-O7	81.0(1)	H8 A	-C8	-C3	113.7
O2	-Ta	-O4	74.9(1)	H8 B	-C8	-C3	110.4
O2	-Ta	-O7	78.2(1)	H8 C	-C8	-C3	109.7
O4	-Ta	-O7	153.0(1)	H8 B	-C8	-H8 A	109.2
Ta	-O1	-S1	100.1(1)	H8 C	-C8	-H8 A	108.9
Ta	-O2	-S1	94.2(1)	H8 C	-C8	-H8 B	104.6
Ta	-O4	-S2	152.6(2)	H9 A	-C9	-C4	110.4
Ta	-O7	-S3	142.0(2)	H9 B	-C9	-C4	110.6
C5	-C1	-C2	108.5(4)	H9 C	-C9	-C4	110.9
C6	-C1	-C2	125.9(4)	H9 B	-C9	-H9 A	107.3
C6	-C1	-C5	124.9(4)	H9 C	-C9	-H9 A	109.1
C3	-C2	-C1	107.4(4)	H9 C	-C9	-H9 B	108.4
C7	-C2	-C1	125.8(4)	H10A	-C10	-C5	110.7
C7	-C2	-C3	126.2(4)	H10B	-C10	-C5	111.9
C4	-C3	-C2	108.3(4)	H10C	-C10	-C5	112.2
C8	-C3	-C2	124.3(4)	H10B	-C10	-H10A	106.8
C8	-C3	-C4	127.0(4)	H10C	-C10	-H10A	107.0
C5	-C4	-C3	107.9(4)	H10C	-C10	-H10B	107.9
C9	-C4	-C3	127.8(4)	O2	-S1	-O1	102.6(2)
C9	-C4	-C5	124.0(4)	O3	-S1	-O1	116.9(2)
C4	-C5	-C1	107.8(4)	O3	-S1	-O2	118.8(2)
C10	-C5	-C1	124.9(4)	F2	-C11	-F1	109.7(4)
C10	-C5	-C4	127.0(4)	F3	-C11	-F1	109.1(4)
H6 A	-C6	-C1	111.9	F3	-C11	-F2	109.0(4)

Angle(°)

O5	–S2	–O4	111.0(2)
O6	–S2	–O4	110.0(2)
O6	–S2	–O5	121.2(2)
F5	–C12	–F4	106.9(4)
F6	–C12	–F4	108.4(5)
F6	–C12	–F5	107.5(5)
O8	–S3	–O7	111.9(2)
O9	–S3	–O7	112.0(2)
O9	–S3	–O8	119.4(3)
F8	–C13	–F7	107.1(5)
F9	–C13	–F7	108.0(5)
F9	–C13	–F8	110.0(5)

Chapter 3

The Preparation and Partial Characterization of N-Alkyl Trimetaphosphimate Derivatives

Abstract

Hexabenzyloxycyclotriphosphatriene was synthesized and thermally rearranged to 1,3,5 - tribenzyl - 2,4,6 tribenzyloxy - 2,4,6 trioxocyclotriphosphazane as per published procedures. Characterization of the rearranged product by NMR techniques revealed the previously undetermined stereochemistry of the product . This ligand precursor has been shown to react with trialkyl silyl chlorides, although the products have not been characterized.

Introduction

Phosphonitrilic chloride trimer provides a simple route into a large number of hexaalkoxy phosphazenes by reactions of the appropriate alcohols or simple metathesis of the chloride with metal alkoxides.(1)

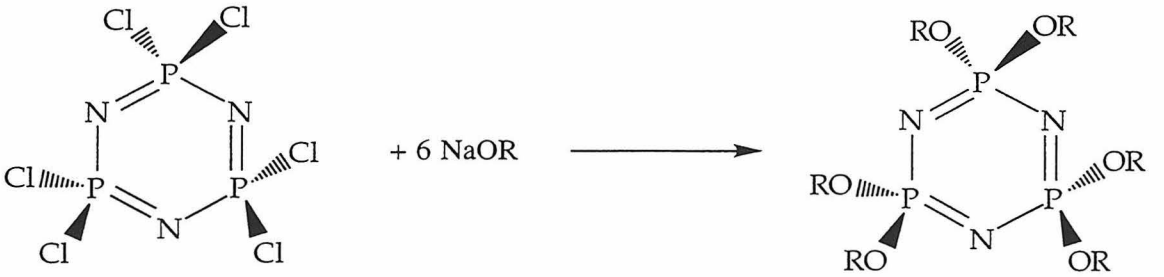

Fitzsimmons and Shaw have reported that these complexes can undergo thermal rearrangement to hexaalkyl trimetaphosphimates.(2,3) This rearrangement can be catalyzed by alkyl halides, and in that case, it is the alkyl group from the alkyl halide which is delivered to the nitrogen.(4,5) For the catalyzed rearrangements, the yields are higher and the conversion temperatures lower than for the uncatalyzed rearrangements.

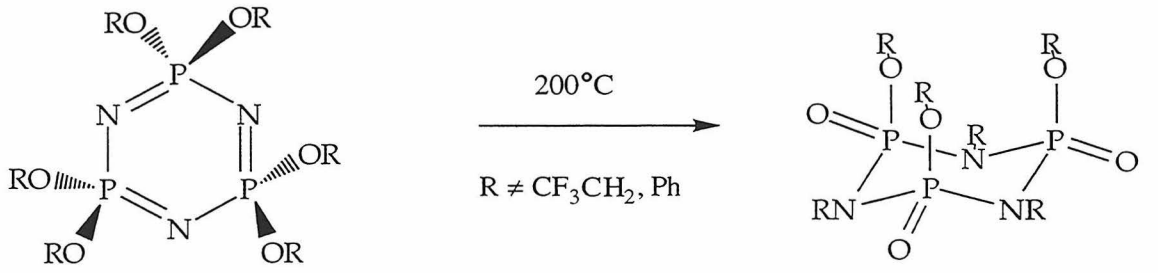

Figure 5: Thermal Formation of Hexaalkyl Trimetaphosphimates

The primary techniques of characterization for these species have been IR spectroscopy and analysis of the hydrolysis products. Primary amines were identified as hydrolysis products instead of ammonia, which is the nitrogen containing product obtained from hydrolysis of the starting materials. It is not known which isomers of hexaalkyl trimetaphosphimate exist, since the stereocenters are lost during hydrolytic decomposition of the compounds. The isomer with all the alkyl groups in equatorial positions is probably the thermodynamically prefered isomer, the final product may be kinetically determined.

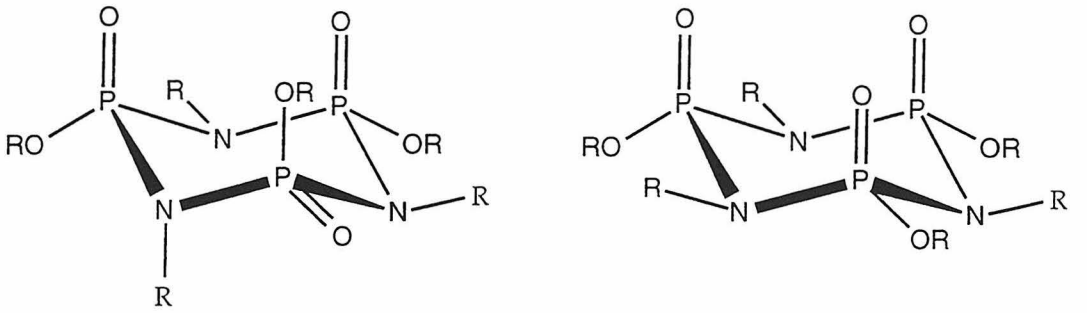

Isomer A Isomer B

Possible Isomers of Hexaalkyltrimetaphosphimates

The neutral hexaalkyl trimetaphosphimate complexes are not expected to be very good ligands for metals due to the low nucleophilicity of possible donor sites. To acquire a more nucleophilic species, dealkyllation to give the trianionic N-alkyl trimetaphoshimate derivatives is desirable. Three such anionic derivatives are pictured. Notably, the barrier to migration of the cations and trialkylsilyl groups in these complexes should allow the thermodynamically favored all-equatorial isomer to be formed as desired.

The stereochemistry of the precursors should not necessarily determine the stereochemistry of the target trimetaphosphimate complexes.

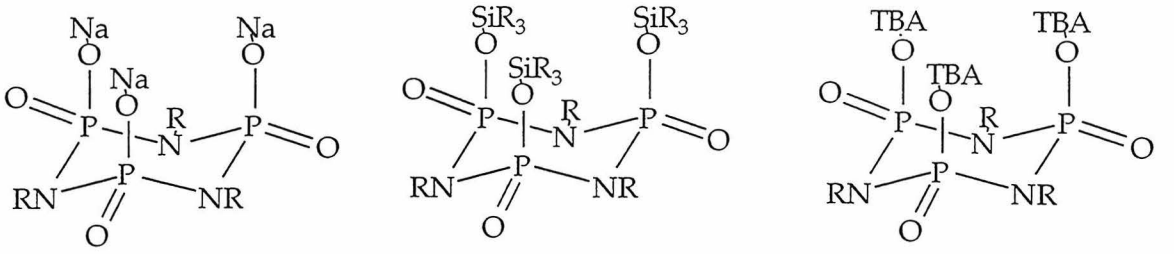

Target Trimetaphosphimate Complexes

At this time, tris N-alkyl trimetaphosphimate complexes of transition metals are not known, although they may be accessible from the above complexes by typical methods. These ligands may have several advantages over the trimetaphosphate (*vide supra*) and trimetaphosphimate anions.

1) The presence of alkyl substituents on the ring nitrogen atoms adds an element of tunability to the ligand.

2) The electron-withdrawing property of the ligand can be adjusted by modification of the substituents at nitrogen.

3) The presence of alkyl groups will increase the solubility of the ligand in organic solvents.

4) The increased steric hindrance at nitrogen will decrease the likelihood of coordination to the metal through the nitrogen atom which was observed for the parent trimetaphosphimate

5) The steric bulk of the alkyls may also prevent oligomerization of the trimetaphosphimate metal complexes.

6) The water of hydration which plagues some of the trimetaphosphate work will be removable for the ligands in which larger, less hydrophillic alkyl groups are used. Also, in some cases, the methods of synthesis of particular derivatives will insure water-free trimetaphosphimates.

7) The bulk of the alkyl substituent may also help to enforce the desired chair conformation of the ring.

Results and Discussion

Hexabenzyloxycyclotriphosphatriene was synthesized in 98% yield using a procedure adapted from Allcock's for the corresponding *ortho*-substituted phenoxy derivatives. The product was characterized by ^{1}H and ^{31}P NMR, which were consistent with the expected symmetry of the complex. The synthesis of 1,3,5 - tribenzyl - 2,4,6 - tribenzyloxy - 2,4,6 - trioxocyclotriphosphazane (hexabenzyl trimetaphosphimate) was accomplished from the thermal rearrangement of hexabenzyloxycyclotriphosphatriene (hexabenzyloxyphosphazene). NMR spectra indicated the presence of inequivalent phosphorus atoms in a 2:1 ratio, strongly suggesting that isomer A was formed in the reaction. This was also supported by an extremely complicated 1H NMR spectrum for the compound. The presence of 4 inequivalent benzyl groups in a 2:2:1:1 ratio is apparent from analysis of the *ortho* protons in the phenyl region of the spectrum. The methylenes on the benzyls show second order effects, which is not surprising given the lack of symmetry in the molecule.

One concern in this work might be that the unexpected assymetric trimetaphosphimate would not be able to coordinate in the desired fashion to a transition metal. Fortunately, upon dealkylation of the oxygen to form trimetaphosphimate salts, the higher symmetry of the molecule would be restored, eliminating such concerns. Three preliminary reactions were performed on an NMR scale (prior to abandonment of the project). In deuterobenzene, hexabenzyl trimetaphosphimate reacts with trimethylsilyl chloride, triphenylsilyl chloride or $Cp^{*}TaCl_4$, liberating benzyl chloride.

Conclusions

Although the hexaalkyl trimetaphosphimates have been synthesized previously, characterization of those compounds did not include identification of the isomer(s) present. This work successfully reproduced the high yield synthesis of hexabenzyl trimetaphosphimates and by utilizing modern NMR techniques of analysis, the stereochemistry of the product has been identified. Very preliminary studies indicate that these complexes may serve as interesting ligand precursors for very oxophilic metals.

Experimental Section

General Considerations. All air and/or moisture sensitive compounds were manipulated using standard Schlenk techniques or in a dry box under a dinitrogen atmosphere. Solvents were stored under vacuum over sodium benzophenone ketyl or calcium hydride (dioxane). Phosphorus NMR spectra were recorded on a JEOL FX90Q (36.28 MHz for ^{31}P) spectrometer and referenced to an external 85% H_3PO_4(aq) standard (δ=0 ppm). Hydrogen NMR spectra were recorded on a General Electric QE 300 (300.152 MHz for ^{1}H) spectrometer. Phosphonitrillic chloride trimer (Aldrich, 99%) was stored in the dry box and used as received. Benzyl alcohol was dried over 4Å molecular sieves overnight prior to use. Tetrabutylammonium bromide (anhydrous) was used as received.

Preparation of Hexabenzyloxycyclotriphosphatriene. 7.95g of freshly cut sodium was loaded into a 1L 3-neck roundbottom flask equipped with a gas inlet adaptor and an addition funnel. 0.67g of tetrabutylammonium bromide was added to the flask against an Ar counterflow, then 75 mL of dioxane was transfered onto the solids via cannula. A mixture of 100 mL of dioxane and 37 mL of benzyl alcohol was added over a period of two hours. This was stirred at 55°C for 3 days. 10g of $P_3N_3Cl_6$ was weighed into a flask and dissolved in 150 mL of dioxane. This was transfered to the addition funnel and added to the mixture dropwise over 1.5 hours. The reaction vessel was heated to 100°C for 2 days. This was pumped to dryness in vacuo, dissolved in 400 mL of dry methylene chloride, filtered to remove excess sodium and sodium chloride, washed with 4x200 mL 10% NaOH(aq) , washed with 2x200 mL of water and pumped again to dryness. A slightly yellow oil which

solidified to a waxy solid was isolated (21.4g, 98%). ^{31}P NMR δ 18.3 ppm (singlet). ^{1}H NMR δ 5.05 ppm (singlet, 12H); δ 7.03 (multiplet, 18H); δ 7.26 (multiplet, 12H).

Preparation of 1,3,5 - tribenzyl - 2,4,6 - tribenzyloxy - 2,4,6 - trioxocyclotriphosphazane. The solid hexabenzyloxycyclotriphosphatriene (5g) from the above preparation was loaded into a medium-walled reaction flask attached to a 8mm teflon Kontes valve. The flask was heated to 160°C for 3 hours. The yellow oil solidified after washing with dry pentane. ^{31}P NMR δ 8.21 (triplet); δ 5.08 (doublet). 1H NMR δ 7.78 (doublet, 2H); δ 7.57 (doublet, 4H); δ 7.26 (doublet, 2H); δ 7.03 (multiplet, 18H); δ 6.70 (doublet, 2H); δ 4.96 (doublet, 1H); δ 4.83 (multiplet, 1H); δ 4.6 (multiplet, 3H); δ 4.32 (mulitplet, 1H).

NMR tube reactions. These reactions were carried out in sealed tubes fitted with a 180° teflon needle valve which was blown directly onto the tube. In each case, a weighed amount of the hexabenzyltrimetaphosphimate was dissolved in d6-benzene and either 3 equivalents of trimethylsilyl chloride, 3 equivalents of triphenylsilyl chloride or 1 equivalent of pentamethylcyclopentadienyl tantalum tetrachloride were added. Over days at room temperature, the characteristic proton resonances for benzyl chloride were apparent in the ^{1}H spectra. Resonances for the other alkyl groups changed as expected for the reaction.

References

1) Emsley; Hall *The cyclophosphazenes*; Emsley; Hall, Ed.; Harper and Row: New York, New York, 1976, pp 405-437.

2) Fitzsimmons, B. W.; Shaw, R. A. *Proceedings of the Chemical Society of London* **1961**, 258.

3) Fitzsimmons, B. W.; Shaw, R. A. *Journal of the Chemical Society of London* **1964**, 1735-1741.

4) Fitzsimmons, B. W.; Hewlett, C.; Shaw, R. A. *Journal of the Chemical Society of London* **1965**, 7432-7436.

5) Fitzsimmons, B. W.; Shaw, R. A. *Journal of the Chemical Society of London* **1964**, 4459-4464.

Chapter 4

The Synthesis, Characterization and Reactivity of $Cp^*_2Ta(=N^tBu)(THF)[B(C_6F_5)_4]$

Abstract

$Cp^*_2Ta(=N^tBu)(THF)[B(C_6F_5)_4]$ **(1)** was synthesized according to the method developed previously in our group. A cationic analog to Bergman's $Cp_2Zr(=N^tBu)$, the reactivity of this complex to hydrocarbon substrates was studied. Contrary to previous reports, this complex does not react with methane, but C-H activation reactions were observed for propyne and phenyl acetylene. In the propyne case, an initial mixture of the [2+2] and C-H activation products was driven to exclusively the C-H activation product thermally. An interesting intramolecular activation of a Cp* methyl group precludes much of the desired C-H activation chemistry. The steric demands of the active site was demonstrated by the observed reaction with ethylene, but the lack of reactivity towards propene. A very interesting dealkylation of the imido group was observed upon reaction with carbon dioxide, which is proposed to involve the intermediacy of a coordinated isocyanate. $Cp^*_2Ta(=N^tBu)(THF)[B(C_6F_5)_4]$ reacts as expected with water, HCl and dihydrogen, and reacts cleanly with methylene chloride to give $Cp^*_2Ta(NH^tBu)Cl[B(C_6F_5)_4]$. Many of the new compounds have been crystallographically and spectroscopically characterized. The reactivity of this complex can be rationalized in terms of the presence of both electrophilic and nucleophilic sites in the same molecule.

Introduction

Transition metal imido complexes have recently attracted a lot of attention for both academic and practical reasons. An excellent, recent and quite comprehensive review of this class of complexes has recently been compiled by Wigley,[1] thus an in depth discussion is not attempted here. Of particular interest is the tremendous range of reactivity of these compounds. Several well-documented studies have taken advantage of the inertness of imido complexes as tunable ancillaries for carbene-containing metathesis catalysts.[2] Other groups have succeeded in making complexes which are extremely reactive, even toward simple hydrocarbons like benzene, which is inert under most conditions. This range of reactivity is certainly mediated by a number of factors and is well worth extended study. Many transition metal imido complexes are of the less reactive variety.[3]

The similarity to transition metal oxo complexes is readily apparent. The two groups are isoelectronic and can be expected to have parallel reactivity patterns. Reactive oxos can be used to make epoxides or alcohols and similarly, imidos can be used to prepare aziridines[4] or amines.[5] The practical chemistry of reactive imido compounds is much less developed than that of oxos. Like the oxo ligand, the imido has a lone pair of electrons which can delocalize into an empty orbital on the metal, stabilizing the complex. One of the major differences between the two groups is the presence of the alkyl group on the imido ligand. This offers the chance to systematically vary the sterics and/or electronics of the system.

Two of the most important reactive imidos were reported in the back-to-back communications of Bergman[6] and Wolczanski,[7] which detail the

generation and reactivity of proposed intermediates [$Cp_2Zr(=N^tBu)$] and [$(^tBu_3SiNH)_2Zr(=NSi^tBu_3)$] respectively. [$Cp_2Zr(=N^tBu)$] was shown to undergo simple C-H activation reactions with hydrocarbons and [2+2] cycloadditions with alkynes.

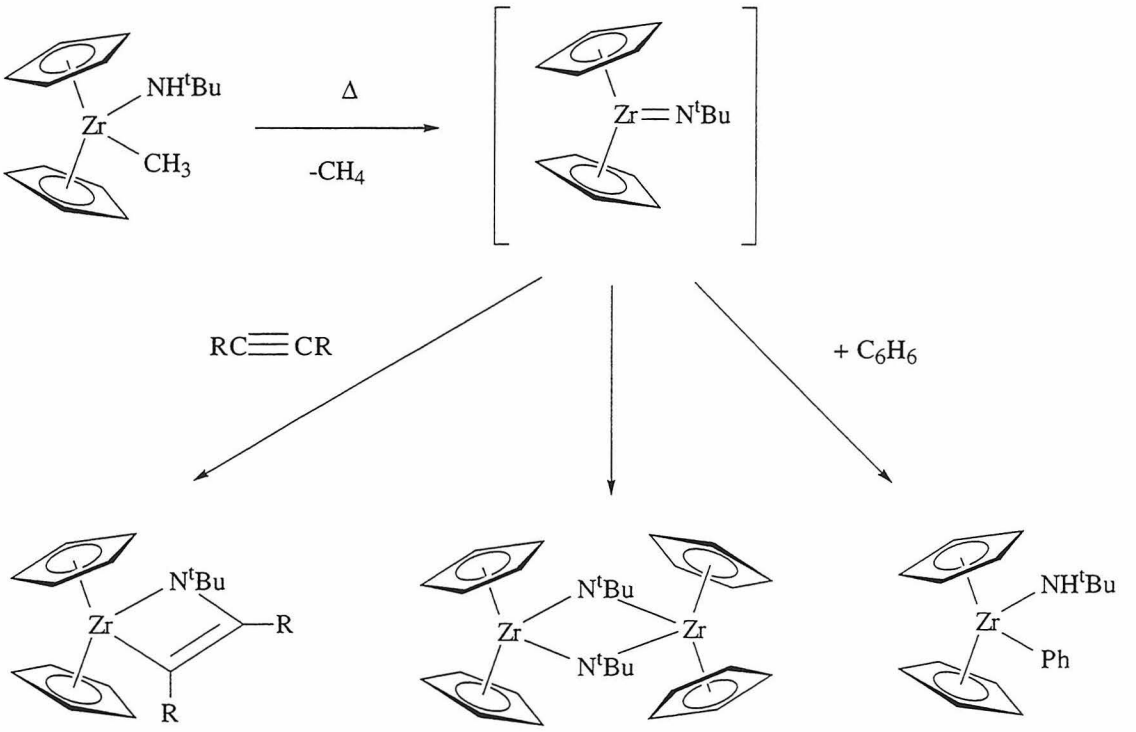

The C-H activation chemistry of [$(^tBu_3SiNH)_2Zr(=NSi^tBu_3)$] is a bit more extensive, including a reaction with methane. Both of these systems involve coordinatedly unsaturated early metals as the active species, which also contained multiple π-bonded ligands in addition to the imido fragment. Theories have been put forth which emphasize the necessity of a basic imido, and suggest that the presence of a so-called π-loaded[8] system is essential. If a surplus of π-donor ligands are attached to the same metal, they will be in competition for the available orbitals of π symmetry and therefore more basic. A slightly different viewpoint, but not mutally exclusive, is that the electrophilicity of the metal center is the key feature for reactivity. This view

suggests that although the basicity of the nitrogen is important, it is secondary. Cundari[9] has suggested that it is the highly polar nature of the imido which allows a formal heterolysis of the C-H bonds of hydrocarbons.

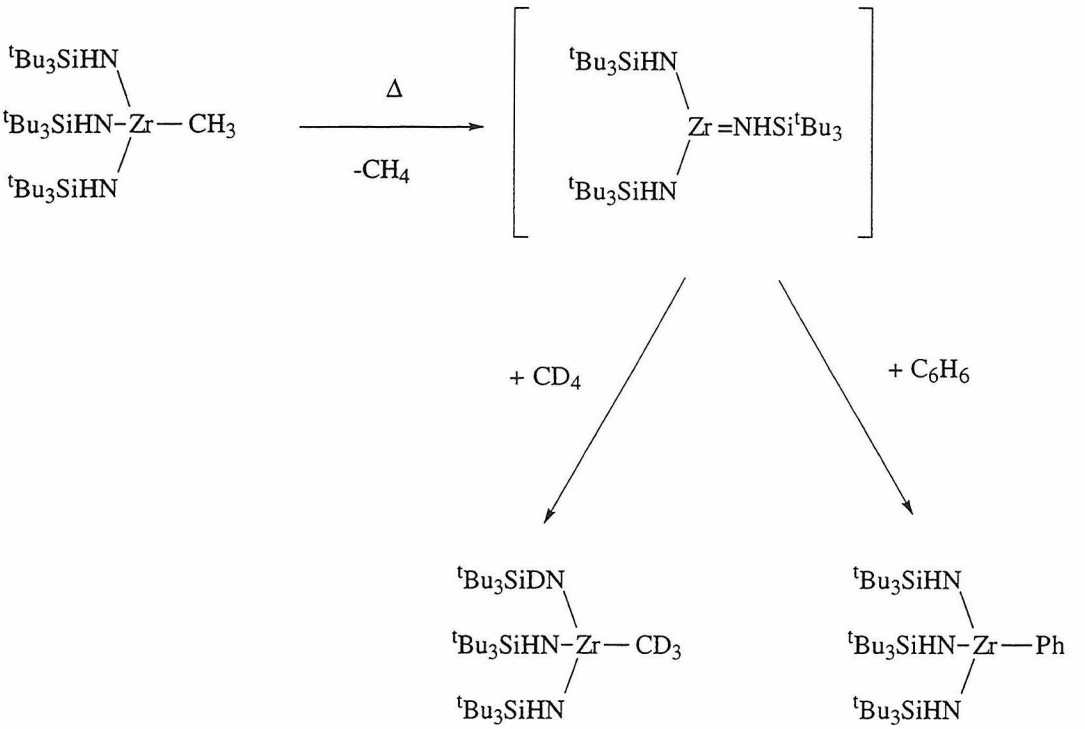

Only by studying a number of imido complexes and their observed reactivities can these theories be examined for validity.

An obvious change to the Bergman system would be to use a group V metal, which would allow the preparation of an isoelectronic cation for comparison. A complex of this type would be far more electrophillic at the metal center, but the imido would be less basic than in the zirconium case. Varying the charge difference between the two compounds would lend insight into the source of reactivity. Ideally, the comparison of the reactivities of $[Cp_2Zr(=N^tBu)]$ and $[Cp_2Ta(=N^tBu)]^+$ would be expected to differentiate between the importance of π-loading and metal electrophilicity in the reactivity of transition metal imido complexes.

One significant consideration in this work is the choice of counterion. Even relatively inert counterions such as tetraphenyl borate and hexafluorophosphate have shown reactivity toward electrophilic metal centers. Non-coordinated anions have been developed for use in Ziegler-Natta and other extremely reactive systems.(10) One of the most useful and unreactive of these is perfluorotetraphenylborate. The synthesis of the triphenyl methyl salt of this anion has been reported.(11) This compound is quite effective for the formation of cations from either hydride or methyl precursors.

Our group has exploited the exceptionally thermally stable Cp^*_2Ta fragment in previous studies.(12) Although the substitution of Cp* for Cp is a significant change, $[Cp^*_2Ta(=N^tBu)]^+$ remains a very interesting target molecule for this study. The Cp* group is more electron donating than Cp, which will decrease the electrophilicity of the analogous target complex, and was demonstrated in previous studies to be non-innocent in some cases. The bulkier Cp* has the advantage of preventing possible dimerization of the desired complex. Starting from the previously known, paramagnetic $Cp^*_2TaCl_2$, Antonelli worked out the preparation of the cation precursor, $Cp^*_2Ta(=N^tBu)(H)$ **(2)** , via an initial reduction with sodium amalgam and subsequent *in situ* metathesis with $LiNH^tBu$.(13) In solution, the metathesis is followed by an alpha hydrogen abstraction, which results in $Cp^*_2Ta(=N^tBu)(H)$ as the isolated product.

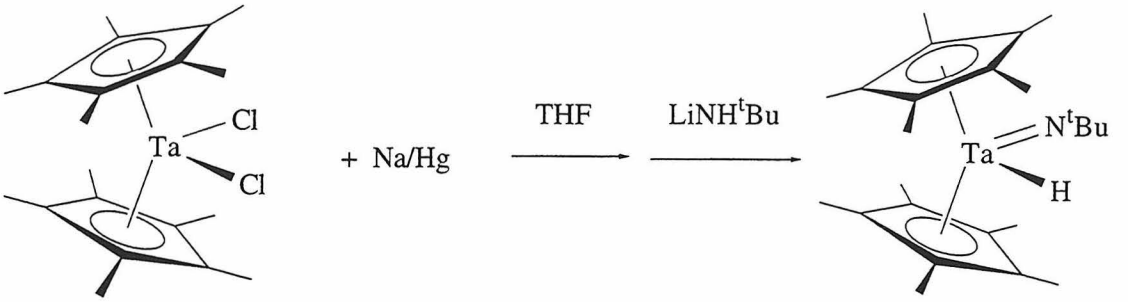

Treatment with $Ph_3C[B(C_6F_5)_4]$ at low temperature in THF gives triphenyl methane and the target cation as a THF adduct.

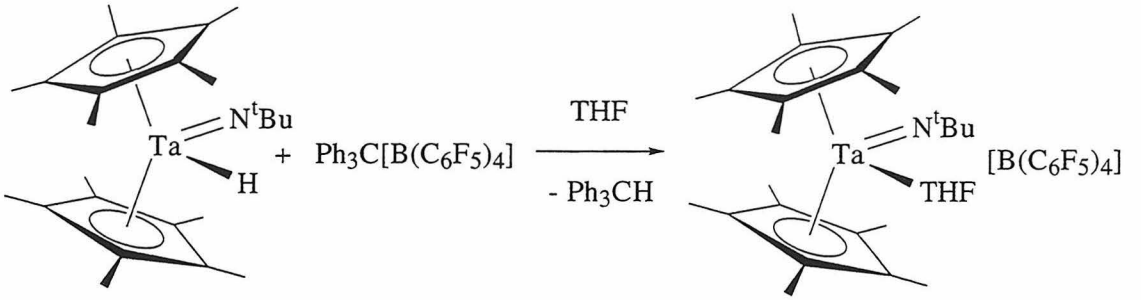

2 **1**

Initial studies of $Cp^*_2Ta(=N^tBu)(THF)[B(C_6F_5)_4]$ were performed by Antonelli. He found that attempted preparation of the cationic species in benzene instead of THF gave an unusual intramolecular activation product **(3)**. The Ta=N bond reacted with a CH_3 group form one of the Cp* rings in preference to the benzene solvent. Similar or intermolecular "tuck-in" complexes have been observed previously in other systems.[14] A unique feature of this product was that the carbon from the methyl group was attached to the nitrogen, not the tantalum. It is not known whether this unusual azametallacycle complex forms directly, or whether a more traditional "tuck-in" species is involved as an intermediate.

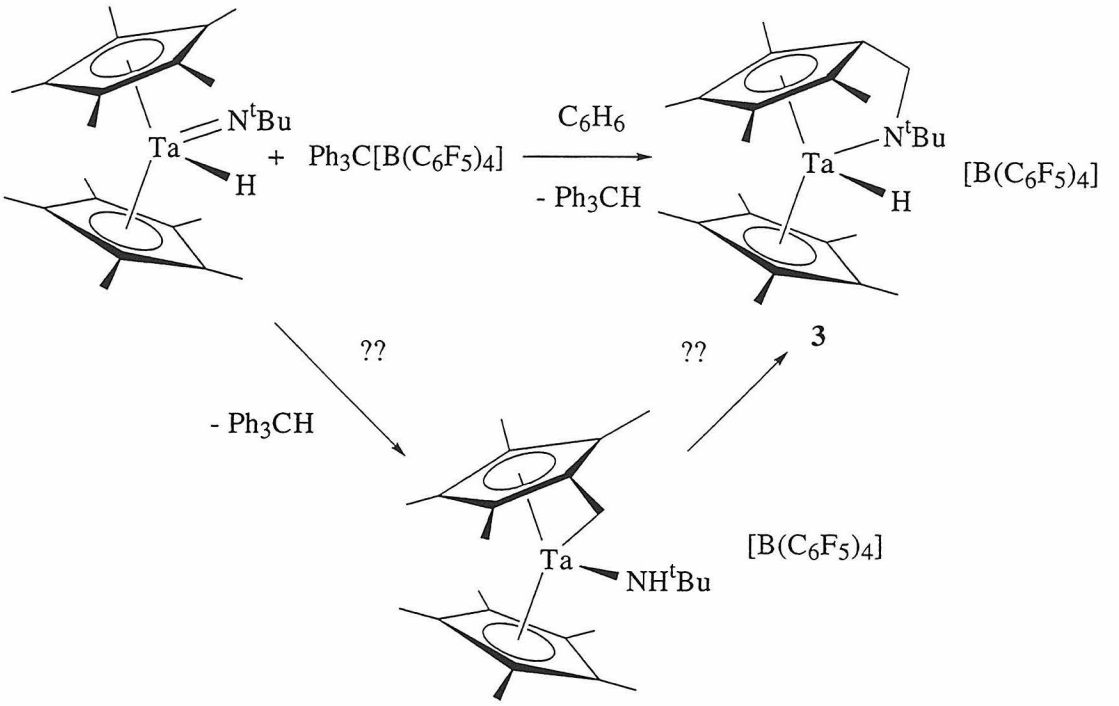

At high temperatures $Cp^*_2Ta(=N^tBu)(THF)[B(C_6F_5)_4]$ was observed to react with methylene chloride, but no product was characterized. The most encouraging feature of the intitial studies was that a clean reaction with methane at low temperature was reported. These interesting and important observations inspired a more complete study of the reactivity of $Cp^*_2Ta(=N^tBu)(THF)[B(C_6F_5)_4]$.

Results and Discussion

Preparation of $Cp^*_2Ta(=N^tBu)(THF)[B(C_6F_5)_4]$ **(1)** was repeated according to the procedure described above. Several difficulties were encountered during this work. Especially problematic was the degree of irreproducibility in the preparation of $Cp^*_2Ta(=N^tBu)H$. Successful syntheses were performed with recrystallized $LiNH^tBu$, under conditions of reasonable dilution, using a 10% excess of sodium and adding a 10% excess of $LiNH^tBu$. Even when these factors were carefully controlled, the success of the experiment seemed to vary from batch to batch of the $Cp^*_2TaCl_2$ starting material and sometimes from experiment to experiment for a single batch. Generally, when the reduction alone of $Cp^*_2TaCl_2$ to "Cp^*_2TaCl" went well, successful $Cp^*_2Ta(=N^tBu)H$ syntheses were possible, supporting the postulate that the $Cp^*_2TaCl_2$ was the source of the difficulty. Despite the vast number of times this reaction was run, the irreproducibility of the reaction was never explained satisfactorily nor eliminated. Also, during the formation of $Cp^*_2Ta(=N^tBu)(THF)[B(C_6F_5)_4]$ with trityl perfluorotetraphenyl borate, it is important to conduct the reaction at low temperatures to prevent the polymerization of the THF solvent by the trityl cation. Even with the difficulties encountered, multigram quantities of **1** for a fairly detailed reactivity study were prepared.

Confirmation of the low temperature reaction of methane and $Cp^*_2Ta(=N^tBu)(THF)[B(C_6F_5)_4]$ in methylene chloride was unsuccessful. Preliminary NMR tube reactions of **1** with methane, toluene, benzene and without reactant were run in deutero-methylene chloride at room temperature. In all cases, the starting material was slowly converted to an

identical product, regardless of the hydrocarbon present. Heating to 80°C resulted in full conversion within 8 hours. Prolonged heating to 120°C converted the new product to a different compound which no longer displayed *tert*-butyl resonances in its NMR spectrum. Apparently, the reaction taking place was an intramolecular rearrangement and/or a reaction with solvent. Similar lack of reactivity was also seen for propene, butadiene and diphenyl acetylene. Methyl iodide and methyl bromide reacted at a rate comparable to methylene chloride to give a mixture of products. The reaction of methane with $Cp^*_2Ta(=N^tBu)(THF)[B(C_6F_5)_4]$ in an inert solvent, chlorobenzene, reproducibly gave the "tuck-in" complex from the intramolecular reaction.

A preparative scale reaction of **1** with methylene chloride was run and the product crystallized from methylene chloride by layering with petroleum ether. NMR studies indicate the presence of a N-H or Ta-H peak at δ=7.18 ppm, the broadness of the peak suggesting the former. X-ray structure determination identified the compound as $Cp^*_2Ta(NH^tBu)Cl[B(C_6F_5)_4]$ **(4)** (Figure 1). The tantalum-nitrogen distance of 1.94 Å is indicative of a single bond and the Ta-N-C1 angle of 155.4° indicates substantial pyramidalization at nitrogen. Infrared spectroscopy confirms the N-H bond by the presence of a weak stretching vibration at 3355 cm^{-1}. Interestingly, when this reaction is run in CD_2Cl_2, the N-***H*** resonance of the final product is prominant, indicating that the solvent is not the source of the proton. This implies that one of the "tuck-in" products (*vide supra*) may be involved in the formation of **4**. No experiments have been conducted to test this hypothesis.

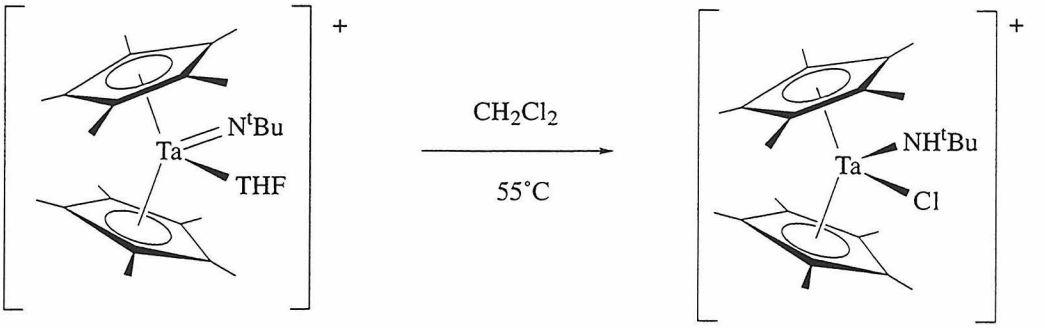

4

Since the reaction between $Cp^*_2Ta(=N^tBu)(THF)[B(C_6F_5)_4]$ and methylene chloride is formally the abstraction of HCl from the solvent, the direct reaction of HCl and **1** was run on an NMR scale in CD_2Cl_2. As the reaction proceeded an unexpected white precipitate formed. After 3 hours at room temperature, unreacted starting materials and multiple products (including the desired product) were identified by NMR spectroscopy. Heating to 60°C for one hour resulted in only two Cp* containing products, primarily the desired $Cp^*_2Ta(NH^tBu)Cl[B(C_6F_5)_4]$. The other product does not contain a tertiary butyl group and is postulated to be $Cp^*_2TaCl_2[B(C_6F_5)_4]$. It is likely that HCl reacted with the desired product to cleave the *tert*-butyl amido group from the metal which precipitated as $^tBuNH_3Cl$. As the reaction proceeded, the *tert*-butyl ammonium chloride may have reacted with **1** that was still in solution to produce more of the desired product.

Given that the reaction with fairly inert hydrocarbons was not possible, reactions were performed with several more reactive small molecules to probe the general reactivity of the tantalum imido compound. In a series of NMR tube reactions in methylene chloride, clean reactions were seen with dihydrogen, propyne, phenyl acetylene, carbon dioxide, dihydrogen and water. The NMR tube reaction with ethylene rapidly gave an adduct as observed by the appearance of two triplets (δ=0.74 ppm, 2H and 2.93 ppm, 2H),

whereas propene shows no reaction whatsoever. The NMR-observed ethylene product reacted with additional equivalents of ethylene to give an intractable oily product which was not pursued. Based upon this NMR evidence, it is probable that the initially-formed product is the result of a formal [2+2] addition of ethylene across the Ta=N bond, which is followed by an insertion reaction (or reactions) to give the subsequent product(s).

$Cp^*_2Ta(=N^tBu)(THF)[B(C_6F_5)_4]$ was reacted cleanly with an excess of hydrogen. The NMR spectrum of the recrystallized product showed two broad downfield peaks, consistent with the expected amido-hydride product $Cp^*_2Ta(NH^tBu)H[B(C_6F_5)_4]$ **(5)**. An IR spectrum was taken in a nujol mull which confirmed the presence of N-H (ν=3336 cm^{-1}) and Ta-H (ν=1862 cm^{-1}) bonds in the product. An X-ray structural determination was done on a suitable single crystal (Figure 2). A tantalum-nitrogen distance of 1.93Å and a Ta-N-C1 angle of 159° are consistent with the expected values for the product. The fact that **1** reacts readily with hydrogen is encouraging given the strength of the H-H bond. Somewhat surprisingly, $Cp^*_2Ta(NH^tBu)H[B(C_6F_5)_4]$ reacts very slowly to form $Cp^*_2Ta(NH^tBu)Cl[B(C_6F_5)_4]$ if left in solution in methylene chloride. Apparently both **1** and **5** are very reactive toward chloride abstractions, even from methylene chloride at room temperature. It is likely that a radical chain mechanism is involved in these transformations.

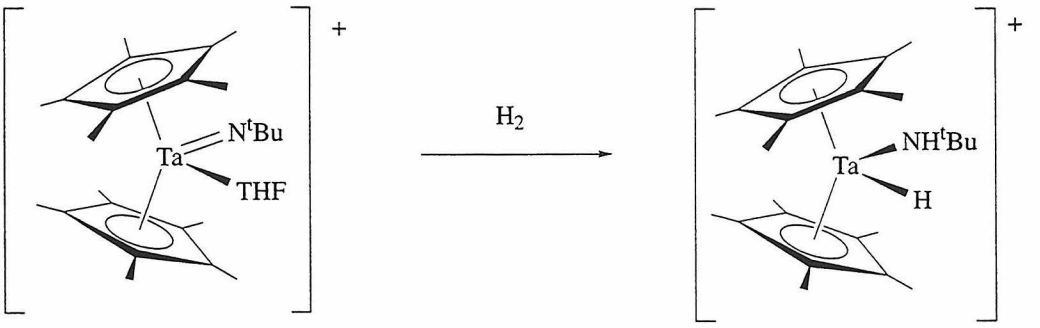

5

Propyne was reacted with complex **1** in the hopes that the relatively reactive sp C-H bond would be heterolyzed by the tantalum imido species. After a few hours at room temperature, the ^{1}H NMR signals for the starting material were replaced by two new Cp* and *tert*-butyl resonances. The presence of a broad peak at δ=7.02 ppm suggested that the expected C-H activation had taken place to form $Cp^*_2Ta(NH^tBu)(C{\equiv}CCH_3)[B(C_6F_5)_4]$ **(6)**. The observation of an N-H stretch in the IR spectrum of the complex at ν=3338 cm^{-1} supported this hypothesis.

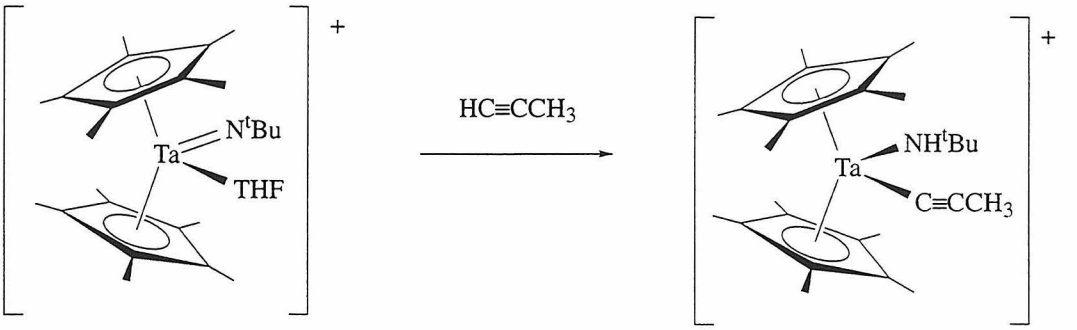

6

The other product was identified as the [2+2] addition product to form the azametallacyclobutene structure pictured below. The identification of coupled ^{1}H NMR signals for the methyl and methine protons supported this supposition. Heating of the compound to 60°C for several hours converted this product entirely to the C-H activation product.

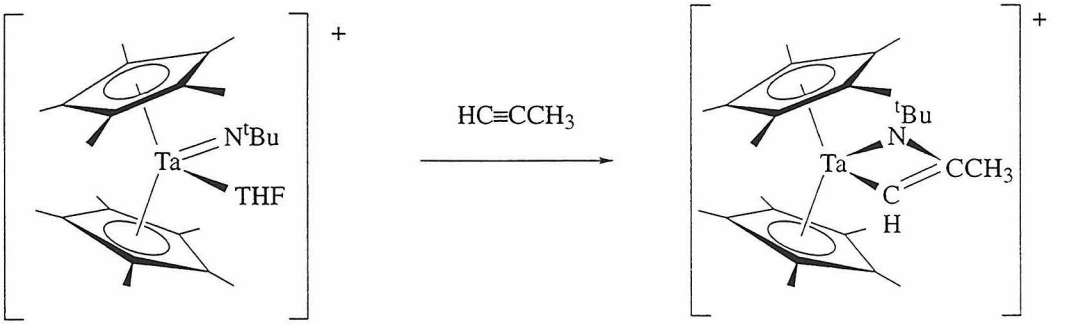

7

The spectroscopic evidence identifying the two products in the reaction of **1** with propyne was quite convincing. Based upon the hypothesis that the C-H activation is essentially a heterolysis reaction, a more acidic substrate was chosen in the hopes that the C-H activation product would predominate. Phenyl acetylene reacted with $Cp^*_2Ta(=N^tBu)(THF)[B(C_6F_5)_4]$ rapidly at room temperature to cleanly give the expected product in high yield. In addition to the collaborating spectroscopic evidence, a crystal structure determination unambiguously identified the product as $Cp^*_2Ta(NH^tBu)(C{\equiv}CPh)[B(C_6F_5)_4]$ **(8)** (Figure 3).

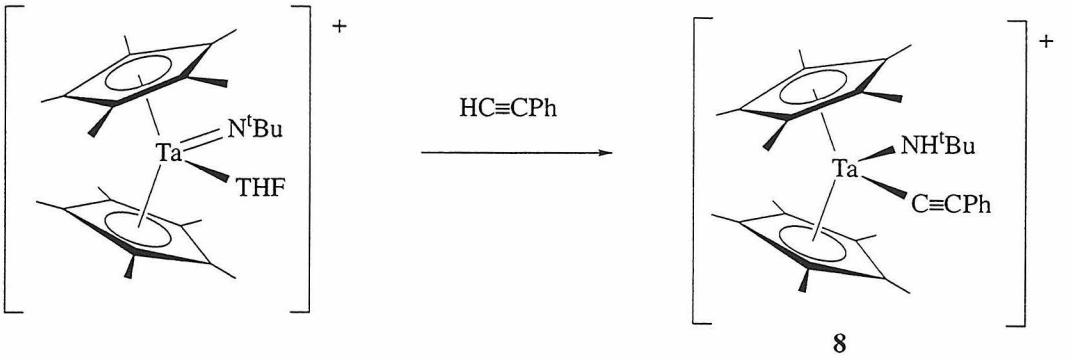

8

The reaction of $Cp^*_2Ta(=N^tBu)(THF)[B(C_6F_5)_4]$ with 5 equivalents of water gave $Cp^*_2Ta(OH)_2[B(C_6F_5)_4]$ **(9)** in high yield. This reaction was notable only in the fact that it answered the question about the initially observed reaction with methane. The ^1H spectrum of **9** in methylene chloride is identical to that obtained from the original reaction with methane. Apparently the reaction was conducted with wet methane.

An interesting and unexpected result was obtained from the reaction of $Cp^*_2Ta(=N^tBu)(THF)[B(C_6F_5)_4]$ with carbon dioxide. Previous work in our group and others gave precedent for a formal [2+2] addition to form an

η^2-carbamate complex. Instead, a rapid reaction gave a product which did not contain a *tert*-butyl group according to elemental analysis or ^{1}H NMR. The nitrogen, however, was contained in the final product. A broad peak at δ=8.26 ppm supported the presence of an N-H proton. Unfortunately, we could not explain how carbon dioxide might displace THF and induce dealkylation of the imido. One of the possible structures of the complex is pictured below.

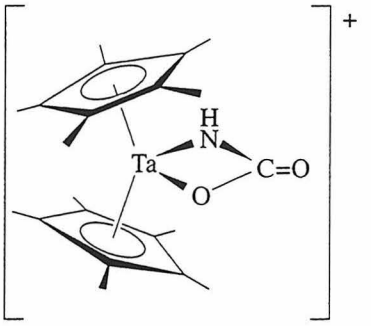

??

A structure was determined of a single crystal of the compound by X-ray diffraction (Figure 4). Initially, a the data was poorly modelled by a structure which contained a linear O-bound OCO group and an imido (=NH). Since carbon dioxide is not known to be a good enough base to displace THF, the thermal parameters were inconsistent with the proposed structure and the proposed C=O bond distance of 1.13 Å was shorter than that of free CO, it was suspected that the compound was not as proposed. In fact, a literature search revealed that to date no linear O-bound CO_2 complexes are known. An isocyanate hydroxide complex was considered as an alternative, which gave a much better fit to the structural data. The revised structure matched the elemental analysis and spectral data as well.

A reasonable mechanism to explain the formation of the observed product is depicted below. The expected [2+2] addition reaction was followed by a productive retro [2+2] reaction to give an oxo complex containing a coordinated organic isocyanate. A six membered transition state could be drawn for the subsequent deprotonation of a methyl on the *tert*-butyl group by the oxo. This would be accompanied by the extrusion of isobutylene and formation of the proposed isocyanate hydroxo complex. Reexamination of data from the original sealed-tube NMR experiment confirmed the presence of isobutylene in the reaction mixture. Reaction with ^{13}C labelled CO_2 allowed unambiguous assignment of the C=O stretch (ν=2252 cm^{-1}) for the complex, which shifted by 62 cm^{-1} to ν=2190 cm^{-1} due to the isotopic substitution. This reaction has implications for hydrodenitrification processes by metal oxos and represents an interesting activation of carbon dioxide.

The availability of $Cp^*_2Ta(NH^tBu)Cl[B(C_6F_5)_4]$ prompted the attempted synthesis of $Cp^*_2Ta(NH^tBu)(CH_3)[B(C_6F_5)_4]$ (**10**), the expected product from the activation of methane by $Cp^*_2Ta(NH^tBu)Cl[B(C_6F_5)_4]$. The stability of this compound would imply that the lack of reactivity with methane is kinetic and not thermodynamic in nature. Despite the possibly favorable driving force for the C-H activation, it is an intramolecular shunt prevents the reaction of **1** with methane. In NMR experiments, the alkylating agents dimethyl mercury and diethyl zinc show no reaction with **4**. Addition of methyl lithium to **4** results in the rapid evolution of methane.

Proposed Mechanism for Product Formation in CO_2 Reaction

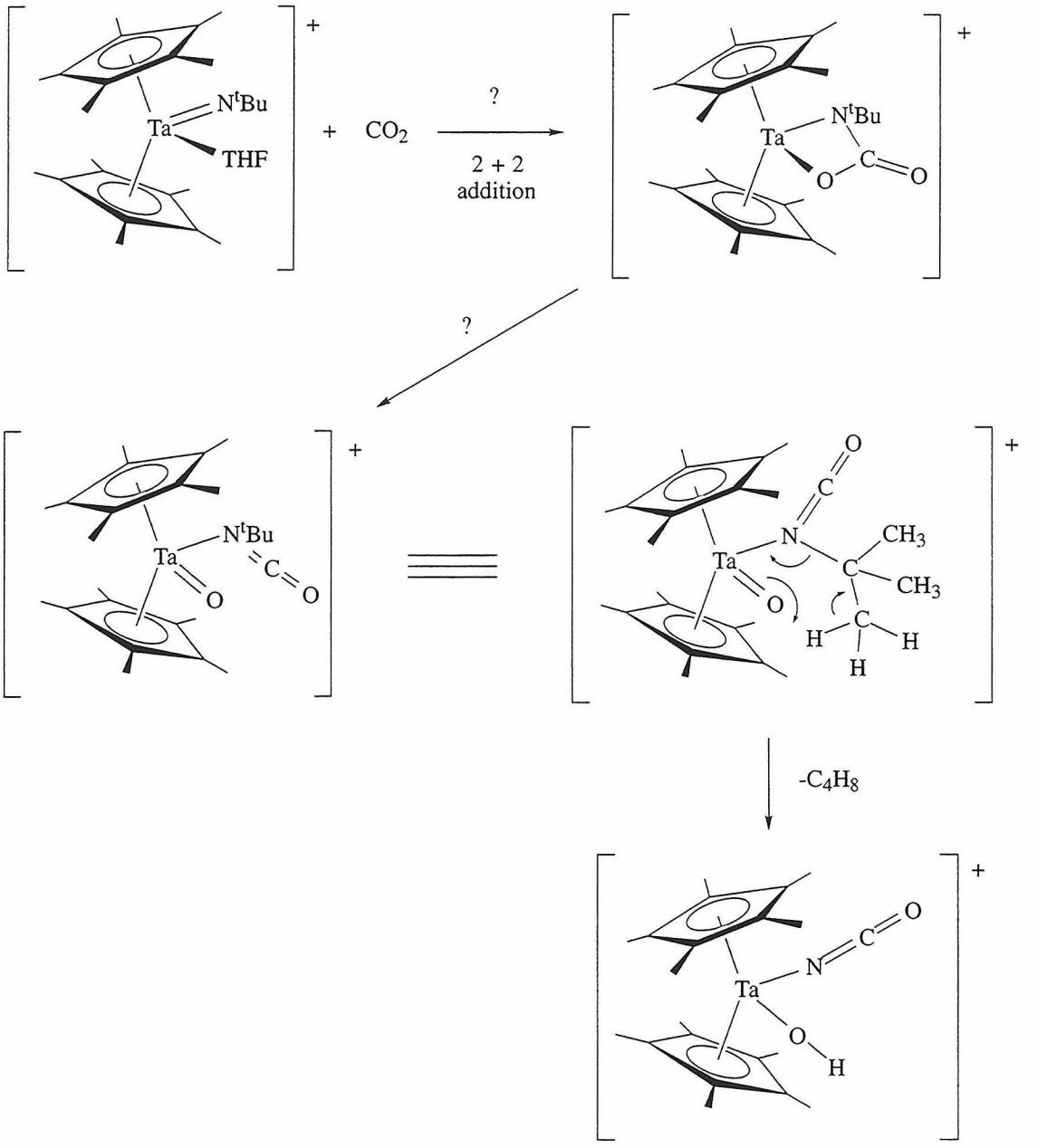

Unfortunately, this negative result did not unambiguously determine the stability of the possible methyl amido product. Due to the presence of the acidic proton of the amido group, the direct deprotonation of the complex by methyl lithium to give neutral $Cp^*_2Ta(=N^tBu)Cl$ was observed by NMR. Metathesis of the chloride ligand followed by methane elimination (the reverse of the desired reaction) would have resulted in the formation of **1** instead of the observed product. These preliminary efforts to probe the thermodynamic stability of $Cp^*_2Ta(NH^tBu)(CH_3)[B(C_6F_5)_4]$ were inconclusive.

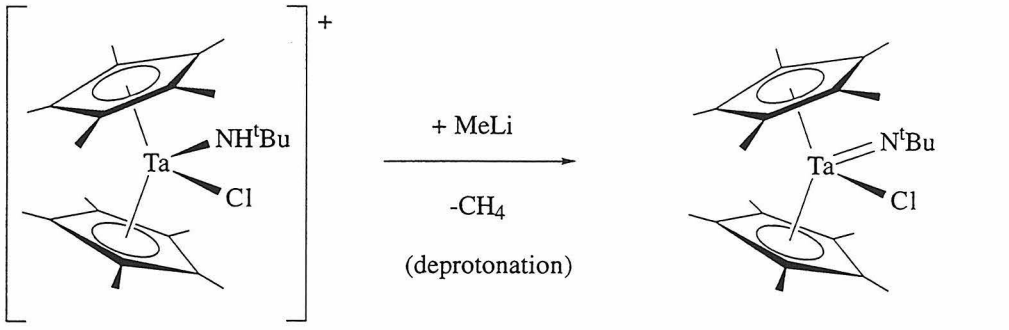

4

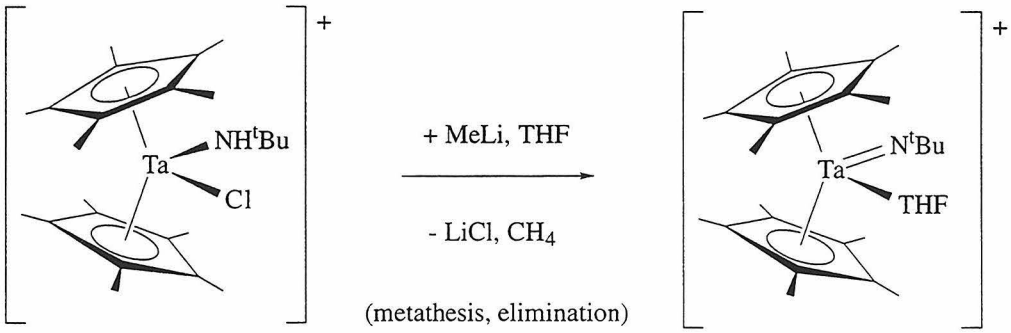

4 **1**

Conclusions

The expected reactivity of $Cp^*_2Ta(=N^tBu)(THF)[B(C_6F_5)_4]$ with methane was not observed due to a facile intramolecular C-H activation reaction. The non-innocence of the ancillary Cp* ligand has proven to be problematic for this extremely reactive compound. Even so, many reactions were found to be competitive with the intramolecular reaction and led to the synthesis and characterization of a number of new cationic complexes of tantalum. The anticipated C-H activation was observed for the fairly reactive and unhindered sp C-H bonds. Particularly interesting was the reaction of $Cp^*_2Ta(=N^tBu)(THF)[B(C_6F_5)_4]$ with carbon dioxide, which proceeded via a complex mechanism to dealkyllate the imido ligand.

The implications of this work for future studies are significant. The importance of unreactive supporting ligands was underscored by the observed reactivity of $Cp^*_2Ta(=N^tBu)(THF)[B(C_6F_5)_4]$. Study of the analog incorporating unsubstituted Cp ligands is encouraged. The original proposal that more electrophilic metal imido complexes would be more reactive toward hydrocarbon C-H bonds is supported by these studies. In our reactions with acetylenes, the C-H activation products predominate over the [2+2] addition products. We believe that the C-H activation is encouraged by the polarity of the Ta=N bond, but that the key feature is indeed the electrophilicity of the metal center. The completely unanticipated reaction with carbon dioxide implies that electrophilic early metal oxos may also be competent for the dealkyllation of amines or other nitrogen-containing substrates.

Experimental Section

General Considerations. All air and/or moisture sensitive compounds were manipulated using standard Schlenk techniques or in a dry box under a nitrogen atmosphere. Hydrogen and carbon NMR spectra were recorded on a General Electric QE 300 (300.152 MHz for ^1H) spectrometer and referenced to residual proton impurities or carbon signals in the NMR solvent. Fluorine spectra were recorded on a Bruker AM500 (500.13 MHz for 1H) spectrometer. Infrared spectra were recorded on a Perkin Elmer 1600 series spectrophotometer in nujol mulls. Elemental analyses were performed by Fenton Harvey at Caltech. Preliminary NMR reactions were all performed using teflon-valved NMR tubes.

Synthesis of $[Cp^*_2Ta(NH^tBu)Cl][B(C_6F_5)_4]$. $[Cp^*_2Ta(=N^tBu)(THF)][B(C_6F_5)_4]$ (0.5g, $3.95x10^{-4}$ mol) was placed in a small teflon-valved flask with 5 mL of methylene chloride in the glovebox. This was placed in an oil bath and heated to 55°C for 12 hours. The yellow/brown solution from the reaction was pumped down to a brown oily solid in vacuo. The product was purified by recrystallization from a methylene chloride and diethyl ether solution which was layered with petroleum ether. The orange crystals were isolated by decanting as much solvent as possible and evaporation of the residual *in vacuo* (0.322g isolated, 69% yield). A suitable crystal for structural analysis by X-Ray diffraction was cleaved from a larger orange needle.

Elemental analysis: Calculated C 46.57% H 3.26% N 1.13%

Found C 46.45% H 3.39% N 0.98%

^{19}F NMR (CD_2Cl_2) δ = -135.2 ppm (d); -165.9 ppm (t); -169.7 ppm (t)

Alternate Synthesis of $[Cp^*_2Ta(NH^tBu)Cl][B(C_6F_5)_4]$ (NMR scale). $[Cp^*_2Ta(=N^tBu)(THF)][B(C_6F_5)_4]$ (0.1g, $7.85x10^{-5}$ mol) was placed in a small teflon-valved NMR tube with 0.7 mL of methylene chloride in the glovebox. A 6.9 mL gas bulb was attached to the NMR tube, evacuated and filled with 220 torr of HCl. The contents of the tube were frozen at 77°K and the HCl opened to the tube. Upon warming to room temperature, a flocculant white precipitate was present in the solution (multiple products by NMR). The tube was warmed to 60°C for 1 hour, during which time the precipitate dissolved. The primary product is $[Cp^*_2Ta(NH^tBu)Cl][B(C_6F_5)_4]$.

Synthesis of $[Cp^*_2Ta(NH^tBu)H][B(C_6F_5)_4]$. $[Cp^*_2Ta(=N^tBu)(THF)][B(C_6F_5)_4]$ (0.5g, $3.95x10^{-4}$ mol) was placed in a small (15 mL) teflon-valved flask with 5 mL of methylene chloride in the glovebox. The flask was evacuated and 1 atm of hydrogen (approximately $6x10^{-4}$ mol) was added at room temperature. The solution was stirred for 3 days, then the resulting yellow solution was pumped down to a yellow solid *in vacuo*. It was purified by recrystallization by layering a methylene chloride solution of the compound with petroleum ether (Yield 0.380g, 80%). A single crystal for structure determination by X-ray diffraction was grown by layering a methylene chloride solution with petroleum ether.

Elemental analysis: Calculated C 47.90% H 3.43% N 1.16%;
Found C 47.54% H 3.45% N 0.96%

^{19}F NMR (CD_2Cl_2) δ = -135.2 ppm (d); -165.9 ppm (t); -169.8 ppm (t)

Initial Reaction of $[Cp^*_2Ta(=N^tBu)(THF)][B(C_6F_5)_4]$ with propyne. $[Cp^*_2Ta(=N^tBu)(THF)][B(C_6F_5)_4]$ (0.5g, 3.95x10-4 mol) was placed in a teflon-valved 100mL flask and 10 mL of dry methylene chloride was vacuum

transferred into the flask. Once the solid dissolved and the solution warmed to room temperature, approximately one atmosphere of propyne (about $3.6x10^{-3}$ mol) was transferred into the flask. This was allowed to stir overnight, during which time the orange solution turned yellow-brown, then pumped to dryness in vacuo. The brownish yellow product was recrystallized by layering a methylene chloride solution with petroleum ether. Yield = 0.336g (69%).

Elemental analysis:	Calculated	C 49.66% H 3.49% N 1.13%;
	Found	C 49.59% H 3.67% N 1.04%

Synthesis of $[Cp^*_2Ta(NH^tBu)(CCCH_3)][B(C_6F_5)_4]$. The solid from the initial reaction of $[Cp^*_2Ta(=N^tBu)(THF)][B(C_6F_5)_4]$ with propyne was placed in a 25 mL teflon-valved flask and 5 mL of dry methylene chloride was added to the flask in the glovebox. This was placed in a 60°C oil bath for 12 hours. After removal of the solvent *in vacuo*, the crude product was recrystallized by layering a methylene chloride solution with petroleum ether.

Synthesis of $[Cp^*_2Ta(NH^tBu)(CCPh)][B(C_6F_5)_4]$.

$[Cp^*_2Ta(=N^tBu)(THF)][B(C_6F_5)_4]$ (0.5g, 3.95x10-4 mol) was placed in a teflon-valved 15 mL flask and 5 mL of dry methylene chloride was pipetted into the flask in the glovebox. Also in the glovebox, 45 mL of phenyl acetylene was syringed into the flask. The reaction mixture was stirred overnight. The resulting red solution was reduced in volume to 2 mL in vacuo, then 6 mL of petroleum ether was layered onto it. Initially a viscous oil sttled out of the solution, but after vigorous shaking the product crystallized. X-ray quality crystals were isolated from the crude product and a structure determined. Yield: 0.453g (88%)

Elemental analysis:	Calculated	C 51.59% H 3.48% N 1.07%;
	Found	C 51.10% H 3.56% N 1.10%

Synthesis of $[Cp^*_2Ta(NCO)(OH)][B(C_6F_5)_4]$. $[Cp^*_2Ta(=N^tBu)(THF)][B(C_6F_5)_4]$ (0.5g, 3.95x10-4 mol) was placed in a teflon-valved 100mL flask and 10 mL of dry methylene chloride was vacuum transferred into the flask. Approximately one atmosphere of carbon dioxide (about $3.6x10^{-3}$ mol) was transferred into the flask. This was allowed to stir for 3 days, during which time the orange solution turned greenish yellow, then pumped to dryness in vacuo. The yellow product was recrystallized by layering a methylene chloride solution with petroleum ether. Yield = 0.400g (85%). Repeated recrystallizations were successful for the isolation of a crystal suitable for an X-ray structure determination.

Elemental analysis:	Calculated	C 45.44% H 2.63% N 1.18%;
	Found	C 45.52% H 2.61% N 1.18%

^{19}F NMR (CD_2Cl_2) δ = -135.2 ppm (d); -165.9 ppm (t); -169.7 ppm (t)

Synthesis of $[Cp^*_2Ta(OH)_2][B(C_6F_5)_4]$. $[Cp^*_2Ta(=N^tBu)(THF)][B(C_6F_5)_4]$ (0.5g, $3.95x10^{-4}$ mol) was placed in a teflon-valved 100mL flask and 10 mL of dry methylene chloride was vacuum transferred into the flask at -78°C. After the flask warmed to room temperature, 35.5 μL of water ($1.96x10^{-3}$ mol) was syringed into the flask under argon counterflow. The orange solution slowly turned pale yellow. After 12 hours, the solvent was removed in vacuo and the product recrystallized by layering a methylene chloride solution with petroleum ether. Large clear crystals were isolated by filtration (0.317g, 69% yield).

Elemental analysis:	Calculated	C 45.38% H 2.77%
	Found	C 45.69% H 2.88%

^{19}F NMR (CD_2Cl_2) δ = -135.2 ppm (d); -165.9 ppm (t); -169.7 ppm (t)

Table 1. ^{1}H NMR Data[a]

compound	assignment	δ, ppm (coupling, Hz)
$Cp^*_2Ta(=N^tBu)(THF)[B(C_6F_5)_4]$	$C_5(CH_3)_5$	2.14
	$(CH_3)_3C$	1.32
	OCH_2	4.19
	OCH_2CH_2	2.21
$Cp^*Ta(N(^tBu)CH_2(\eta^5\text{-}C_5(CH_3)_4))(H)[B(C_6F_5)_4]$	$C_5(CH_3)_5$	2.19
	$(CH_3)_3C$	1.18
	TaH	8.58
	NCH_2	4.59 (d of d)
	$C_5(CH_3)_4$	1.95
		2.06
		2.27
		2.64
$Cp^*_2Ta(NH^tBu)(H)[B(C_6F_5)_4]$	$C_5(CH_3)_5$	2.22
	$(CH_3)_3C$	1.30
	TaH	8.52
	NH	7.74
$Cp^*_2Ta(NH^tBu)(Cl)[B(C_6F_5)_4]$	$C_5(CH_3)_5$	2.22
	$(CH_3)_3C$	1.26
	NH	7.18
$Cp^*_2Ta(NCO)(OH)[B(C_6F_5)_4]$	$C_5(CH_3)_5$	2.21
	OH	8.26 (br)
$Cp^*_2Ta(OH)_2[B(C_6F_5)_4]$	$C_5(CH_3)_5$	2.10
	OH	5.93
$Cp^*_2Ta(NH^tBu)(CCPh)[B(C_6F_5)_4]$	$C_5(CH_3)_5$	2.24
	$(CH_3)_3C$	1.29

	N*H*		7.33 (br)
	C_6H_5		7.35 (m)
			7.40 (m)
$Cp^*_2Ta(=N^tBu)(THF)[B(C_6F_5)_4]$ + CH_3CCH	$C_5(CH_3)_5$	[2+2]	2.07
	$(CH_3)_3C$	[2+2]	1.35
	C*C*H	[2+2]	4.57 (q, J = 2 Hz)
	CH_3CC	[2+2]	2.84 (d, J = 2 Hz)
	$C_5(CH_3)_5$	C-H activation	2.17
	$(CH_3)_3C$	C-H activation	1.24
	N*H*	C-H activation	7.02
	CH_3CC	C-H activation	1.95[b]

[a] Spectra were taken in CD_2Cl_2 solvent and referenced to residual proton impurities at 5.32 ppm unless indicated otherwise.
[b] Chemical shift was not unambiguously resolved.

Table 2. ^{13}C NMR Data[a]

compound	assignment	δ, ppm (coupling, Hz)
$Cp^*_2Ta(=N^tBu)(THF)[B(C_6F_5)_4]$	$\boldsymbol{C}_5(CH_3)_5$	123.4
	$(\boldsymbol{C}H_3)_3C$	34.9
	$C_5(\boldsymbol{C}H_3)_5$	12.7
	$(CH_3)_3\boldsymbol{C}$	68.6
	$O\boldsymbol{C}H_2$	88 (br)
	$OCH_2\boldsymbol{C}H_2$	27.4
	$\boldsymbol{C}_6F_5$[b]	136.3 (d, J_{CF} =246)
		138.3 (d, J_{CF} = 245)
		148.1 (d, J_{CF} = 242)
$Cp^*_2Ta(NH^tBu)(H)[B(C_6F_5)_4]$	$\boldsymbol{C}_5(CH_3)_5$	118.4
	$(\boldsymbol{C}H_3)_3C$	34.0
	$C_5(\boldsymbol{C}H_3)_5$	12.1
	$(CH_3)_3\boldsymbol{C}$	64.3
$Cp^*_2Ta(NH^tBu)(Cl)[B(C_6F_5)_4]$	$\boldsymbol{C}_5(CH_3)_5$	124.5
	$(\boldsymbol{C}H_3)_3C$	31.9
	$C_5(\boldsymbol{C}H_3)_5$	11.9
	$(CH_3)_3\boldsymbol{C}$	65.5
$Cp^*_2Ta(NCO)(OH)[B(C_6F_5)_4]$	$\boldsymbol{C}_5(CH_3)_5$	126.0
	$C_5(\boldsymbol{C}H_3)_5$	10.9
	$N\boldsymbol{C}O$	140.8
$Cp^*_2Ta(OH)_2[B(C_6F_5)_4]$	$\boldsymbol{C}_5(CH_3)_5$	124.1
	$C_5(\boldsymbol{C}H_3)_5$	10.5
$Cp^*_2Ta(NH^tBu)(CCPh)[B(C_6F_5)_4]$	$\boldsymbol{C}_5(CH_3)_5$	122.0
	$(\boldsymbol{C}H_3)_3C$	32.6
	$C_5(\boldsymbol{C}H_3)_5$	12.4
	$(CH_3)_3\boldsymbol{C}$	65.5

	$\boldsymbol{C}C$Ph		133.3
			124.0
	$\boldsymbol{C}_6H_5$		128.3
			128.7
			130.4
			146.5
$Cp^*_2Ta(=N^tBu)(THF)[B(C_6F_5)_4]$ + CH_3CCH	$\boldsymbol{C}_5(CH_3)_5$	[2+2]	121.9
	$(\boldsymbol{C}H_3)_3C$	[2+2]	33.4
	$C_5(\boldsymbol{C}H_3)_5$	[2+2]	11.9
	$(CH_3)_3\boldsymbol{C}$	[2+2]	61.1
	$\boldsymbol{C}_5(CH_3)_5$	C-H activation	121.9
	$(\boldsymbol{C}H_3)_3C$	C-H activation	32.6
	$C_5(\boldsymbol{C}H_3)_5$	C-H activation	12.3
	$(CH_3)_3\boldsymbol{C}$	C-H activation	64.83
	$\boldsymbol{C}\boldsymbol{C}CH_3$	C-H activation	119.7
			131.8
	$CC\boldsymbol{C}H_3$	C-H activation	11.35[c]

[a] All spectra were recorded in CD_2Cl_2. [b]The chemical shifts of the anion for all compounds in this table were within experimental error of these values. [c] Peak assignment is ambiguous due to impurities in the sample and/or low signal to noise ratio.

Table 3. Infrared Absorption Data[a]

compound	assignment	ν, cm^{-1} (intensity)
$Cp^*_2Ta(=N^tBu)(THF)[B(C_6F_5)_4]$	C-O-C or C-N[b]	1213.5 (m)
	C-O-C or Ta=N[b]	847.4 (m)
$Cp^*_2Ta(NH^tBu)(H)[B(C_6F_5)_4]$	N-H	3336 (w)
	Ta-H	1862 (w, br)
	C-N[c]	1182 (m)
$Cp^*_2Ta(NH^tBu)(Cl)[B(C_6F_5)_4]$	N-H	3355 (w)
	C-N[c]	1180.5 (m)
$Cp^*_2Ta(NCO)(OH)[B(C_6F_5)_4]$	O-H	3490.4 (w, br)
		3610.7 (w)
	C=O	2251.6 (s)
$Cp^*_2Ta(N^{13}CO)(OH)[B(C_6F_5)_4]$	$^{13}C=O$	2189.8 (s)
$Cp^*_2Ta(NH^tBu)(CCPh)[B(C_6F_5)_4]$	N-H	3341.9 (w)
	C≡C	2097.5 (w)
	C-N[c]	1183.7 (m)
$Cp^*_2Ta(=N^tBu)(THF)[B(C_6F_5)_4] + CH_3CCH$	N-H	3337.8 (w)
	C≡C	2115.1 (w)
	C-N[c]	1189.4 (m)

[a] Spectra were taken in nujol mulls [b]The indicated peaks are unique to the imido complex. The origin of the absorbances has not been determined, although by comparison to the amido complexes in this chapter, assignment as C-N and Ta-N stretches is reasonable. [c]The peak is obseved in all the amido complexes. The assignment is tentative.

References

1)Wigley, D. E. *Progress in Inorganic Chemistry* **1994**, *42*, 239-482.

2)Schaverian, C. J.; Dewan, J. C.; Schrock, R. R. *Journal of the American Chemical Society* **1986**, *108*, 2771-2773.

3)Nugent, W. A.; Mayer, J. M. *Metal-Ligand Multiple Bonds*; Wiley: New York, 1988.

4)Allain, E. J.; Hager, L. P.; Deng, L.; Jacobsen, E. N. *Journal of the American Chemical Society* **1993**, *115*, 4415.

5)Herranz, E.; Biller, S.; Sharpless, K. B. *Journal of the American Chemical Society* **1978**, *100*, 3596.

6)Walsh, P. J.; Hollander, F. J.; Bergman, R. G. *Journal of the American Chemical Society* **1988**, *110*, 8729.

7)Cummins, C. C.; Baxter, S. M.; Wolczanski, P. T. *Journal of the American Chemical Society* **1988**, *110*, 8731.

8)Huber, S. R.; Baldwin, T. C.; Wigley, D. E. *Organometallics* **1993**, *12*, 91.

9)Cundari, T. R. *Journal of the American Chemical Society* **1992**, *114*, 7879.

10)Strauss, S. H. *Chemical Reviews* **1993**, *93*, 927.

11)Chien, J. C. W.; Tsai, W.-M.; Rausch, M. D. *Journal of the American Chemical Society* **1991**, *113*, 8570.

12)Nelson, J. E.; Parkin, G.; Bercaw, J. E. *Organometallics* **1991**, *11*, 2181.

13)Antonelli, D. M.; Schaefer, W. P.; Parkin, G.; Bercaw, J. E. *Journal of Organometallic Chemistry* **1993**, *462*, 213.

14)Thompson, M. E.; Baxter, S. M.; Bulls, A. R.; Burger, B. J.; Nolan, M. C.; Santarsiero, B. D.; Schaefer, W. P.; Bercaw, J. E. *Journal of the American Chemical Society* **1987**, *109*, 203.

Appendix 2: X-Ray Structure Data for Cp^*_2Ta Complexes

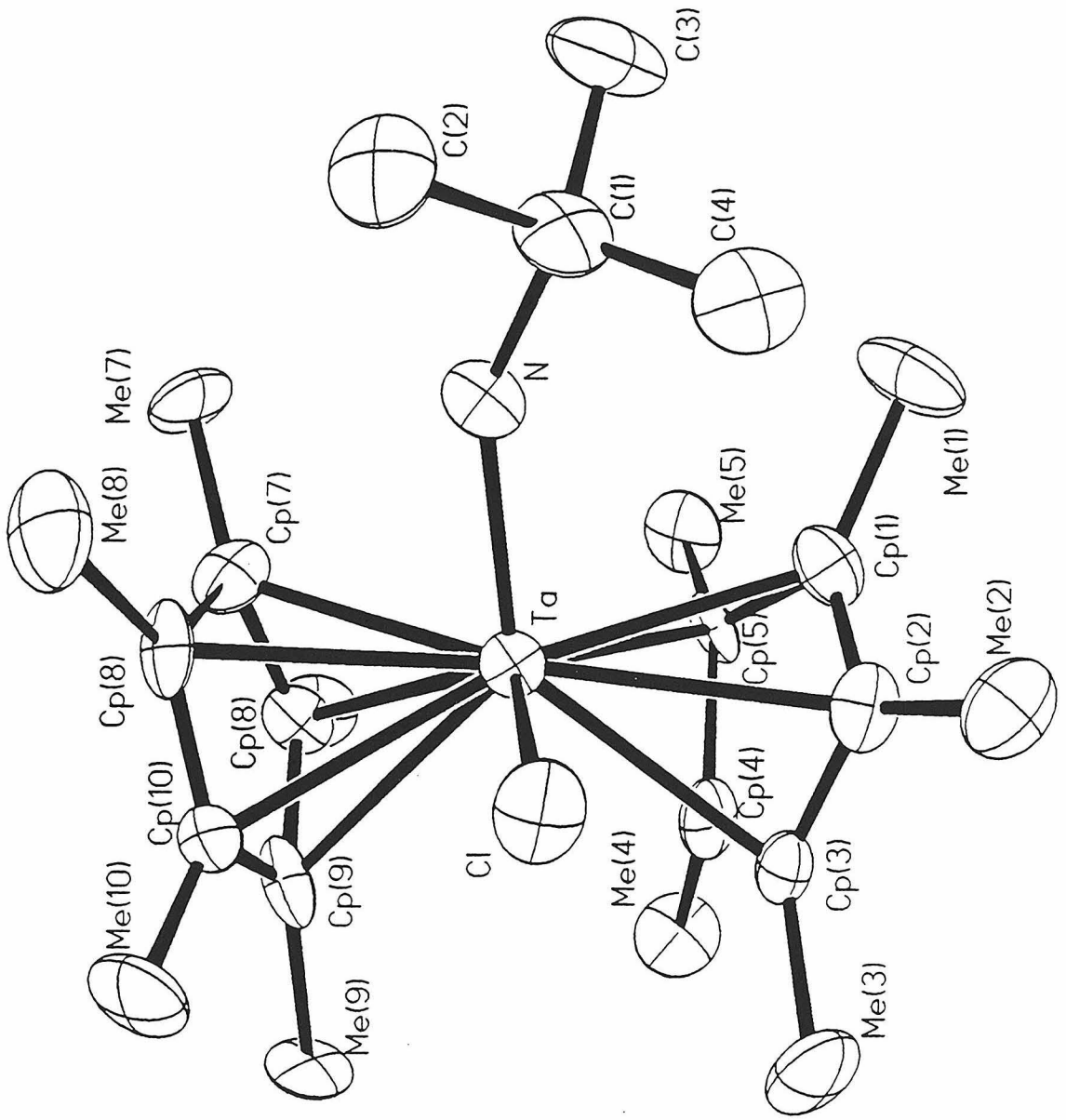

Figure 1: ORTEP diagram of the structure of $Cp^*_2Ta(NH^tBu)(Cl)[B(C_6F_5)_4]$

Table 1: Crystal and Intensity Data for $Cp^*_2Ta(NH^tBu)Cl[B(C_6F_5)_4]$

chemical formula	$C_{48}H_{40}BClF_{20}NTa$
crystal dimension, mm	0.15 x 0.04 x 0.37
crystal system	monoclinic
space group	$P2_1/c$
a, Å	15.200(3)
b, Å	16.540(4)
c, Å	18.702(4)
β, deg	92.30(3)
V, Å^3	4698(2)
ρ_{calc}, gcm^{-3}	1.750
Z	4
λ, Å	0.71073
μ, mm^{-1}	2.513
temp, °K	293(2)
2θ range, deg	2.6 to 40
no. of reflections measured, total	8948
R	0.0498
GOF	1.28

Table 2. Final Heavy Atom Parameters for $Cp^*_2Ta(NH^tBu)Cl[B(C_6F_5)_4$.

U(eq) is defined as one third of the trace of the orthogonalized Uij tensor.

	x	y	z	U(eq)
Ta	1107(1)	1933(1)	2309(1)	55(1)
CP1	-1029(22)	2096(16)	1969(25)	94(8)
CP2	-436(23)	1606(21)	1384(13)	88(9)
CP3	-89(15)	780(17)	1865(16)	80(6)
CP4	-428(19)	819(16)	2746(12)	65(6)
CP5	-1107(19)	1650(21)	2789(18)	82(7)
CP6	3373(16)	2109(14)	2009(15)	68(6)
CP7	3125(16)	1311(18)	1746(11)	68(6)
CP8	2713(16)	687(13)	2490(15)	64(5)
CP9	2597(16)	1113(14)	3222(11)	58(5)
CP10	3111(16)	1951(15)	2927(13)	62(6)
ME1	-1755(23)	3010(16)	1596(22)	239(19)
ME2	-247(22)	1700(17)	351(13)	167(12)
ME3	334(19)	-107(15)	1453(15)	151(11)
ME4	-467(18)	1(15)	3495(13)	135(9)
ME5	-1779(20)	1919(18)	3616(15)	205(16)
ME6	4012(17)	2886(14)	1421(13)	128(9)
ME7	3458(18)	1087(17)	804(12)	150(11)
ME8	2736(18)	-336(13)	2546(14)	124(8)
ME9	2390(17)	713(12)	4196(10)	93(7)
ME10	3533(18)	2533(13)	3553(13)	118(8)
N	586(17)	3052(11)	2734(12)	125(6)
C(1)	699(29)	4010(17)	3007(18)	126(9)
C(2)	-393(25)	4579(18)	2694(23)	239(18)
C(3)	638(24)	3873(17)	4046(19)	181(12)
C(4)	1906(21)	4440(15)	2489(17)	149(11)
B	3274(17)	2478(12)	7209(11)	43(5)
C(10)	1739(15)	2633(10)	7299(11)	44(4)
C(11)	957(20)	2931(11)	7997(12)	56(5)
C(12)	-312(22)	3007(14)	8051(13)	70(6)
C(13)	-926(19)	2811(13)	7411(17)	76(7)
C(14)	-244(21)	2491(13)	6707(15)	71(6)
C(15)	1052(19)	2429(10)	6650(11)	56(5)
C(20)	3976(15)	2924(13)	7927(9)	40(4)
C(21)	3814(16)	3825(16)	7959(11)	59(5)
C(22)	4428(23)	4306(17)	8459(14)	75(7)
C(23)	5279(22)	3834(21)	8961(13)	80(7)
C(24)	5550(18)	2940(17)	8958(12)	64(6)

C(25)	4879(17)	2508(14)	8458(11)	55(5)
C(30)	3934(16)	3004(11)	6214(10)	44(4)
C(31)	3419(18)	3677(13)	5633(12)	54(5)
C(32)	4029(23)	4145(14)	4839(13)	67(6)
C(33)	5267(28)	3904(15)	4665(12)	74(7)
C(34)	5885(19)	3277(15)	5214(15)	65(5)
C(35)	5188(20)	2844(11)	5986(12)	51(5)
C(40)	3472(15)	1402(12)	7306(12)	50(5)
C(41)	3101(16)	909(13)	8146(13)	57(5)
C(42)	3225(16)	-26(17)	8300(13)	68(5)
C(43)	3703(17)	-516(13)	7601(18)	71(6)
C(44)	4019(15)	-44(16)	6775(15)	65(5)
C(45)	3915(15)	864(14)	6657(12)	51(5)
F(11)	1448(8)	3147(6)	8687(6)	69(3)
F(12)	-1028(9)	3298(7)	8726(7)	96(4)
F(13)	-2176(10)	2845(8)	7398(7)	110(4)
F(14)	-765(9)	2246(7)	6019(7)	95(3)
F(15)	1719(8)	2106(6)	5918(6)	69(3)
F(21)	2953(9)	4332(6)	7461(6)	71(3)
F(22)	4168(12)	5199(8)	8429(7)	111(4)
F(23)	5890(11)	4277(8)	9460(7)	121(4)
F(24)	6385(10)	2488(8)	9470(6)	98(4)
F(25)	5223(8)	1624(7)	8489(5)	71(3)
F(31)	2192(10)	3975(6)	5779(6)	77(3)
F(32)	3456(11)	4772(8)	4301(7)	99(4)
F(33)	5930(11)	4310(7)	3891(6)	113(4)
F(34)	7135(11)	3058(7)	5050(6)	104(4)
F(35)	5886(8)	2227(7)	6518(6)	68(3)
F(41)	2623(9)	1307(7)	8823(6)	75(3)
F(42)	2887(10)	-500(7)	9132(7)	99(4)
F(43)	3812(9)	-1446(7)	7782(7)	104(4)
F(44)	4447(9)	-525(6)	6112(7)	95(4)
F(45)	4238(8)	1245(6)	5799(6)	72(3)

Table 3. Assigned Hydrogen Atom Parameters for $Cp^*_2Ta(NH^tBu)Cl[B(C_6F_5)_4]$.

	x	y	z	U(eq)
H(1A)	-1504(23)	3169(16)	967(22)	358
H(1B)	-1557(23)	3480(16)	1900(22)	358
H(1C)	-2645(23)	2937(16)	1693(22)	358
H(2A)	256(22)	1189(17)	180(13)	250
H(2B)	171(22)	2242(17)	104(13)	250
H(2C)	-1052(22)	1728(17)	128(13)	250
H(3A)	526(19)	48(15)	818(15)	226
H(3B)	-336(19)	-513(15)	1583(15)	226
H(3C)	1068(19)	-393(15)	1710(15)	226
H(4A)	-735(18)	197(15)	4057(13)	203
H(4B)	358(18)	-296(15)	3512(13)	203
H(4C)	-1047(18)	-410(15)	3384(13)	203
H(5A)	-1656(20)	1449(18)	4112(15)	307
H(5B)	-2662(20)	2019(18)	3553(15)	307
H(5C)	-1456(20)	2464(18)	3719(15)	307
H(6A)	4056(17)	2806(14)	807(13)	191
H(6B)	4847(17)	2907(14)	1580(13)	191
H(6C)	3539(17)	3440(14)	1500(13)	191
H(7A)	3193(18)	497(17)	786(12)	225
H(7B)	4352(18)	1098(17)	647(12)	225
H(7C)	3038(18)	1523(17)	388(12)	225
H(8A)	2823(18)	-483(13)	1954(14)	187
H(8B)	1966(18)	-555(13)	2867(14)	187
H(8C)	3434(18)	-612(13)	2852(14)	187
H(9A)	2350(17)	1183(12)	4552(10)	139
H(9B)	3073(17)	285(12)	4345(10)	139
H(9C)	1613(17)	415(12)	4312(10)	139
H(1D)	3243(18)	2294(13)	4161(13)	177
H(1E)	3186(18)	3140(13)	3408(13)	177
H(1F)	4436(18)	2532(13)	3484(13)	177
H(2D)	-1155(25)	4332(18)	3000(23)	359
H(2E)	-390(25)	4597(18)	2063(23)	359
H(2F) -	344(25)	5179(18)	2815(23)	359
H(3D)	1359(24)	3504(17)	4235(19)	271
H(3E)	-116(24)	3582(17)	4305(19)	271
H(3F)	633(24)	4448(17)	4236(19)	271
H(4D)	2638(21)	4087(15)	2680(17)	224
H(4E)	1932(21)	5043(15)	2607(17)	224
H(4F)	1890(21)	4454(15)	1859(17)	224

Table 4. Anisotropic Displacement Parameters for $Cp^*_2Ta(NH^tBu)Cl[B(C_6F_5)_4]$.
The anisotropic displacement factor exponent takes the form:
$-2\pi^2 [h^2 a^{*2} U11 + ... + 2 h k a^* b^* U12]$

	U11	U22	U33	U23	U13	U12
Ta	49(1)	63(1)	53(1)	-10(1)	-7(1)	-7(1)
CP1	73(18)	70(20)	140(27)	-24(19)	1(19)	-17(14)
CP2	88(19)	121(23)	51(16)	55(16)	-50(14)	-59(17)
CP3	37(12)	131(22)	82(17)	-37(17)	-4(12)	-39(13)
CP4	69(15)	90(17)	35(13)	9(12)	-11(11)	-24(14)
CP5	45(14)	110(23)	101(20)	-57(18)	29(14)	-26(15)
CP6	40(12)	74(16)	88(18)	-2(14)	-11(12)	-12(11)
CP7	39(12)	126(20)	44(13)	-35(14)	-7(10)	14(13)
CP8	55(13)	69(16)	77(15)	-27(14)	-9(11)	-15(11)
CP9	65(13)	66(14)	41(13)	-1(12)	3(9)	-21(11)
CP10	50(13)	94(18)	51(13)	-43(13)	-14(10)	17(12)
ME1	124(24)	80(21)	514(57)	54(27)	-171(31)	-31(18)
ME2	172(25)	247(32)	83(17)	39(18)	-54(16)	-99(23)
ME3	105(19)	173(25)	219(27)	-160(23)	1(18)	-34(18)
ME4	81(17)	183(26)	132(19)	34(19)	-36(15)	-44(17)
ME5	117(20)	347(39)	203(26)	-238(29)	101(20)	-106(23)
ME6	74(16)	129(20)	145(19)	68(16)	12(14)	-26(15)
ME7	78(16)	313(35)	75(15)	-90(19)	-8(13)	15(19)
ME8	81(16)	85(18)	220(25)	-47(17)	-51(16)	17(14)
ME9	90(16)	128(19)	53(13)	3(12)	-8(11)	-7(14)
ME10	103(18)	106(18)	170(21)	-63(16)	-63(16)	5(15)
N	138(17)	55(12)	187(18)	-9(12)	-67(14)	13(12)
C(1)	165(29)	89(21)	129(21)	-14(17)	-59(21)	18(21)
C(2)	125(26)	117(26)	464(55)	-3(29)	-82(31)	53(21)
C(3)	173(28)	180(29)	220(32)	-106(26)	-45(25)	-3(23)
C(4)	93(20)	103(21)	253(31)	-11(20)	-26(20)	-39(17)
B	46(14)	45(14)	36(11)	-6(10)	1(10)	-2(11)
C(10)	48(12)	38(11)	46(11)	-2(9)	-10(11)	-13(9)
C(11)	50(15)	66(14)	49(13)	5(10)	-11(12)	-9(11)
C(12)	61(19)	105(17)	46(14)	-19(12)	-7(13)	-12(14)
C(13)	35(15)	77(17)	97(20)	7(13)	35(15)	10(13)
C(14)	54(16)	69(15)	100(18)	7(12)	-58(15)	-31(13)
C(15)	74(16)	43(12)	52(12)	-9(9)	-9(12)	-6(11)
C(20)	36(11)	40(13)	38(12)	-4(10)	11(9)	0(10)
C(21)	41(13)	88(18)	38(12)	9(12)	2(10)	11(13)
C(22)	82(18)	96(21)	61(15)	-42(16)	-3(13)	-30(17)
C(23)	72(17)	130(26)	56(14)	-46(16)	-5(12)	-49(18)

C(24)	49(14)	95(20)	58(14)	-35(14)	-10(11)	-11(14)
C(25)	46(13)	77(16)	40(11)	-10(12)	2(10)	11(13)
C(30)	28(12)	54(13)	54(12)	-26(10)	-8(10)	6(10)
C(31)	47(13)	67(14)	49(13)	-13(11)	-12(12)	0(12)
C(32)	80(18)	79(17)	43(15)	-12(13)	7(14)	-26(15)
C(33)	124(23)	67(16)	31(13)	-11(12)	19(16)	-50(17)
C(34)	52(15)	72(16)	73(16)	-29(13)	9(14)	-12(13)
C(35)	71(16)	38(12)	48(13)	-10(10)	-14(12)	-5(12)
C(40)	50(12)	56(14)	47(12)	-17(12)	-1(10)	-8(11)
C(41)	45(12)	47(15)	78(17)	18(13)	-24(11)	-24(11)
C(42)	49(13)	87(19)	65(15)	9(15)	-12(11)	-17(13)
C(43)	49(13)	41(15)	126(20)	-1(16)	-35(13)	-10(12)
C(44)	38(12)	70(19)	89(17)	-21(15)	-1(11)	-14(12)
C(45)	46(12)	48(15)	58(14)	8(12)	-10(10)	-23(11)
F(11)	61(7)	95(8)	55(6)	-23(6)	1(5)	-9(6)
F(12)	70(8)	129(10)	79(8)	-13(7)	18(6)	1(7)
F(13)	41(8)	149(12)	139(10)	-21(8)	-6(7)	-5(7)
F(14)	66(7)	115(9)	111(9)	-21(7)	-28(7)	-17(7)
F(15)	65(7)	77(7)	72(7)	-20(6)	-18(6)	-3(6)
F(21)	85(8)	56(7)	72(7)	-16(5)	0(6)	-6(6)
F(22)	152(12)	69(9)	127(10)	-45(8)	-20(8)	-25(8)
F(23)	126(10)	148(11)	112(9)	-59(8)	-30(8)	-46(9)
F(24)	77(8)	150(11)	77(7)	-29(7)	-37(7)	-5(8)
F(25)	62(7)	86(8)	66(7)	-19(6)	-19(5)	11(6)
F(31)	74(8)	75(8)	75(7)	5(6)	-19(6)	2(6)
F(32)	138(11)	89(9)	67(7)	23(6)	-31(7)	-29(8)
F(33)	152(11)	122(10)	66(7)	-19(7)	26(7)	-67(9)
F(34)	85(9)	129(10)	96(8)	-40(7)	40(7)	-24(8)
F(35)	55(7)	84(8)	68(7)	-29(6)	9(5)	-4(6)
F(41)	91(8)	89(8)	40(6)	-11(6)	3(5)	2(6)
F(42)	99(9)	83(8)	105(8)	27(7)	-16(7)	-22(7)
F(43)	77(8)	48(8)	188(11)	-7(7)	-32(7)	-9(7)
F(44)	90(8)	77(8)	132(9)	-59(7)	-7(7)	-1(7)
F(45)	76(7)	78(7)	67(7)	-33(6)	-1(6)	-8(6)

Table 3. Complete Distances and Angles for $Cp^*_2Ta(NH^tBu)Cl[B(C_6F_5)_4]$.

Ta-N	1.93(2)
Ta-CP9	2.38(2)
Ta-CP1	2.39(2)
Ta-CP4	2.40(2)
Ta-CP7	2.41(2)
Ta-CP2	2.43(2)
Ta-CP6	2.44(2)
Ta-CP5	2.45(2)
Ta-CP8	2.45(2)
Ta-CP10	2.45(2)
Ta-CP3	2.47(2)
CP1-CP5	1.31(3)
CP1-CP2	1.33(3)
CP1-ME1	1.58(3)
CP2-CP3	1.38(3)
CP2-ME2	1.55(2)
CP3-CP4	1.36(2)
CP3-ME3	1.58(2)
CP4-CP5	1.41(3)
CP4-ME4	1.53(2)
CP5-ME5	1.48(2)
CP6-CP10	1.38(2)
CP6-CP7	1.39(2)
CP6-ME6	1.51(2)
CP7-CP8	1.40(2)
CP7-ME7	1.53(2)
CP8-CP9	1.37(2)
CP8-ME8	1.53(2)
CP9-CP10	1.40(2)
CP9-ME9	1.50(2)
CP10-ME10	1.53(2)
ME1-H(1A)	0.96
ME1-H(1B)	0.96
ME1-H(1C)	0.96
ME2-H(2A)	0.96
ME2-H(2B)	0.96
ME2-H(2C)	0.96
ME3-H(3A)	0.96
ME3-H(3B)	0.96
ME3-H(3C)	0.96
ME4-H(4A)	0.96
ME4-H(4B)	0.96
ME4-H(4C)	0.96
ME5-H(5A)	0.96
ME5-H(5B)	0.96
ME5-H(5C)	0.96
ME6-H(6A)	0.96
ME6-H(6B)	0.96
ME6-H(6C)	0.96
ME7-H(7A)	0.96

ME7-H(7B)	0.96
ME7-H(7C)	0.96
ME8-H(8A)	0.96
ME8-H(8B)	0.96
ME8-H(8C)	0.96
ME9-H(9A)	0.96
ME9-H(9B)	0.96
ME9-H(9C)	0.96
ME10-H(1D)	0.96
ME10-H(1E)	0.96
ME10-H(1F)	0.96
N-C(1)	1.59(3)
C(1)-C(2)	1.47(3)
C(1)-C(4)	1.56(3)
C(1)-C(3)	1.56(3)
C(2)-H(2D)	0.96
C(2)-H(2E)	0.96
C(2)-H(2F)	0.96
C(3)-H(3D)	0.96
C(3)-H(3E)	0.96
C(3)-H(3F)	0.96
C(4)-H(4D)	0.96
C(4)-H(4E)	0.96
C(4)-H(4F)	0.96
B-C(40)	1.60(2)
B-C(10)	1.64(2)
B-C(20)	1.66(2)
B-C(30)	1.69(2)
C(10)-C(11)	1.39(2)
C(10)-C(15)	1.39(2)
C(11)-F(11)	1.33(2)
C(11)-C(12)	1.35(2)
C(12)-F(12)	1.33(2)
C(12)-C(13)	1.33(3)
C(13)-F(13)	1.34(2)
C(13)-C(14)	1.36(2)
C(14)-F(14)	1.36(2)
C(14)-C(15)	1.38(2)
C(15)-F(15)	1.39(2)
C(20)-C(21)	1.36(2)
C(20)-C(25)	1.38(2)
C(21)-F(21)	1.37(2)
C(21)-C(22)	1.39(2)
C(22)-F(22)	1.35(2)
C(22)-C(23)	1.34(3)
C(23)-F(23)	1.35(2)
C(23)-C(24)	1.36(3)
C(24)-F(24)	1.33(2)
C(24)-C(25)	1.38(2)
C(25)-F(25)	1.35(2)
C(30)-C(35)	1.36(2)
C(30)-C(31)	1.36(2)
C(31)-F(31)	1.36(2)
C(31)-C(32)	1.41(2)

C(32)-F(32)	1.31(2)
C(32)-C(33)	1.35(3)
C(33)-C(34)	1.34(2)
C(33)-F(33)	1.38(2)
C(34)-F(34)	1.36(2)
C(34)-C(35)	1.41(2)
C(35)-F(35)	1.37(2)
C(40)-C(45)	1.40(2)
C(40)-C(41)	1.40(2)
C(41)-F(41)	1.31(2)
C(41)-C(42)	1.39(2)
C(42)-F(42)	1.37(2)
C(42)-C(43)	1.42(2)
C(43)-C(44)	1.36(2)
C(43)-F(43)	1.38(2)
C(44)-C(45)	1.35(2)
C(44)-F(44)	1.36(2)
C(45)-F(45)	1.35(2)

N-Ta-CP9	109.2(7)
N-Ta-CP1	80.3(8)
CP9-Ta-CP1	146.5(9)
N-Ta-CP4	112.8(8)
CP9-Ta-CP4	93.6(7)
CP1-Ta-CP4	54.1(7)
N-Ta-CP7	132.6(8)
CP9-Ta-CP7	55.6(5)
CP1-Ta-CP7	139.4(9)
CP4-Ta-CP7	112.8(9)
N-Ta-CP2	108.9(10)
CP9-Ta-CP2	137.7(9)
CP1-Ta-CP2	31.9(7)
CP4-Ta-CP2	54.6(6)
CP7-Ta-CP2	107.5(9)
N-Ta-CP6	99.5(8)
CP9-Ta-CP6	56.8(6)
CP1-Ta-CP6	155.6(10)
CP4-Ta-CP6	142.6(8)
CP7-Ta-CP6	33.2(5)
CP2-Ta-CP6	132.1(8)
N-Ta-CP5	81.3(8)
CP9-Ta-CP5	116.3(9)
CP1-Ta-CP5	31.5(7)
CP4-Ta-CP5	33.7(6)
CP7-Ta-CP5	145.9(9)
CP2-Ta-CP5	53.4(7)
CP6-Ta-CP5	172.9(9)
N-Ta-CP8	140.7(7)
CP9-Ta-CP8	32.9(5)
CP1-Ta-CP8	135.6(7)
CP4-Ta-CP8	87.0(7)
CP7-Ta-CP8	33.4(5)
CP2-Ta-CP8	110.2(10)
CP6-Ta-CP8	55.6(6)

CP5-Ta-CP8	119.7(9)
N-Ta-CP10	88.5(7)
CP9-Ta-CP10	33.6(5)
CP1-Ta-CP10	167.2(8)
CP4-Ta-CP10	126.7(7)
CP7-Ta-CP10	53.4(5)
CP2-Ta-CP10	160.8(9)
CP6-Ta-CP10	32.7(5)
CP5-Ta-CP10	140.7(8)
CP8-Ta-CP10	53.6(6)
N-Ta-CP3	132.2(7)
CP9-Ta-CP3	105.4(8)
CP1-Ta-CP3	53.2(7)
CP4-Ta-CP3	32.5(5)
CP7-Ta-CP3	94.3(7)
CP2-Ta-CP3	32.8(6)
CP6-Ta-CP3	127.2(7)
CP5-Ta-CP3	53.8(6)
CP8-Ta-CP3	82.6(7)
CP10-Ta-CP3	135.9(8)
CP5-CP1-CP2	112(3)
CP5-CP1-ME1	129(3)
CP2-CP1-ME1	118(3)
CP5-CP1-Ta	77(2)
CP2-CP1-Ta	75.5(14)
ME1-CP1-Ta	126(2)
CP1-CP2-CP3	107(2)
CP1-CP2-ME2	135(3)
CP3-CP2-ME2	117(3)
CP1-CP2-Ta	72.5(14)
CP3-CP2-Ta	75.1(10)
ME2-CP2-Ta	125.3(13)
CP4-CP3-CP2	108(2)
CP4-CP3-ME3	126(3)
CP2-CP3-ME3	125(3)
CP4-CP3-Ta	71.1(10)
CP2-CP3-Ta	72.1(11)
ME3-CP3-Ta	132.5(12)
CP3-CP4-CP5	107(2)
CP3-CP4-ME4	125(3)
CP5-CP4-ME4	125(2)
CP3-CP4-Ta	76.5(10)
CP5-CP4-Ta	75.0(11)
ME4-CP4-Ta	130.2(12)
CP1-CP5-CP4	106(2)
CP1-CP5-ME5	129(3)
CP4-CP5-ME5	125(3)
CP1-CP5-Ta	72.0(13)
CP4-CP5-Ta	71.3(11)
ME5-CP5-Ta	122.5(13)
CP10-CP6-CP7	104(2)
CP10-CP6-ME6	129(2)
CP7-CP6-ME6	126(2)
CP10-CP6-Ta	74.0(10)

CP7-CP6-Ta	72.1(10)
ME6-CP6-Ta	126.6(12)
CP6-CP7-CP8	110(2)
CP6-CP7-ME7	125(2)
CP8-CP7-ME7	124(2)
CP6-CP7-Ta	74.8(10)
CP8-CP7-Ta	74.9(10)
ME7-CP7-Ta	125.0(11)
CP9-CP8-CP7	108(2)
CP9-CP8-ME8	124(2)
CP7-CP8-ME8	127(2)
CP9-CP8-Ta	70.7(10)
CP7-CP8-Ta	71.7(10)
ME8-CP8-Ta	135.5(12)
CP8-CP9-CP10	105.9(14)
CP8-CP9-ME9	129(2)
CP10-CP9-ME9	122(2)
CP8-CP9-Ta	76.3(11)
CP10-CP9-Ta	76.0(10)
ME9-CP9-Ta	128.0(12)
CP6-CP10-CP9	111(2)
CP6-CP10-ME10	124(2)
CP9-CP10-ME10	124(2)
CP6-CP10-Ta	73.3(10)
CP9-CP10-Ta	70.4(10)
ME10-CP10-Ta	131.6(11)
CP1-ME1-H(1A)	110(2)
CP1-ME1-H(1B)	110(2)
H(1A)-ME1-H(1B)	109.5
CP1-ME1-H(1C)	109.5(12)
H(1A)-ME1-H(1C)	109.5
H(1B)-ME1-H(1C)	109.5
CP2-ME2-H(2A)	110(2)
CP2-ME2-H(2B)	109.5(12)
H(2A)-ME2-H(2B)	109.5
CP2-ME2-H(2C)	109.5(12)
H(2A)-ME2-H(2C)	109.5
H(2B)-ME2-H(2C)	109.5
CP3-ME3-H(3A)	109.5(14)
CP3-ME3-H(3B)	109.5(10)
H(3A)-ME3-H(3B)	109.5
CP3-ME3-H(3C)	109.5(11)
H(3A)-ME3-H(3C)	109.5
H(3B)-ME3-H(3C)	109.5
CP4-ME4-H(4A)	109.5(13)
CP4-ME4-H(4B)	109.5(11)
H(4A)-ME4-H(4B)	109.5
CP4-ME4-H(4C)	109.5(10)
H(4A)-ME4-H(4C)	109.5
H(4B)-ME4-H(4C)	109.5
CP5-ME5-H(5A)	110(2)
CP5-ME5-H(5B)	109.5(13)
H(5A)-ME5-H(5B)	109.5
CP5-ME5-H(5C)	109.5(12)

H(5A)-ME5-H(5C)	109.5
H(5B)-ME5-H(5C)	109.5
CP6-ME6-H(6A)	109.5(13)
CP6-ME6-H(6B)	109.5(10)
H(6A)-ME6-H(6B)	109.5
CP6-ME6-H(6C)	109.5(11)
H(6A)-ME6-H(6C)	109.5
H(6B)-ME6-H(6C)	109.5
CP7-ME7-H(7A)	109.5(14)
CP7-ME7-H(7B)	109.5(10)
H(7A)-ME7-H(7B)	109.5
CP7-ME7-H(7C)	109.5(11)
H(7A)-ME7-H(7C)	109.5
H(7B)-ME7-H(7C)	109.5
CP8-ME8-H(8A)	109.5(12)
CP8-ME8-H(8B)	109.5(10)
H(8A)-ME8-H(8B)	109.5
CP8-ME8-H(8C)	109.5(10)
H(8A)-ME8-H(8C)	109.5
H(8B)-ME8-H(8C)	109.5
CP9-ME9-H(9A)	109.5(11)
CP9-ME9-H(9B)	109.5(10)
H(9A)-ME9-H(9B)	109.5
CP9-ME9-H(9C)	109.5(10)
H(9A)-ME9-H(9C)	109.5
H(9B)-ME9-H(9C)	109.5
CP10-ME10-H(1D)	109.5(12)
CP10-ME10-H(1E)	109.5(10)
H(1D)-ME10-H(1E)	109.5
CP10-ME10-H(1F)	109.5(10)
H(1D)-ME10-H(1F)	109.5
H(1E)-ME10-H(1F)	109.5
C(1)-N-Ta	159(2)
C(2)-C(1)-C(4)	107(2)
C(2)-C(1)-C(3)	111(3)
C(4)-C(1)-C(3)	115(2)
C(2)-C(1)-N	106(2)
C(4)-C(1)-N	109(2)
C(3)-C(1)-N	107(2)
C(1)-C(2)-H(2D)	110(2)
C(1)-C(2)-H(2E)	109(2)
H(2D)-C(2)-H(2E)	109.5
C(1)-C(2)-H(2F)	110(2)
H(2D)-C(2)-H(2F)	109.5
H(2E)-C(2)-H(2F)	109.5
C(1)-C(3)-H(3D)	110(2)
C(1)-C(3)-H(3E)	110(2)
H(3D)-C(3)-H(3E)	109.5
C(1)-C(3)-H(3F)	109.5(13)
H(3D)-C(3)-H(3F)	109.5
H(3E)-C(3)-H(3F)	109.5
C(1)-C(4)-H(4D)	109.5(13)
C(1)-C(4)-H(4E)	109.5(13)
H(4D)-C(4)-H(4E)	109.5

C(1)-C(4)-H(4F)	109.5(14)
H(4D)-C(4)-H(4F)	109.5
H(4E)-C(4)-H(4F)	109.5
C(40)-B-C(10)	102.1(13)
C(40)-B-C(20)	114.4(14)
C(10)-B-C(20)	115.1(13)
C(40)-B-C(30)	112.1(13)
C(10)-B-C(30)	111.3(13)
C(20)-B-C(30)	102.2(12)
C(11)-C(10)-C(15)	112(2)
C(11)-C(10)-B	128(2)
C(15)-C(10)-B	121(2)
F(11)-C(11)-C(12)	115(2)
F(11)-C(11)-C(10)	120(2)
C(12)-C(11)-C(10)	125(2)
F(12)-C(12)-C(13)	115(2)
F(12)-C(12)-C(11)	123(2)
C(13)-C(12)-C(11)	122(2)
C(12)-C(13)-F(13)	127(2)
C(12)-C(13)-C(14)	118(2)
F(13)-C(13)-C(14)	115(3)
F(14)-C(14)-C(13)	124(2)
F(14)-C(14)-C(15)	116(2)
C(13)-C(14)-C(15)	120(2)
C(14)-C(15)-C(10)	124(2)
C(14)-C(15)-F(15)	118(2)
C(10)-C(15)-F(15)	118(2)
C(21)-C(20)-C(25)	112(2)
C(21)-C(20)-B	121(2)
C(25)-C(20)-B	127(2)
C(20)-C(21)-F(21)	119(2)
C(20)-C(21)-C(22)	127(2)
F(21)-C(21)-C(22)	115(2)
F(22)-C(22)-C(23)	123(2)
F(22)-C(22)-C(21)	121(3)
C(23)-C(22)-C(21)	116(2)
F(23)-C(23)-C(22)	118(3)
F(23)-C(23)-C(24)	120(3)
C(22)-C(23)-C(24)	122(2)
F(24)-C(24)-C(23)	120(2)
F(24)-C(24)-C(25)	121(2)
C(23)-C(24)-C(25)	118(2)
F(25)-C(25)-C(24)	114(2)
F(25)-C(25)-C(20)	121(2)
C(24)-C(25)-C(20)	125(2)
C(35)-C(30)-C(31)	112(2)
C(35)-C(30)-B	119(2)
C(31)-C(30)-B	129(2)
F(31)-C(31)-C(30)	121(2)
F(31)-C(31)-C(32)	112(2)
C(30)-C(31)-C(32)	127(2)
F(32)-C(32)-C(33)	122(2)
F(32)-C(32)-C(31)	123(2)
C(33)-C(32)-C(31)	115(2)

C(34)-C(33)-C(32)	123(2)
C(34)-C(33)-F(33)	118(3)
C(32)-C(33)-F(33)	119(2)
C(33)-C(34)-F(34)	123(2)
C(33)-C(34)-C(35)	117(2)
F(34)-C(34)-C(35)	120(2)
C(30)-C(35)-F(35)	121(2)
C(30)-C(35)-C(34)	125(2)
F(35)-C(35)-C(34)	114(2)
C(45)-C(40)-C(41)	114(2)
C(45)-C(40)-B	130(2)
C(41)-C(40)-B	117(2)
F(41)-C(41)-C(42)	117(2)
F(41)-C(41)-C(40)	122(2)
C(42)-C(41)-C(40)	121(2)
F(42)-C(42)-C(41)	121(2)
F(42)-C(42)-C(43)	118(2)
C(41)-C(42)-C(43)	121(2)
C(44)-C(43)-F(43)	123(2)
C(44)-C(43)-C(42)	118(2)
F(43)-C(43)-C(42)	119(2)
C(45)-C(44)-C(43)	119(2)
C(45)-C(44)-F(44)	124(2)
C(43)-C(44)-F(44)	117(2)
C(44)-C(45)-F(45)	113(2)
C(44)-C(45)-C(40)	127(2)
F(45)-C(45)-C(40)	121(2)

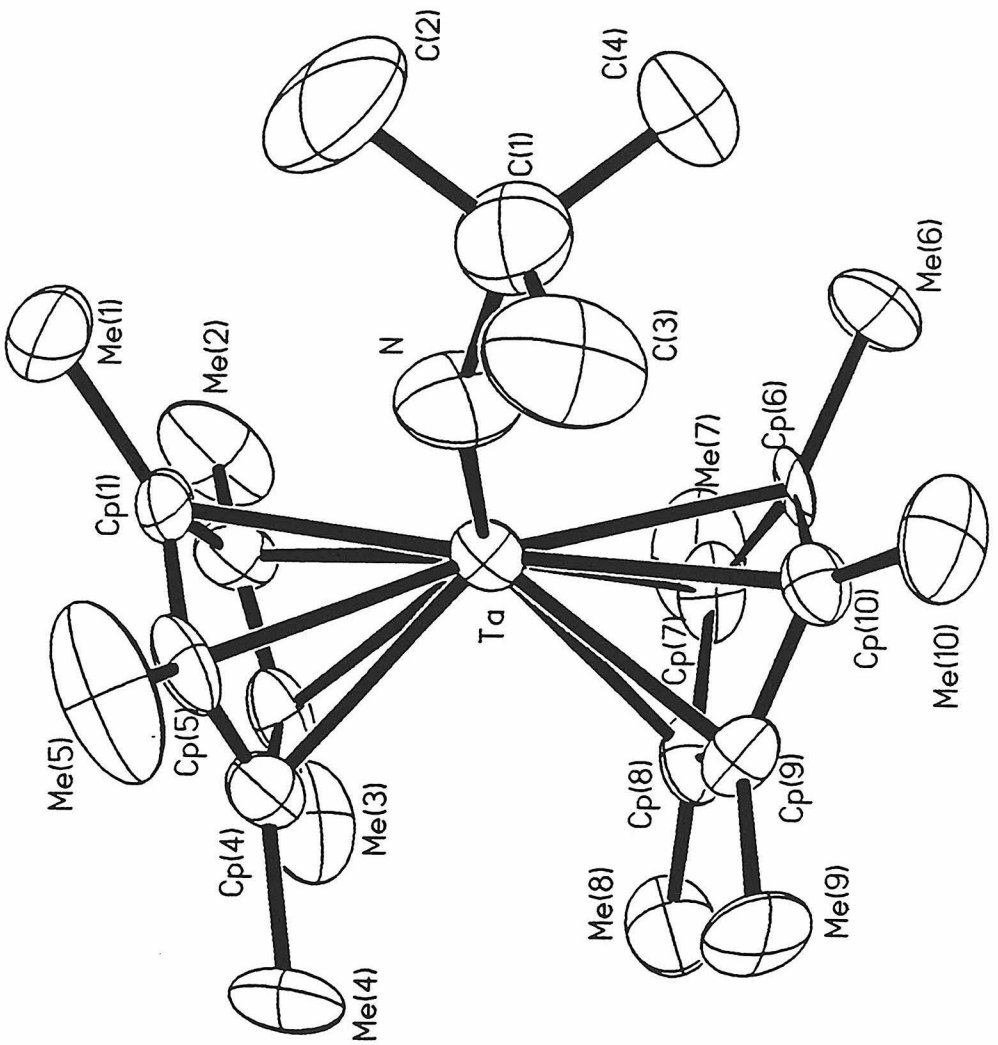

Figure 2: ORTEP diagram of the structure of $Cp^*_2Ta(NH^tBu)(H)[B(C_6F_5)_4]$

Table 6: Crystal and Intensity Data for $Cp^*_2Ta(NH^tBu)H[B(C_6F_5)_4]$

chemical formula	$C_{48}H_{41}BF_{20}NTa$
crystal dimension, mm	0.55 x 0.44 x 0.37
crystal system	triclinic
space group	P -1
a, Å	10.719(2)
b, Å	15.076(3)
c, Å	15.275(4)
α, deg	80.21(3)
β, deg	83.08(3)
γ, deg	85.50(3)
V, Å^3	2410.5(8)
ρ_{calc}, g cm^{-3}	1.658
Z	2
λ, Å	0.71073
μ, mm^{-1}	2.392
temp, °K	293(2)
2θ range, deg	2.6 to 40
no. of reflections measured, total	8034
R	0.0554
GOF	2.843

Table 7. Final Heavy Atom Parameters for $Cp^*_2Ta(NH^tBu)H[B(C_6F_5)_4$.

U(eq) is defined as one third of the trace of the orthogonalized Uij tensor.

	x	y	z	U(eq)
Ta	1575(1)	694(1)	1620(1)	44(1)
F(46)	1904(5)	6035(4)	2882(3)	60(2)
F(31)	4850(5)	4793(5)	1433(4)	70(2)
F(11)	2047(4)	4483(4)	2166(3)	57(2)
F(22)	526(5)	6947(6)	649(4)	86(3)
F(34)	4656(5)	7702(5)	141(4)	74(3)
F(15)	4893(4)	5488(4)	2772(3)	63(2)
F(13)	3961(5)	3007(5)	3670(4)	74(2)
F(12)	2351(5)	3229(4)	2993(3)	67(2)
F(21)	1760(4)	7073(4)	1677(4)	63(2)
F(26)	2987(5)	4611(4)	906(3)	62(2)
F(14)	5210(5)	4171(5)	3561(4)	84(3)
F(41)	4642(5)	7215(4)	2394(4)	66(2)
F(24)	1699(5)	4492(5)	-104(4)	86(3)
F(35)	3499(5)	7345(4)	1112(3)	62(2)
C(22)	1127(9)	6373(10)	708(8)	56(4)
C(33)	5354(9)	6432(11)	315(7)	53(4)
C(14)	4430(9)	4265(11)	3200(7)	54(4)
C(13)	3788(12)	3680(8)	3245(7)	60(5)
C(10)	3475(9)	5059(8)	2382(6)	39(3)
C(34)	4714(12)	6971(9)	480(7)	55(4)
C(20)	2441(8)	5845(8)	1363(6)	42(3)
F(33)	5962(5)	6646(5)	-161(4)	81(3)
C(40)	3265(8)	6571(7)	2555(6)	34(3)
C(25)	2393(10)	5213(9)	868(7)	50(4)
C(12)	2990(9)	3791(9)	2909(7)	48(4)
C(30)	4111(8)	6062(8)	1352(6)	38(3)
C(45)	2566(9)	6559(8)	3018(7)	48(4)
C(15)	4247(9)	4921(9)	2794(7)	48(4)
C(43)	3154(12)	7586(9)	3774(9)	62(5)
C(35)	4121(9)	6769(8)	970(7)	45(4)
C(21)	1802(10)	6421(8)	1245(7)	45(4)
C(11)	2868(8)	4449(9)	2485(6)	41(4)
C(41)	3895(10)	7131(9)	2775(7)	49(4)
C(31)	4772(9)	5555(8)	1166(6)	41(3)
B	3333(9)	5894(8)	1909(7)	44(4)

F(23)	488(5)	5689(6)	-270(4)	98(3)
F(32)	6022(5)	5182(5)	499(4)	74(3)
F(43)	3069(5)	8074(5)	4346(4)	88(3)
CP7	1948(9)	-677(9)	1980(7)	47(3)
CP6	1234(10)	-765(9)	1453(6)	54(4)
CP4	1555(9)	1622(8)	2687(7)	51(4)
C(32)	5393(9)	5694(10)	652(6)	44(3)
C(23)	1122(10)	5739(11)	258(7)	61(4)
N	2446(7)	529(7)	904(6)	88(4)
H(1)	2319	-175	889	150
CP2	1661(12)	2219(8)	1574(7)	57(4)
CP3	1064(9)	1992(8)	2123(7)	48(4)
C(1)	2868(9)	664(10)	196(6)	63(4)
CP1	2494(10)	1937(8)	1801(7)	53(4)
CP5	2428(9)	1504(7)	2451(7)	47(4)
ME8	2046(8)	-411(7)	3313(6)	69(5)
ME7	2849(9)	-1062(7)	1945(7)	80(5)
CP8	1616(9)	-336(8)	2576(7)	49(4)
ME9	-5(8)	49(8)	2948(6)	76(5)
ME10	-407(8)	-514(9)	1412(7)	94(5)
ME5	3234(8)	1241(8)	2902(6)	75(5)
C(3)	3883(8)	635(10)	277(6)	99(5)
C(24)	1736(11)	5130(9)	335(7)	54(4)
ME2	1423(10)	2776(8)	992(7)	84(5)
CP10	502(9)	-428(8)	1747(8)	61(4)
CP9	695(10)	-127(9)	2430(8)	71(5)
ME4	1287(9)	1566(8)	3443(6)	78(5)
ME6	1244(10)	-1184(8)	715(7)	94(6)
C(2)	2595(10)	-30(9)	-354(6)	104(6)
F(44)	1778(5)	7013(5)	4006(4)	88(3)
F(42)	4507(6)	8156(5)	3512(4)	89(3)
C(44)	2488(10)	7056(10)	3599(7)	57(4)
ME1	3372(9)	2174(9)	1507(7)	96(6)
ME3	135(9)	2292(9)	2155(7)	92(5)
C(4)	2508(9)	1465(8)	-87(6)	91(6)
C(42)	3870(12)	7642(9)	3362(10)	65(5)
Cl	430(2)	1016(2)	769(2)	77(1)

Table 8. Assigned Hydrogen Atom Parameters for $Cp^*_2Ta(NH^tBu)H[B(C_6F_5)_4]$.

	x	y	z	U(eq)
H(8A)	1702(8)	-126(7)	3651(6)	135(10)
H(8B)	2627(8)	-183(7)	3313(6)	135(10)
H(8C)	2084(8)	-971(7)	3445(6)	135(10)
H(7A)	2931(9)	-1258(7)	1469(7)	135(10)
H(7B)	2893(9)	-1504(7)	2277(7)	135(10)
H(7C)	3294(9)	-668(7)	2067(7)	135(10)
H(9A)	262(8)	251(8)	3386(6)	135(10)
H(9B)	-324(8)	-438(8)	3043(6)	135(10)
H(9C)	-402(8)	447(8)	2747(6)	135(10)
H(10A)	-821(8)	-237(9)	1699(7)	135(10)
H(10B)	-561(8)	-1076(9)	1381(7)	135(10)
H(10C)	-422(8)	-283(9)	940(7)	135(10)
H(5A)	3050(8)	957(8)	3318(6)	135(10)
H(5B)	3570(8)	1708(8)	3047(6)	135(10)
H(5C)	3591(8)	891(8)	2624(6)	135(10)
H(3A)	4064(8)	115(10)	457(6)	135(10)
H(3B)	4085(8)	1048(10)	605(6)	135(10)
H(3C)	4131(8)	725(10)	-180(6)	135(10)
H(2A)	796(10)	2853(8)	968(7)	135(10)
H(2B)	1607(10)	2555(8)	547(7)	135(10)
H(2C)	1709(10)	3287(8)	1077(7)	135(10)
H(4A)	1734(9)	1286(8)	3723(6)	135(10)
H(4B)	741(9)	1277(8)	3461(6)	135(10)
H(4C)	1214(9)	2101(8)	3633(6)	135(10)
H(6A)	1829(10)	-1368(8)	630(7)	135(10)
H(6B)	1059(10)	-808(8)	349(7)	135(10)
H(6C)	849(10)	-1638(8)	709(7)	135(10)
H(2D)	2820(10)	-538(9)	-179(6)	135(10)
H(2E)	2835(10)	85(9)	-810(6)	135(10)
H(2F)	1965(10)	-58(9)	-406(6)	135(10)
H(1D)	3836(9)	1888(9)	1762(7)	135(10)
H(1E)	3460(9)	2746(9)	1566(7)	135(10)
H(1F)	3377(9)	2039(9)	1008(7)	135(10)
H(3A)	-48(9)	2519(9)	1700(7)	135(10)
H(3B)	103(9)	2699(9)	2519(7)	135(10)
H(3C)	-246(9)	1850(9)	2266(7)	135(10)
H(4D)	1877(9)	1441(8)	-124(6)	135(10)
H(4E)	2733(9)	1568(8)	-550(6)	135(10)
H(4F)	2687(9)	1892(8)	235(6)	135(10)

Table 9. Anisotropic Displacement Parameters for $Cp^*_2Ta(NH^tBu)H[B(C_6F_5)_4]$.
The anisotropic displacement factor exponent takes the form:
$-2\pi^2 [h^2 a^{*2} U11 + ... + 2 h k a^* b^* U12]$

	U11	U22	U33	U23	U13	U12
Ta	43(1)	48(1)	42(1)	3(1)	-4(1)	-1(1)
F(46)	49(5)	64(6)	68(5)	-12(4)	15(4)	-9(5)
F(31)	78(6)	58(6)	77(6)	7(5)	33(5)	23(5)
F(11)	46(5)	58(6)	65(5)	2(4)	-5(4)	-19(4)
F(22)	51(6)	109(8)	97(7)	14(6)	-21(5)	-4(6)
F(34)	91(7)	71(6)	59(5)	16(5)	-8(5)	-22(5)
F(15)	42(5)	73(6)	73(5)	13(4)	-6(4)	-11(5)
F(13)	78(6)	66(6)	78(6)	20(5)	-1(5)	1(5)
F(12)	84(6)	44(5)	73(5)	6(4)	1(5)	-17(5)
F(21)	51(6)	57(5)	79(5)	3(5)	-10(4)	8(5)
F(26)	83(6)	56(6)	47(5)	-16(4)	7(4)	7(5)
F(14)	67(6)	88(7)	94(6)	31(5)	-19(5)	1(6)
F(41)	60(6)	68(6)	68(6)	-4(4)	-10(5)	-23(5)
F(24)	136(8)	75(7)	46(5)	-17(5)	-6(5)	-20(6)
F(35)	72(6)	42(5)	73(6)	6(4)	5(5)	4(5)
C(22)	24(10)	76(14)	67(11)	6(10)	-8(9)	4(9)
C(33)	29(10)	92(14)	38(10)	4(10)	-3(8)	-22(10)
C(14)	47(10)	66(11)	49(9)	11(10)	-6(8)	-15(12)
C(13)	98(15)	36(11)	47(10)	31(8)	15(10)	28(11)
C(10)	22(9)	53(10)	41(9)	-4(7)	9(7)	-3(8)
C(34)	75(13)	42(11)	49(11)	15(9)	-8(10)	-25(10)
C(20)	47(9)	39(10)	39(8)	9(8)	-3(7)	-9(9)
F(33)	80(6)	91(7)	72(6)	10(5)	27(5)	-17(5)
C(40)	17(8)	37(9)	46(9)	12(7)	-6(8)	-5(7)
C(25)	64(12)	57(11)	28(9)	5(8)	1(9)	-10(9)
C(12)	43(11)	47(11)	54(10)	11(8)	-4(8)	4(9)
C(30)	38(9)	34(9)	42(8)	4(7)	1(7)	1(8)
C(45)	31(10)	54(11)	60(11)	10(9)	-2(9)	-3(8)
C(15)	38(11)	58(12)	49(10)	1(8)	2(8)	-21(9)
C(43)	57(13)	54(12)	73(14)	-14(10)	-28(11)	12(11)
C(35)	48(11)	37(11)	50(10)	-9(8)	-13(8)	-4(9)
C(21)	59(11)	36(10)	41(9)	-1(8)	2(8)	-9(9)
C(11)	38(9)	56(12)	28(8)	-8(8)	-11(7)	-3(9)
C(41)	51(12)	44(11)	51(11)	19(9)	-4(9)	13(10)
C(31)	49(10)	33(10)	41(8)	-6(8)	-2(8)	-14(9)
B	45(10)	49(13)	38(9)	-3(8)	-7(8)	15(9)
F(23)	98(7)	114(7)	78(5)	15(6)	-37(5)	-23(7)

F(32)	57(6)	90(7)	78(6)	-20(5)	16(5)	14(5)
F(43)	107(7)	89(7)	65(5)	-37(5)	-22(5)	24(6)
CP7	56(9)	48(9)	36(8)	6(9)	-8(8)	12(10)
CP6	91(13)	31(9)	41(9)	16(8)	-7(9)	-12(10)
CP4	39(10)	50(10)	62(11)	16(8)	1(9)	-14(8)
C(32)	54(10)	44(10)	34(8)	4(9)	-1(8)	-14(10)
C(23)	79(13)	55(11)	48(10)	2(11)	-11(9)	-27(12)
CP2	94(14)	43(9)	32(9)	1(8)	-9(10)	3(11)
CP3	44(10)	48(10)	53(10)	1(8)	-11(9)	4(9)
CP1	54(11)	63(11)	41(10)	-6(8)	0(9)	-9(10)
CP5	47(11)	51(10)	41(9)	16(8)	-14(8)	-25(8)
ME8	87(12)	64(11)	56(9)	11(8)	-7(8)	5(9)
ME7	84(13)	63(11)	91(12)	7(8)	0(10)	16(10)
CP8	37(10)	71(11)	39(9)	15(8)	4(8)	-1(8)
ME9	63(11)	95(12)	73(11)	7(9)	30(9)	-20(10)
ME10	56(11)	115(15)	109(12)	16(11)	-23(9)	-40(11)
ME5	71(11)	77(11)	76(11)	-18(9)	-14(9)	-26(10)
C(3)	79(12)	135(14)	85(11)	31(12)	20(9)	-12(13)
C(24)	74(12)	51(12)	36(10)	-2(9)	5(9)	-8(10)
ME2	96(13)	73(12)	83(12)	13(10)	-12(10)	1(11)
CP10	44(10)	77(13)	64(11)	-4(9)	15(9)	1(9)
CP9	64(13)	98(13)	51(11)	1(9)	6(10)	-2(10)
ME4	100(13)	90(12)	44(10)	5(8)	15(9)	-11(10)
ME6	130(16)	69(12)	83(12)	-21(10)	-9(11)	-31(11)
C(2)	150(17)	112(14)	49(10)	-1(10)	7(10)	-22(13)
F(44)	76(7)	119(8)	69(6)	-18(5)	8(5)	23(6)
F(42)	102(7)	72(6)	92(7)	-24(5)	-23(6)	-30(6)
C(44)	51(12)	89(13)	31(10)	-13(9)	6(9)	30(11)
ME1	65(12)	113(15)	111(14)	-20(11)	11(11)	-42(11)
ME3	70(13)	89(13)	115(14)	-7(10)	-9(11)	17(11)
C(4)	101(14)	112(14)	61(10)	24(10)	6(10)	33(11)
C(42)	58(13)	50(12)	83(14)	-6(11)	-39(12)	0(11)
Cl	73(3)	77(3)	78(3)	2(2)	-33(2)	5(2)

Table 10. Complete Distances and Angles for $Cp^*_2Ta(NH^tBu)H[B(C_6F_5)_4]$.

Ta-N	1.940(11)
Ta-H(1)	2.3105(7)
Ta-Cl	2.372(3)
Ta-CP5	2.394(12)
Ta-CP7	2.425(14)
Ta-CP9	2.468(14)
Ta-CP8	2.469(12)
Ta-CP3	2.481(13)
Ta-CP6	2.485(14)
Ta-CP10	2.488(14)
Ta-CP1	2.502(13)
Ta-CP4	2.518(13)
F(46)-C(45)	1.345(13)
F(31)-C(31)	1.359(12)
F(11)-C(11)	1.363(12)
F(22)-C(22)	1.319(14)
F(34)-C(34)	1.366(14)
F(15)-C(15)	1.359(13)
F(13)-C(13)	1.387(13)
F(12)-C(12)	1.359(13)
F(21)-C(21)	1.351(13)
F(26)-C(25)	1.344(13)
F(14)-C(14)	1.349(13)
F(41)-C(41)	1.372(14)
F(24)-C(24)	1.337(13)
F(35)-C(35)	1.374(13)
C(22)-C(23)	1.34(2)
C(22)-C(21)	1.41(2)
C(33)-F(33)	1.356(14)
C(33)-C(34)	1.36(2)
C(33)-C(32)	1.37(2)
C(14)-C(15)	1.35(2)
C(14)-C(13)	1.38(2)
C(13)-C(12)	1.36(2)
C(10)-C(11)	1.38(2)
C(10)-C(15)	1.40(2)
C(10)-B	1.65(2)
C(34)-C(35)	1.35(2)
C(20)-C(21)	1.37(2)
C(20)-C(25)	1.40(2)
C(20)-B	1.67(2)
C(40)-C(41)	1.38(2)
C(40)-C(45)	1.40(2)
C(40)-B	1.65(2)
C(25)-C(24)	1.39(2)
C(12)-C(11)	1.35(2)
C(30)-C(31)	1.37(2)
C(30)-C(35)	1.37(2)
C(30)-B	1.63(2)

C(45)-C(44)	1.37(2)
C(43)-F(43)	1.35(2)
C(43)-C(42)	1.36(2)
C(43)-C(44)	1.37(2)
C(41)-C(42)	1.39(2)
C(31)-C(32)	1.39(2)
F(23)-C(23)	1.354(13)
F(32)-C(32)	1.318(14)
CP7-CP8	1.36(2)
CP7-CP6	1.444(14)
CP7-ME7	1.51(2)
CP6-CP10	1.38(2)
CP6-ME6	1.54(2)
CP4-CP3	1.41(2)
CP4-CP5	1.43(2)
CP4-ME4	1.49(2)
C(23)-C(24)	1.38(2)
N-H(1)	1.180(11)
N-C(1)	1.511(14)
CP2-CP1	1.40(2)
CP2-CP3	1.45(2)
CP2-ME2	1.46(2)
CP3-ME3	1.50(2)
C(1)-C(4)	1.52(2)
C(1)-C(3)	1.55(2)
C(1)-C(2)	1.59(2)
CP1-CP5	1.42(2)
CP1-ME1	1.51(2)
CP5-ME5	1.52(2)
ME8-CP8	1.507(14)
CP8-CP9	1.46(2)
ME9-CP9	1.50(2)
ME10-CP10	1.50(2)
CP10-CP9	1.39(2)
F(44)-C(44)	1.348(14)
F(42)-C(42)	1.31(2)

N-Ta-H(1)	30.7(3)
N-Ta-Cl	94.1(3)
H(1)-Ta-Cl	96.10(9)
N-Ta-CP5	99.2(5)
H(1)-Ta-CP5	117.8(4)
Cl-Ta-CP5	132.4(3)
N-Ta-CP7	84.4(5)
H(1)-Ta-CP7	57.9(3)
Cl-Ta-CP7	123.6(3)
CP5-Ta-CP7	103.2(4)
N-Ta-CP9	138.4(5)
H(1)-Ta-CP9	108.1(4)
Cl-Ta-CP9	97.7(4)
CP5-Ta-CP9	101.7(5)
CP7-Ta-CP9	56.1(5)

N-Ta-CP8	113.9(5)
H(1)-Ta-CP8	90.0(3)
Cl-Ta-CP8	129.6(3)
CP5-Ta-CP8	85.3(4)
CP7-Ta-CP8	32.3(3)
CP9-Ta-CP8	34.3(4)
N-Ta-CP3	128.0(5)
H(1)-Ta-CP3	158.5(3)
Cl-Ta-CP3	80.1(3)
CP5-Ta-CP3	55.9(4)
CP7-Ta-CP3	140.9(5)
CP9-Ta-CP3	93.3(5)
CP8-Ta-CP3	108.8(5)
N-Ta-CP6	85.4(5)
H(1)-Ta-CP6	55.0(3)
Cl-Ta-CP6	89.4(3)
CP5-Ta-CP6	136.9(4)
CP7-Ta-CP6	34.2(3)
CP9-Ta-CP6	55.1(4)
CP8-Ta-CP6	54.6(4)
CP3-Ta-CP6	145.2(5)
N-Ta-CP10	115.4(5)
H(1)-Ta-CP10	86.0(3)
Cl-Ta-CP10	76.5(3)
CP5-Ta-CP10	134.1(5)
CP7-Ta-CP10	54.8(4)
CP9-Ta-CP10	32.6(4)
CP8-Ta-CP10	54.1(4)
CP3-Ta-CP10	113.2(5)
CP6-Ta-CP10	32.2(4)
N-Ta-CP1	79.4(4)
H(1)-Ta-CP1	107.9(3)
Cl-Ta-CP1	107.3(4)
CP5-Ta-CP1	33.6(4)
CP7-Ta-CP1	127.4(5)
CP9-Ta-CP1	133.1(5)
CP8-Ta-CP1	118.1(4)
CP3-Ta-CP1	54.5(4)
CP6-Ta-CP1	158.1(5)
CP10-Ta-CP1	164.8(5)
N-Ta-CP4	131.5(4)
H(1)-Ta-CP4	150.4(3)
Cl-Ta-CP4	111.3(3)
CP5-Ta-CP4	33.7(4)
CP7-Ta-CP4	111.1(4)
CP9-Ta-CP4	79.9(5)
CP8-Ta-CP4	81.2(4)
CP3-Ta-CP4	32.7(4)
CP6-Ta-CP4	133.0(4)
CP10-Ta-CP4	110.5(5)
CP1-Ta-CP4	54.3(4)
F(22)-C(22)-C(23)	121.5(14)
F(22)-C(22)-C(21)	120(2)
C(23)-C(22)-C(21)	118(2)

F(33)-C(33)-C(34)	119(2)
F(33)-C(33)-C(32)	121(2)
C(34)-C(33)-C(32)	119.7(14)
C(15)-C(14)-F(14)	122.1(14)
C(15)-C(14)-C(13)	118.0(13)
F(14)-C(14)-C(13)	120(2)
C(12)-C(13)-C(14)	119.9(13)
C(12)-C(13)-F(13)	121(2)
C(14)-C(13)-F(13)	119(2)
C(11)-C(10)-C(15)	110.7(12)
C(11)-C(10)-B	127.6(12)
C(15)-C(10)-B	121.4(12)
C(35)-C(34)-C(33)	119.5(14)
C(35)-C(34)-F(34)	120(2)
C(33)-C(34)-F(34)	120(2)
C(21)-C(20)-C(25)	113.3(12)
C(21)-C(20)-B	128.2(12)
C(25)-C(20)-B	117.6(13)
C(41)-C(40)-C(45)	111.1(12)
C(41)-C(40)-B	127.4(13)
C(45)-C(40)-B	121.0(12)
F(26)-C(25)-C(24)	115.2(13)
F(26)-C(25)-C(20)	120.2(13)
C(24)-C(25)-C(20)	124.5(14)
C(11)-C(12)-C(13)	118.6(14)
C(11)-C(12)-F(12)	122.4(13)
C(13)-C(12)-F(12)	118.9(14)
C(31)-C(30)-C(35)	111.5(12)
C(31)-C(30)-B	128.2(12)
C(35)-C(30)-B	120.1(12)
F(46)-C(45)-C(44)	116.6(14)
F(46)-C(45)-C(40)	118.2(13)
C(44)-C(45)-C(40)	125.1(14)
C(14)-C(15)-F(15)	116.1(13)
C(14)-C(15)-C(10)	126.3(13)
F(15)-C(15)-C(10)	117.6(13)
F(43)-C(43)-C(42)	121(2)
F(43)-C(43)-C(44)	119(2)
C(42)-C(43)-C(44)	121(2)
C(34)-C(35)-C(30)	125.8(14)
C(34)-C(35)-F(35)	116.3(14)
C(30)-C(35)-F(35)	117.9(13)
F(21)-C(21)-C(20)	120.6(12)
F(21)-C(21)-C(22)	114.8(14)
C(20)-C(21)-C(22)	124.5(13)
C(12)-C(11)-F(11)	113.0(13)
C(12)-C(11)-C(10)	126.1(12)
F(11)-C(11)-C(10)	120.9(13)
F(41)-C(41)-C(40)	119.5(13)
F(41)-C(41)-C(42)	114(2)
C(40)-C(41)-C(42)	127(2)
F(31)-C(31)-C(30)	122.0(12)
F(31)-C(31)-C(32)	110.8(13)
C(30)-C(31)-C(32)	126.9(13)

C(30)-B-C(10)	113.7(10)
C(30)-B-C(40)	114.8(11)
C(10)-B-C(40)	100.8(9)
C(30)-B-C(20)	102.0(9)
C(10)-B-C(20)	112.0(11)
C(40)-B-C(20)	114.1(10)
CP8-CP7-CP6	107.9(12)
CP8-CP7-ME7	125.1(12)
CP6-CP7-ME7	125.7(13)
CP8-CP7-Ta	75.6(8)
CP6-CP7-Ta	75.2(8)
ME7-CP7-Ta	125.7(9)
CP10-CP6-CP7	106.4(12)
CP10-CP6-ME6	125.1(14)
CP7-CP6-ME6	128.4(14)
CP10-CP6-Ta	74.0(9)
CP7-CP6-Ta	70.7(9)
ME6-CP6-Ta	122.6(8)
CP3-CP4-CP5	107.4(12)
CP3-CP4-ME4	125.5(14)
CP5-CP4-ME4	125.3(13)
CP3-CP4-Ta	72.2(8)
CP5-CP4-Ta	68.4(7)
ME4-CP4-Ta	136.6(9)
F(32)-C(32)-C(33)	119.3(13)
F(32)-C(32)-C(31)	124.1(14)
C(33)-C(32)-C(31)	116.5(14)
C(22)-C(23)-F(23)	119(2)
C(22)-C(23)-C(24)	121.2(14)
F(23)-C(23)-C(24)	119(2)
H(1)-N-C(1)	101.6(10)
H(1)-N-Ta	92.3(7)
C(1)-N-Ta	155.4(9)
N-H(1)-Ta	57.0(5)
CP1-CP2-CP3	106.5(12)
CP1-CP2-ME2	129(2)
CP3-CP2-ME2	123(2)
CP1-CP2-Ta	72.9(8)
CP3-CP2-Ta	71.5(7)
ME2-CP2-Ta	130.0(9)
CP4-CP3-CP2	108.4(12)
CP4-CP3-ME3	125.9(14)
CP2-CP3-ME3	124.1(14)
CP4-CP3-Ta	75.1(8)
CP2-CP3-Ta	75.0(8)
ME3-CP3-Ta	127.6(9)
N-C(1)-C(4)	106.0(11)
N-C(1)-C(3)	111.5(10)
C(4)-C(1)-C(3)	113.9(13)
N-C(1)-C(2)	110.6(12)
C(4)-C(1)-C(2)	109.0(11)
C(3)-C(1)-C(2)	106.0(12)
CP2-CP1-CP5	109.4(13)
CP2-CP1-ME1	127.2(14)

CP5-CP1-ME1	122.4(13)
CP2-CP1-Ta	74.9(8)
CP5-CP1-Ta	69.0(7)
ME1-CP1-Ta	131.2(9)
CP1-CP5-CP4	107.2(12)
CP1-CP5-ME5	122.4(13)
CP4-CP5-ME5	127.2(12)
CP1-CP5-Ta	77.4(7)
CP4-CP5-Ta	77.9(7)
ME5-CP5-Ta	127.0(9)
CP7-CP8-CP9	109.2(12)
CP7-CP8-ME8	123.5(12)
CP9-CP8-ME8	124.7(13)
CP7-CP8-Ta	72.1(8)
CP9-CP8-Ta	72.8(8)
ME8-CP8-Ta	135.8(9)
F(24)-C(24)-C(23)	120.1(14)
F(24)-C(24)-C(25)	122(2)
C(23)-C(24)-C(25)	117.9(14)
CP6-CP10-CP9	111.6(13)
CP6-CP10-ME10	122.6(14)
CP9-CP10-ME10	125.0(14)
CP6-CP10-Ta	73.8(9)
CP9-CP10-Ta	72.9(9)
ME10-CP10-Ta	128.7(10)
CP10-CP9-CP8	104.6(13)
CP10-CP9-ME9	122.4(14)
CP8-CP9-ME9	128.9(13)
CP10-CP9-Ta	74.5(8)
CP8-CP9-Ta	72.9(8)
ME9-CP9-Ta	135.0(11)
F(44)-C(44)-C(43)	120(2)
F(44)-C(44)-C(45)	121(2)
C(43)-C(44)-C(45)	119(2)
F(42)-C(42)-C(43)	122(2)
F(42)-C(42)-C(41)	121(2)
C(43)-C(42)-C(41)	117(2)

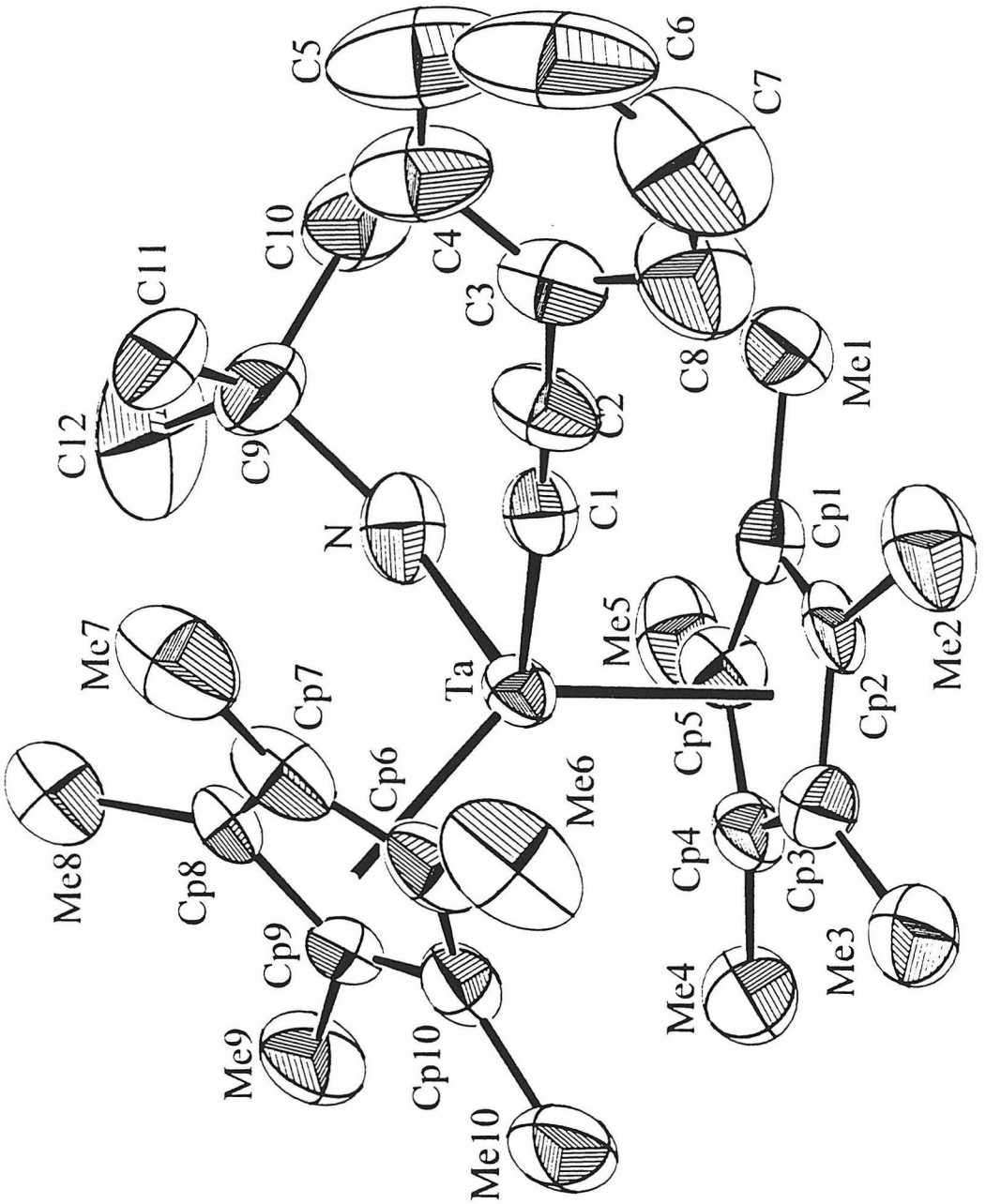

Figure 3: ORTEP diagram of the structure of $Cp^*_2Ta(NH^tBu)(C{\equiv}CPh)[B(C_6F_5)_4]$

Table 11: Crystal and Intensity Data for $Cp^*_2Ta(NH^tBu)(C{\equiv}CPh)[B(C_6F_5)_4]$

chemical formula	$C_{56}H_{45}BF_{20}NTa$
crystal dimension, mm	0.15 x 0.30 x 0.40
crystal system	triclinic
space group	$P\bar{1}$ (#2)
a, Å	12.470(3)
b, Å	12.748(4)
c, Å	15.880(4)
α, deg	100.32(2)
β, deg	109.39(2)
γ, deg	97.98(2)
V, Å^3	2647.6(12)
ρ_{calc}, g cm^{-3}	1.635
Z	2
λ, Å	0.71073
μ, mm^{-1}	2.156
temp, °K	295(2)
2θ range, deg	3 to 40
no. of reflections measured, total	9449
R	0.049
GOF	1.41

Table 12: Final Heavy Atom Parameters for $Cp^*_2Ta(NH^tBu)(C{\equiv}CPh)[B(C_6F_5)_4]$

	x, y, z and $U_{eq}{}^a \times 10^4$			
Atom	x	y	z	U_{eq}
Ta	2058.5(3)	2919.9(3)	2390.9(3)	430(1)
Cp1	3273(7)	2513(5)	3777(5)	474(23)
Cp2	2152(8)	2428(6)	3837(5)	544(28)
Cp3	1371(7)	1690(6)	3101(6)	600(26)
Cp4	2011(8)	1309(5)	2590(5)	535(27)
Cp5	3184(7)	1804(5)	3025(5)	503(25)
Me1	4336(7)	3154(6)	4518(5)	752(28)
Me2	1843(8)	2915(7)	4626(6)	998(33)
Me3	195(8)	1247(7)	3082(6)	973(33)
Me4	1643(8)	382(6)	1897(6)	867(33)
Me5	4191(8)	1540(6)	2803(6)	781(27)
Cp6	86(7)	3145(8)	1640(5)	642(30)
Cp7	801(8)	3784(7)	1387(6)	659(31)
Cp8	1273(7)	3288(7)	846(6)	609(31)
Cp9	889(7)	2307(6)	760(5)	524(27)
Cp10	95(7)	2238(7)	1197(6)	567(28)
Me6	−699(8)	3433(8)	2110(7)	1192(39)
Me7	843(8)	4838(7)	1512(6)	1077(37)
Me8	1907(8)	3596(7)	229(6)	1003(36)
Me9	1076(8)	1523(6)	93(5)	870(32)

Atom	x	y	z	U_{eq}
Me10	−830(7)	1364(7)	979(6)	949(35)
C1	2050(7)	4129(6)	3312(6)	609(26)
C2	2065(7)	4842(7)	3824(6)	709(30)
C3	2069(8)	5707(7)	4436(7)	712(33)
C4	2530(8)	6560(10)	4366(8)	1075(42)
C5	2506(13)	7391(13)	4922(14)	1611(75)
C6	1981(17)	7329(15)	5516(15)	1821(90)
C7	1519(14)	6508(13)	5637(10)	1609(57)
C8	1565(10)	5665(8)	5093(9)	1171(42)
N	3574(6)	3449(5)	2412(4)	712(19)
C9	4472(8)	4273(7)	2357(7)	931(35)
C10	5451(9)	4585(8)	3314(8)	1608(50)
C11	3912(9)	5117(7)	2248(7)	1120(38)
C12	4982(9)	3961(9)	1652(8)	1523(43)
B	6424(8)	8550(7)	2389(6)	513(27)
C30	6633(7)	8976(5)	3488(5)	473(22)
C31	7631(8)	9625(6)	4056(7)	564(26)
C32	7893(10)	10047(7)	4969(7)	736(39)
C33	7082(13)	9828(8)	5353(7)	841(45)
C34	6101(10)	9189(8)	4846(8)	729(35)

Atom	x	y	z	U_{eq}
C35	5900(8)	8757(6)	3950(7)	591(28)
F31	8440(4)	9901(3)	3695(3)	759(15)
F32	8897(5)	10677(4)	5442(3)	1146(22)
F33	7307(6)	10277(4)	6230(4)	1418(28)
F34	5305(5)	8973(4)	5220(4)	1088(18)
F35	4914(4)	8098(4)	3530(3)	811(14)
C40	7484(7)	7981(6)	2476(5)	506(26)
C41	8483(8)	8225(6)	2292(5)	556(27)
C42	9361(8)	7719(8)	2417(6)	692(33)
C43	9260(10)	6922(8)	2740(7)	803(34)
C44	8301(10)	6664(7)	2950(6)	758(32)
C45	7468(8)	7183(7)	2818(6)	581(28)
F41	8677(3)	9002(3)	1980(3)	722(14)
F42	10293(4)	8012(4)	2217(3)	1051(19)
F43	10085(5)	6417(4)	2851(4)	1296(20)
F44	8191(5)	5878(4)	3270(4)	1154(19)
F45	6546(4)	6880(3)	3046(3)	769(14)
C50	5121(7)	7909(6)	1772(5)	447(23)
C51	4156(8)	8262(6)	1749(6)	516(25)
C52	3020(9)	7795(8)	1238(7)	691(33)

Atom	x	y	z	U_{eq}
C53	2824(9)	6921(9)	677(7)	753(39)
C54	3742(11)	6555(7)	635(6)	725(35)
C55	4860(8)	7041(7)	1174(6)	625(29)
F51	4283(4)	9139(4)	2264(3)	715(13)
F52	2115(4)	8189(4)	1266(4)	1060(19)
F53	1723(4)	6450(4)	170(4)	1191(21)
F54	3554(4)	5692(4)	68(3)	1072(20)
F55	5703(4)	6593(3)	1073(3)	810(16)
C60	6484(6)	9396(6)	1832(6)	463(24)
C61	6460(6)	9183(7)	937(7)	558(27)
C62	6433(7)	9830(9)	406(7)	686(30)
C63	6381(7)	10717(9)	740(8)	726(31)
C64	6389(6)	10986(7)	1597(8)	626(28)
C65	6446(6)	10324(7)	2124(6)	529(25)
F61	6466(3)	8298(4)	562(3)	721(15)
F62	6414(4)	9551(4)	−451(4)	1051(20)
F63	6336(4)	11364(4)	232(4)	1107(18)
F64	6360(4)	11886(4)	1953(4)	940(16)
F65	6419(4)	10668(3)	2972(3)	688(13)

Table 13: Assigned Hydrogen Atom Parameters for $Cp^*_2Ta(NH^tBu)(C{\equiv}CPh)[B(C_6F_5)_4]$

	x, y and $z \times 10^4$			
Atom	x	y	z	B
H0	3988	3135	2307	6.6
HMe1a	4956	3187	4296	7.1
HMe1b	4519	2898	5042	7.1
HMe1c	4170	3759	4657	7.1
HMe2a	2340	3523	4890	9.5
HMe2b	1952	2546	5067	9.5
HMe2c	1055	2967	4388	9.5
HMe3a	306	1025	3624	9.2
HMe3b	−158	739	2552	9.2
HMe3c	−261	1710	3061	9.2
HMe4a	2213	333	1626	8.2
HMe4b	913	363	1443	8.2
HMe4c	1583	−109	2203	8.2
HMe5a	4813	2077	3041	7.4
HMe5b	3957	1342	2156	7.4
HMe5c	4410	1043	3083	7.4
HMe6a	−284	3975	2596	11.3
HMe6b	−941	2928	2347	11.3
HMe6c	−1347	3572	1678	11.3
HMe7a	1427	5104	1312	10.2
HMe7b	1024	5110	2143	10.2
HMe7c	104	4924	1151	10.2
HMe8a	2532	3282	286	9.5
HMe8b	2188	4259	429	9.5
HMe8c	1368	3427	−387	9.5
HMe9a	896	944	249	8.3
HMe9b	1866	1657	148	8.3
HMe9c	577	1505	−512	8.3
HMe10a	−1300	1488	1331	9.0
HMe10b	−458	864	1134	9.0
HMe10c	−1285	1211	341	9.0
H4	2882	6592	3923	10.2
H5	2855	7987	4878	15.3
H6	1928	7897	5877	17.3
H7	1168	6498	6083	15.2
H8	1256	5073	5171	11.1
H10a	6023	5087	3320	15.2
H10b	5136	4794	3765	15.2
H10c	5799	4068	3448	15.2

Atom	x	y	z	B
H11a	4450	5620	2215	10.6
H11b	3239	4946	1701	10.6
H11c	3697	5312	2762	10.6
H12a	5519	4478	1641	14.4
H12b	5373	3470	1804	14.4
H12c	4377	3735	1064	14.4

Table 14: Anisotropic Displacement Parameters for
$Cp^*_2Ta(NH^tBu)(C{\equiv}CPh)[B(C_6F_5)_4]$

Atom	U_{11}	U_{22}	U_{33}	U_{12}	U_{13}	U_{23}
Ta	506(2)	432(2)	335(2)	117(2)	148(2)	46(1)
Cp1	521(58)	479(58)	510(61)	164(46)	226(49)	216(50)
Cp2	885(71)	583(61)	276(55)	239(54)	309(53)	129(47)
Cp3	602(61)	630(62)	568(64)	21(52)	254(55)	152(52)
Cp4	804(69)	396(55)	365(54)	131(51)	171(52)	75(44)
Cp5	649(65)	404(55)	473(58)	252(49)	218(50)	14(44)
Me1	782(64)	744(64)	595(61)	113(52)	103(52)	156(51)
Me2	1380(88)	1167(85)	691(72)	441(69)	595(65)	278(63)
Me3	879(74)	1255(87)	731(71)	−95(64)	301(58)	346(62)
Me4	1287(80)	507(62)	716(67)	178(55)	270(58)	123(53)
Me5	1134(78)	694(67)	733(67)	443(59)	433(60)	338(53)
Cp6	535(60)	976(84)	416(59)	258(59)	201(47)	41(60)
Cp7	752(71)	725(79)	463(64)	444(63)	131(52)	11(57)
Cp8	623(62)	714(76)	351(60)	34(57)	−7(49)	226(54)
Cp9	548(56)	516(65)	358(54)	12(46)	34(44)	67(46)
Cp10	447(57)	841(77)	410(57)	117(52)	158(46)	159(54)
Me6	798(72)	1921(118)	937(83)	673(76)	371(64)	146(77)
Me7	1355(89)	869(81)	817(74)	572(67)	71(62)	109(60)
Me8	1106(82)	1125(87)	636(72)	70(65)	211(62)	199(63)
Me9	1196(78)	754(68)	526(61)	155(57)	286(55)	−77(53)
Me10	601(61)	1283(88)	697(68)	−102(61)	69(51)	148(61)
C1	679(59)	563(63)	547(63)	154(49)	98(47)	270(50)
C2	672(62)	695(74)	612(69)	294(55)	54(50)	33(57)
C3	670(66)	602(80)	706(79)	270(57)	68(54)	22(64)
C4	818(78)	699(83)	1411(107)	223(69)	139(68)	−4(83)
C5	1053(120)	867(115)	2292(222)	225(90)	224(107)	−411(135)
C6	1467(178)	1005(134)	1975(214)	367(143)	−169(128)	−667(157)
C7	2241(170)	1495(136)	1218(113)	821(137)	922(110)	−244(121)
C8	1619(112)	1074(100)	899(93)	469(80)	574(85)	77(79)
N	856(51)	794(53)	719(51)	355(43)	464(41)	280(42)
C9	839(75)	723(75)	1017(86)	−99(61)	55(67)	442(65)
C10	978(84)	1708(117)	1458(108)	−565(79)	−338(78)	883(92)
C11	1311(90)	749(77)	1067(86)	−196(67)	220(68)	386(66)
C12	1371(100)	2457(149)	1680(121)	697(96)	1377(98)	999(108)
B	572(67)	584(69)	448(68)	172(53)	192(53)	239(55)
C30	531(56)	497(56)	473(60)	176(47)	206(54)	221(48)
C31	638(69)	657(65)	554(74)	262(55)	325(60)	233(56)
C32	1007(90)	637(72)	432(80)	278(65)	82(71)	79(62)
C33	1432(116)	777(85)	413(82)	482(80)	342(86)	189(69)

Atom	U_{11}	U_{22}	U_{33}	U_{12}	U_{13}	U_{23}
C34	1173(97)	785(79)	477(81)	386(70)	465(73)	312(64)
C35	635(67)	665(66)	501(73)	167(52)	184(58)	234(57)
F31	675(32)	762(35)	665(34)	33(26)	133(27)	49(27)
F32	1418(52)	911(43)	633(38)	134(39)	−53(36)	−69(32)
F33	2644(78)	1259(51)	504(39)	758(49)	655(43)	176(36)
F34	1750(56)	1304(50)	882(43)	702(42)	998(43)	625(37)
F35	980(39)	927(39)	759(37)	183(32)	510(32)	419(31)
C40	545(68)	565(63)	377(53)	126(54)	145(49)	79(46)
C41	548(63)	651(68)	434(58)	119(58)	158(49)	93(48)
C42	487(69)	1054(91)	554(66)	290(69)	200(52)	124(60)
C43	826(87)	918(92)	668(72)	579(79)	154(62)	129(63)
C44	866(85)	697(80)	754(75)	302(73)	230(65)	302(61)
C45	550(66)	585(70)	565(64)	96(57)	181(51)	94(52)
F41	654(32)	843(37)	742(35)	101(27)	365(26)	206(30)
F42	662(36)	1587(53)	1024(43)	393(35)	432(33)	255(37)
F43	1144(46)	1590(56)	1321(53)	990(45)	355(38)	409(42)
F44	1461(52)	1024(47)	1183(49)	680(41)	446(40)	525(40)
F45	896(38)	658(34)	838(37)	217(28)	287(31)	410(28)
C50	503(59)	530(62)	378(54)	163(50)	190(44)	188(49)
C51	519(65)	570(65)	489(60)	81(60)	151(53)	290(51)
C52	608(85)	878(87)	681(73)	110(70)	220(64)	489(66)
C53	538(79)	918(97)	579(73)	−196(74)	−37(61)	369(70)
C54	876(88)	596(77)	549(71)	7(75)	95(69)	197(59)
C55	648(75)	734(77)	567(66)	225(63)	242(59)	240(59)
F51	720(33)	733(36)	823(36)	279(28)	325(28)	331(30)
F52	619(35)	1383(49)	1288(48)	320(34)	308(33)	593(38)
F53	756(39)	1316(49)	1066(44)	−249(36)	−132(34)	479(38)
F54	1304(46)	751(39)	772(38)	−93(34)	64(33)	77(33)
F55	942(38)	726(35)	627(33)	165(30)	195(28)	21(26)
C60	418(49)	455(62)	524(67)	52(41)	202(43)	115(49)
C61	595(56)	674(71)	416(66)	129(48)	235(47)	69(62)
C62	597(60)	1069(93)	578(80)	263(61)	275(52)	477(80)
C63	561(59)	1166(106)	749(90)	315(61)	305(57)	734(87)
C64	559(57)	556(72)	824(84)	164(47)	221(54)	343(71)
C65	538(55)	720(75)	428(63)	154(48)	252(45)	218(63)
F61	797(33)	945(40)	436(30)	180(28)	298(25)	71(28)
F62	901(38)	1920(60)	549(36)	348(36)	361(31)	613(39)
F63	882(38)	1484(51)	1190(47)	208(34)	330(33)	1030(44)
F64	1020(39)	711(38)	1319(48)	278(31)	518(34)	562(35)
F65	869(34)	563(31)	732(36)	263(25)	330(29)	248(27)

Table 15: Complete Distances and Angles for
$Cp^*_2Ta(NH^tBu)(C{\equiv}CPh)[B(C_6F_5)_4]$

		Distance(Å)			Distance(Å)
Ta	–N	1.928(7)	Me5	–HMe5c	0.950
Ta	–C1	2.097(9)	Cp6	–Cp7	1.408(14)
Ta	–CpA	2.157	Cp6	–Cp10	1.398(13)
Ta	–CpB	2.172	Cp6	–Me6	1.478(14)
Ta	–Cp1	2.451(8)	Cp7	–Cp8	1.361(14)
Ta	–Cp2	2.502(9)	Cp7	–Me7	1.523(14)
Ta	–Cp3	2.497(9)	Cp8	–Cp9	1.426(12)
Ta	–Cp4	2.447(8)	Cp8	–Me8	1.538(14)
Ta	–Cp5	2.447(9)	Cp9	–Cp10	1.388(12)
Ta	–Cp6	2.450(10)	Cp9	–Me9	1.521(12)
Ta	–Cp7	2.500(10)	Cp10	–Me10	1.508(13)
Ta	–Cp8	2.511(9)	Me6	–HMe6a	0.950
Ta	–Cp9	2.438(8)	Me6	–HMe6b	0.950
Ta	–Cp10	2.480(9)	Me6	–HMe6c	0.946
Cp1	–Cp2	1.422(12)	Me7	–HMe7a	0.951
Cp1	–Cp5	1.402(12)	Me7	–HMe7b	0.947
Cp1	–Me1	1.500(12)	Me7	–HMe7c	0.949
Cp2	–Cp3	1.412(12)	Me8	–HMe8a	0.948
Cp2	–Me2	1.520(13)	Me8	–HMe8b	0.948
Cp3	–Cp4	1.415(12)	Me8	–HMe8c	0.948
Cp3	–Me3	1.508(13)	Me9	–HMe9a	0.949
Cp4	–Cp5	1.414(12)	Me9	–HMe9b	0.949
Cp4	–Me4	1.497(12)	Me9	–HMe9c	0.948
Cp5	–Me5	1.494(12)	Me10	–HMe10a	0.948
Me1	–HMe1a	0.949	Me10	–HMe10b	0.951
Me1	–HMe1b	0.948	Me10	–HMe10c	0.948
Me1	–HMe1c	0.948	C1	–C2	1.202(13)
Me2	–HMe2a	0.950	C2	–C3	1.459(14)
Me2	–HMe2b	0.947	C3	–C4	1.347(16)
Me2	–HMe2c	0.948	C3	–C8	1.390(16)
Me3	–HMe3a	0.950	C4	–C5	1.39(2)
Me3	–HMe3b	0.949	C4	–H4	0.950
Me3	–HMe3c	0.946	C5	–C6	1.32(3)
Me4	–HMe4a	0.950	C5	–H5	0.950
Me4	–HMe4b	0.948	C6	–C7	1.34(3)
Me4	–HMe4c	0.949	C6	–H6	0.950
Me5	–HMe5a	0.948	C7	–C8	1.40(2)
Me5	–HMe5b	0.947	C7	–H7	0.950

	Distance(Å)		Distance(Å)
C8 –H8	0.950	C43 –F43	1.336(13)
N –C9	1.570(12)	C44 –C45	1.357(15)
N –H0	0.779	C44 –F44	1.354(13)
C9 –C10	1.541(16)	C45 –F45	1.358(11)
C9 –C11	1.517(15)	C50 –C51	1.368(12)
C9 –C12	1.496(17)	C50 –C55	1.375(13)
C9 –H0	1.682	C51 –C52	1.380(15)
C10 –H10a	0.950	C51 –F51	1.357(10)
C10 –H10b	0.950	C52 –C53	1.368(16)
C10 –H10c	0.950	C52 –F52	1.348(13)
C11 –H11a	0.950	C53 –C54	1.347(16)
C11 –H11b	0.950	C53 –F53	1.349(13)
C11 –H11c	0.950	C54 –C55	1.378(15)
C12 –H12a	0.950	C54 –F54	1.362(12)
C12 –H12b	0.950	C55 –F55	1.355(11)
C12 –H12c	0.950	C60 –C61	1.388(12)
B –C30	1.663(13)	C60 –C65	1.377(12)
B –C40	1.643(13)	C61 –C62	1.378(14)
B –C50	1.637(13)	C61 –F61	1.335(10)
B –C60	1.661(13)	C62 –C63	1.340(16)
C30 –C31	1.375(13)	C62 –F62	1.341(12)
C30 –C35	1.389(13)	C63 –C64	1.343(16)
C31 –C32	1.380(15)	C63 –F63	1.351(13)
C31 –F31	1.366(11)	C64 –C65	1.391(14)
C32 –C33	1.373(17)	C64 –F64	1.356(11)
C32 –F32	1.341(13)	C65 –F65	1.365(10)
C33 –C34	1.337(18)		
C33 –F33	1.348(14)		
C34 –C35	1.372(16)		
C34 –F34	1.346(14)		
C35 –F35	1.339(11)		
C40 –C41	1.386(12)		
C40 –C45	1.383(13)		
C41 –C42	1.390(14)		
C41 –F41	1.350(10)		
C42 –C43	1.370(16)		
C42 –F42	1.338(12)		
C43 –C44	1.368(16)		

			Angle(°)				Angle(°)
C1	-Ta	-N	92.5(3)	HMe3c	-Me3	-HMe3b	110.6
C1	-Ta	-CpA	101.5	HMe4a	-Me4	-Cp4	108.5
C1	-Ta	-CpB	100.5	HMe4b	-Me4	-Cp4	108.5
N	-Ta	-CpA	104.0	HMe4c	-Me4	-Cp4	108.6
N	-Ta	-CpB	114.0	HMe4b	-Me4	-HMe4a	110.3
CpA	-Ta	-CpB	134.7	HMe4c	-Me4	-HMe4a	110.4
Cp5	-Cp1	-Cp2	107.3(7)	HMe4c	-Me4	-HMe4b	110.5
Me1	-Cp1	-Cp2	122.2(7)	HMe5a	-Me5	-Cp5	108.4
Me1	-Cp1	-Cp5	129.7(8)	HMe5b	-Me5	-Cp5	108.5
Cp3	-Cp2	-Cp1	108.5(8)	HMe5c	-Me5	-Cp5	108.3
Me2	-Cp2	-Cp1	127.4(8)	HMe5b	-Me5	-HMe5a	110.6
Me2	-Cp2	-Cp3	123.4(8)	HMe5c	-Me5	-HMe5a	110.4
Cp4	-Cp3	-Cp2	107.4(8)	HMe5c	-Me5	-HMe5b	110.6
Me3	-Cp3	-Cp2	122.4(8)	Cp10	-Cp6	-Cp7	106.9(8)
Me3	-Cp3	-Cp4	127.7(8)	Me6	-Cp6	-Cp7	123.3(9)
Cp5	-Cp4	-Cp3	107.9(7)	Me6	-Cp6	-Cp10	128.5(9)
Me4	-Cp4	-Cp3	126.8(8)	Cp8	-Cp7	-Cp6	108.8(9)
Me4	-Cp4	-Cp5	123.0(8)	Me7	-Cp7	-Cp6	126.0(9)
Cp4	-Cp5	-Cp1	108.7(7)	Me7	-Cp7	-Cp8	124.0(9)
Me5	-Cp5	-Cp1	124.9(8)	Cp9	-Cp8	-Cp7	108.4(8)
Me5	-Cp5	-Cp4	125.9(8)	Me8	-Cp8	-Cp7	131.1(9)
HMe1a	-Me1	-Cp1	108.4	Me8	-Cp8	-Cp9	119.4(8)
HMe1b	-Me1	-Cp1	108.4	Cp10	-Cp9	-Cp8	106.5(8)
HMe1c	-Me1	-Cp1	108.4	Me9	-Cp9	-Cp8	124.0(8)
HMe1b	-Me1	-HMe1a	110.4	Me9	-Cp9	-Cp10	127.4(8)
HMe1c	-Me1	-HMe1a	110.4	Cp9	-Cp10	-Cp6	108.9(8)
HMe1c	-Me1	-HMe1b	110.6	Me10	-Cp10	-Cp6	125.6(8)
HMe2a	-Me2	-Cp2	108.3	Me10	-Cp10	-Cp9	123.2(8)
HMe2b	-Me2	-Cp2	108.4	HMe6a	-Me6	-Cp6	108.4
HMe2c	-Me2	-Cp2	108.4	HMe6b	-Me6	-Cp6	108.4
HMe2b	-Me2	-HMe2a	110.5	HMe6c	-Me6	-Cp6	108.6
HMe2c	-Me2	-HMe2a	110.4	HMe6b	-Me6	-HMe6a	110.3
HMe2c	-Me2	-HMe2b	110.7	HMe6c	-Me6	-HMe6a	110.5
HMe3a	-Me3	-Cp3	108.4	HMe6c	-Me6	-HMe6b	110.6
HMe3b	-Me3	-Cp3	108.5	HMe7a	-Me7	-Cp7	108.4
HMe3c	-Me3	-Cp3	108.5	HMe7b	-Me7	-Cp7	108.5
HMe3b	-Me3	-HMe3a	110.3	HMe7c	-Me7	-Cp7	108.5
HMe3c	-Me3	-HMe3a	110.5	HMe7b	-Me7	-HMe7a	110.5

			Angle(°)				Angle(°)
HMe7c	-Me7	-HMe7a	110.3	H8	-C8	-C3	120.5
HMe7c	-Me7	-HMe7b	110.6	H8	-C8	-C7	120.5
HMe8a	-Me8	-Cp8	108.3	Ta	-N	-C9	151.8(6)
HMe8b	-Me8	-Cp8	108.3	Ta	-N	-H0	122.2
HMe8c	-Me8	-Cp8	108.3	H0	-N	-C9	84.3
HMe8b	-Me8	-HMe8a	110.6	C10	-C9	-N	105.9(8)
HMe8c	-Me8	-HMe8a	110.7	C11	-C9	-N	108.9(8)
HMe8c	-Me8	-HMe8b	110.6	C12	-C9	-N	112.1(8)
HMe9a	-Me9	-Cp9	108.3	H0	-C9	-N	27.4
HMe9b	-Me9	-Cp9	108.4	C11	-C9	-C10	105.1(9)
HMe9c	-Me9	-Cp9	108.4	C12	-C9	-C10	108.9(9)
HMe9b	-Me9	-HMe9a	110.5	H0	-C9	-C10	101.3
HMe9c	-Me9	-HMe9a	110.6	C12	-C9	-C11	115.2(9)
HMe9c	-Me9	-HMe9b	110.6	H0	-C9	-C11	134.9
HMe10a	-Me10	-Cp10	108.7	H0	-C9	-C12	89.1
HMe10b	-Me10	-Cp10	108.5	H10a	-C10	-C9	109.5
HMe10c	-Me10	-Cp10	108.7	H10b	-C10	-C9	109.5
HMe10b	-Me10	-HMe10a	110.2	H10c	-C10	-C9	109.5
HMe10c	-Me10	-HMe10a	110.5	H10b	-C10	-H10a	109.5
HMe10c	-Me10	-HMe10b	110.2	H10c	-C10	-H10a	109.5
Ta	-C1	-C2	177.6(8)	H10c	-C10	-H10b	109.5
C3	-C2	-C1	179.2(10)	H11a	-C11	-C9	109.5
C4	-C3	-C2	121.2(10)	H11b	-C11	-C9	109.5
C8	-C3	-C2	120.1(10)	H11c	-C11	-C9	109.5
C8	-C3	-C4	118.7(10)	H11b	-C11	-H11a	109.5
C5	-C4	-C3	121.9(13)	H11c	-C11	-H11a	109.5
H4	-C4	-C3	119.0	H11c	-C11	-H11b	109.5
H4	-C4	-C5	119.0	H12a	-C12	-C9	109.5
C6	-C5	-C4	117.9(18)	H12b	-C12	-C9	109.5
H5	-C5	-C4	121.0	H12c	-C12	-C9	109.5
H5	-C5	-C6	121.0	H12b	-C12	-H12a	109.5
C7	-C6	-C5	123.6(20)	H12c	-C12	-H12a	109.5
H6	-C6	-C5	118.2	H12c	-C12	-H12b	109.5
H6	-C6	-C7	118.2	C40	-B	-C30	101.8(7)
C8	-C7	-C6	118.8(16)	C50	-B	-C30	114.3(7)
H7	-C7	-C6	120.6	C60	-B	-C30	112.3(7)
H7	-C7	-C8	120.6	C50	-B	-C40	114.8(7)
C7	-C8	-C3	119.0(12)	C60	-B	-C40	113.0(7)

	Angle(°)		Angle(°)
C60 –B –C50	101.2(7)	C55 –C50 –B	126.3(8)
C31 –C30 –B	120.4(8)	C55 –C50 –C51	113.0(8)
C35 –C30 –B	127.8(8)	C52 –C51 –C50	125.4(9)
C35 –C30 –C31	111.8(8)	F51 –C51 –C50	119.6(8)
C32 –C31 –C30	125.9(9)	F51 –C51 –C52	115.0(8)
F31 –C31 –C30	118.3(8)	C53 –C52 –C51	118.4(10)
F31 –C31 –C32	115.8(9)	F52 –C52 –C51	121.6(10)
C33 –C32 –C31	118.1(10)	F52 –C52 –C53	120.0(10)
F32 –C32 –C31	119.7(9)	C54 –C53 –C52	119.0(11)
F32 –C32 –C33	122.2(10)	F53 –C53 –C52	119.6(10)
C34 –C33 –C32	119.2(12)	F53 –C53 –C54	121.4(10)
F33 –C33 –C32	118.3(11)	C55 –C54 –C53	120.4(10)
F33 –C33 –C34	122.5(11)	F54 –C54 –C53	119.3(10)
C35 –C34 –C33	120.6(11)	F54 –C54 –C55	120.2(9)
F34 –C34 –C33	119.3(11)	C54 –C55 –C50	123.7(9)
F34 –C34 –C35	120.1(10)	F55 –C55 –C50	121.7(8)
C34 –C35 –C30	124.2(9)	F55 –C55 –C54	114.6(9)
F35 –C35 –C30	120.9(8)	C61 –C60 –B	120.4(7)
F35 –C35 –C34	114.9(9)	C65 –C60 –B	126.9(8)
C41 –C40 –B	128.0(8)	C65 –C60 –C61	112.4(8)
C45 –C40 –B	119.6(8)	C62 –C61 –C60	124.0(9)
C45 –C40 –C41	112.3(8)	F61 –C61 –C60	118.4(8)
C42 –C41 –C40	124.3(9)	F61 –C61 –C62	117.5(8)
F41 –C41 –C40	121.2(8)	C63 –C62 –C61	119.7(10)
F41 –C41 –C42	114.6(8)	F62 –C62 –C61	119.3(9)
C43 –C42 –C41	119.5(10)	F62 –C62 –C63	120.9(10)
F42 –C42 –C41	119.7(9)	C64 –C63 –C62	120.5(11)
F42 –C42 –C43	120.8(9)	F63 –C63 –C62	121.1(10)
C44 –C43 –C42	118.4(11)	F63 –C63 –C64	118.5(10)
F43 –C43 –C42	120.5(10)	C65 –C64 –C63	118.6(10)
F43 –C43 –C44	121.1(10)	F64 –C64 –C63	121.3(9)
C45 –C44 –C43	119.9(10)	F64 –C64 –C65	120.1(8)
F44 –C44 –C43	118.9(10)	C64 –C65 –C60	124.8(9)
F44 –C44 –C45	121.2(9)	F65 –C65 –C60	121.6(8)
C44 –C45 –C40	125.7(9)	F65 –C65 –C64	113.5(8)
F45 –C45 –C40	118.2(8)		
F45 –C45 –C44	116.1(8)		
C51 –C50 –B	120.4(8)		

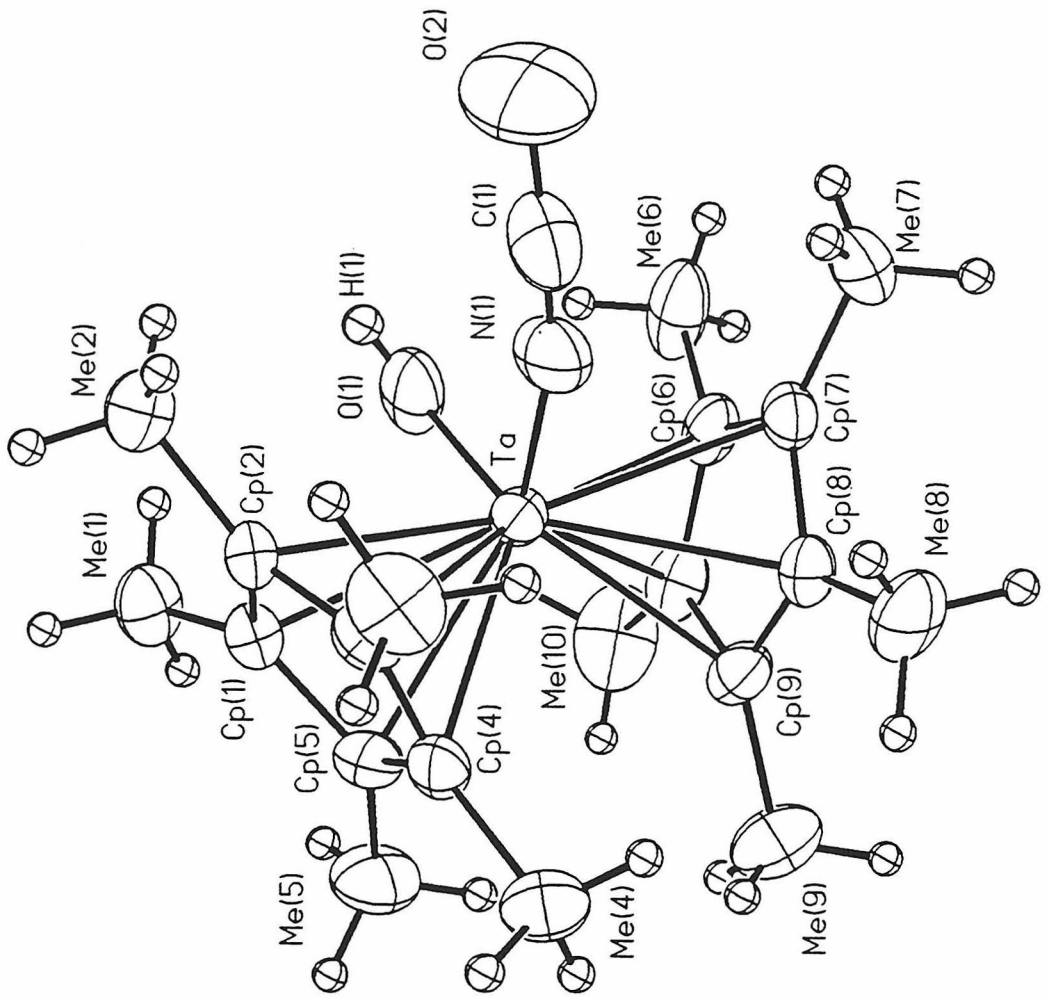

Figure 4: ORTEP diagram of the structure of $Cp^*_2Ta(OH)(NCO)[B(C_6F_5)_4]$

Table 16: Crystal and Intensity Data for $Cp^*_2Ta(NCO)(OH)[B(C_6F_5)_4]$

chemical formula	$C_{48}H_{31}BF_{20}NO_2Ta$
crystal dimension, mm	0.30 x 0.36 x 0.45
crystal system	triclinic
space group	P -1
a, Å	12.626(3)
b, Å	12.763(3)
c, Å	15.352(3)
α, deg	70.84(3)
β, deg	69.45(3)
γ, deg	77.43(3)
V, $Å^3$	2173.4(8)
ρ_{calc}, g cm^{-3}	1.818
Z	2
λ, Å	0.71073
μ, mm^{-1}	2.656
temp, °K	293(2)
2θ range, deg	2.8 to 45
no. of reflections measured, total	11863
R	0.0417
GOF	1.466

Table 17: Final Heavy Atom Parameters for $Cp^*_2Ta(OH)(NCO)[B(C_6F_5)_4]$

	x	y	z	U(eq)
Ta	2140(1)	1272(1)	3224(1)	45(1)
CP1	1145(6)	3005(5)	3619(5)	48(2)
CP2	366(5)	2540(5)	3420(5)	48(2)
CP3	774(6)	2562(6)	2428(6)	53(2)
CP4	1815(6)	3028(5)	2015(5)	55(2)
CP5	2056(6)	3286(5)	2760(5)	51(2)
CP6	3724(6)	-119(7)	3611(5)	58(2)
CP7	3453(5)	-408(6)	2911(5)	51(2)
CP8	3687(6)	473(6)	2035(5)	54(2)
CP9	4142(6)	1289(6)	2199(5)	56(2)
CP10	4115(6)	947(7)	3185(6)	61(2)
ME1	986(6)	3262(6)	4552(5)	71(2)
ME2	-750(6)	2149(6)	4116(5)	73(2)
ME3	153(7)	2286(7)	1874(6)	84(3)
ME4	2391(7)	3393(6)	950(5)	83(3)
ME5	2917(6)	4005(6)	2642(6)	84(3)
ME6	3667(7)	-816(7)	4618(6)	100(3)
ME7	3095(6)	-1499(6)	3037(6)	84(3)
ME8	3622(7)	432(7)	1096(5)	83(3)
ME9	4846(7)	2151(7)	1422(6)	101(3)
ME10	4600(7)	1508(8)	3663(7)	111(3)
B	7863(6)	-3095(6)	2412(5)	40(2)
C(10)	7778(5)	-1707(5)	2135(5)	41(2)
C(11)	7600(5)	-1068(6)	2756(5)	47(2)
C(12)	7696(6)	70(6)	2446(6)	59(2)
C(13)	7956(7)	611(6)	1490(7)	69(2)
C(14)	8139(6)	22(6)	836(6)	62(2)
C(15)	8048(5)	-1098(6)	1164(5)	48(2)
C(20)	7372(5)	-3712(5)	3597(5)	42(2)
C(21)	7917(6)	-4608(5)	4145(5)	45(2)
C(22)	7399(7)	-5149(6)	5089(5)	54(2)
C(23)	6309(7)	-4824(6)	5540(5)	53(2)
C(24)	5714(6)	-3956(6)	5051(5)	51(2)
C(25)	6247(6)	-3426(6)	4101(5)	49(2)
C(30)	9255(5)	-3403(5)	1931(4)	36(2)
C(31)	9783(5)	-3713(5)	1075(5)	40(2)
C(32)	10926(6)	-3777(5)	632(5)	46(2)
C(33)	11623(6)	-3533(6)	1014(5)	55(2)
C(34)	11170(6)	-3235(6)	1863(5)	54(2)

C(35)	10018(6)	-3164(5)	2284(5)	46(2)
C(40)	7058(5)	-3544(6)	1988(4)	44(2)
C(41)	6194(6)	-2910(7)	1606(5)	51(2)
C(42)	5523(6)	-3361(8)	1327(5)	63(2)
C(43)	5696(7)	-4457(9)	1386(5)	68(3)
C(44)	6507(7)	-5139(7)	1779(5)	62(2)
C(45)	7161(6)	-4668(6)	2058(5)	51(2)
F(11)	7342(3)	-1521(3)	3718(3)	65(1)
F(12)	7518(4)	631(3)	3092(3)	86(1)
F(13)	8049(4)	1712(3)	1182(4)	103(2)
F(14)	8409(4)	533(4)	-117(3)	99(2)
F(15)	8262(3)	-1629(3)	480(3)	62(1)
F(21)	9009(3)	-5009(3)	3751(3)	64(1)
F(22)	7999(4)	-6005(3)	5575(3)	79(1)
F(23)	5802(4)	-5372(4)	6468(3)	85(1)
F(24)	4627(4)	-3627(4)	5476(3)	83(1)
F(25)	5616(3)	-2576(3)	3633(3)	64(1)
F(31)	9162(3)	-3949(3)	617(2)	55(1)
F(32)	11362(3)	-4063(3)	-209(3)	64(1)
F(33)	12757(3)	-3593(4)	578(3)	87(1)
F(34)	11844(4)	-2986(4)	2262(3)	91(2)
F(35)	9608(3)	-2848(3)	3109(3)	65(1)
F(41)	5939(3)	-1810(4)	1537(3)	67(1)
F(42)	4696(4)	-2690(4)	964(3)	92(2)
F(43)	5065(4)	-4894(5)	1060(4)	113(2)
F(44)	6649(4)	-6236(4)	1882(3)	95(2)
F(45)	7957(3)	-5366(3)	2441(3)	66(1)
N(1)	1200(6)	296(6)	3157(6)	81(2)
C(1)	566(9)	-244(9)	3330(8)	98(3)
O(1)	1816(4)	891(4)	4606(4)	90(2)
O(2)	-231(7)	-899(6)	3579(6)	152(3)

Table 18: Assigned Hydrogen Atom Parameters for $Cp^*_2Ta(OH)(NCO)[B(C_6F_5)_4]$

	x	y	z	U(eq)
H(1A)	1664(6)	3539(6)	4471(5)	106
H(1B)	863(6)	2624(6)	5096(5)	106
H(1C)	359(6)	3823(6)	4651(5)	106
H(2A)	-1106(6)	1885(6)	3789(5)	109
H(2B)	-1215(6)	2774(6)	4313(5)	109
H(2C)	-650(6)	1573(6)	4668(5)	109
H(3A)	-528(7)	1991(7)	2312(6)	125
H(3B)	614(7)	1752(7)	1547(6)	125
H(3C)	-30(7)	2949(7)	1415(6)	125
H(4A)	3075(7)	3682(6)	833(5)	125
H(4B)	1912(7)	3948(6)	630(5)	125
H(4C)	2564(7)	2757(6)	710(5)	125
H(5A)	2908(6)	4028(6)	3257(6)	127
H(5B)	2769(6)	4743(6)	2260(6)	127
H(5C)	3643(6)	3679(6)	2327(6)	127
H(6A)	3346(7)	-1465(7)	4705(6)	150
H(6B)	3210(7)	-452(7)	5098(6)	150
H(6C)	4415(7)	-1025(7)	4674(6)	150
H(7A)	2993(6)	-1944(6)	3687(6)	126
H(7B)	3674(6)	-1871(6)	2612(6)	126
H(7C)	2402(6)	-1384(6)	2888(6)	126
H(8A)	3809(7)	1127(7)	638(5)	124
H(8B)	2877(7)	321(7)	1154(5)	124
H(8C)	4153(7)	-154(7)	884(5)	124
H(9A)	5068(7)	2589(7)	1710(6)	151
H(9B)	4381(7)	2614(7)	1039(6)	151
H(9C)	5504(7)	1819(7)	1026(6)	151
H(10A)	4848(7)	2219(8)	3299(7)	166
H(10B)	5219(7)	1006(8)	3831(7)	166
H(10C)	4006(7)	1576(8)	4236(7)	166
H(1)	1223(4)	708(4)	4897(4)	250

Table 19: Anisotropic Displacement Parameters for $Cp^*_2Ta(OH)(NCO)[B(C_6F_5)_4]$

	U11	U22	U33	U23	U13	U12
Ta	43(1)	46(1)	41(1)	-10(1)	-9(1)	-3(1)
CP1	49(5)	47(4)	52(5)	-18(4)	-19(4)	2(4)
CP2	42(4)	44(4)	53(5)	-20(4)	-10(4)	5(3)
CP3	56(5)	46(5)	59(6)	-13(4)	-26(4)	1(4)
CP4	66(5)	44(4)	44(5)	-5(4)	-17(4)	6(4)
CP5	56(5)	42(4)	56(5)	-9(4)	-17(4)	-11(4)
CP6	47(5)	69(6)	45(5)	-13(5)	-13(4)	12(4)
CP7	43(4)	51(5)	58(5)	-23(4)	-11(4)	2(4)
CP8	57(5)	60(5)	46(5)	-26(4)	-10(4)	-1(4)
CP9	43(4)	64(5)	48(5)	-10(4)	-6(4)	-6(4)
CP10	38(4)	91(6)	64(6)	-31(5)	-23(4)	1(4)
ME1	83(6)	78(6)	59(5)	-32(5)	-27(5)	4(5)
ME2	54(5)	75(6)	82(6)	-24(5)	-13(4)	0(4)
ME3	96(7)	90(7)	86(7)	-28(5)	-55(6)	-2(5)
ME4	103(7)	72(6)	54(6)	3(5)	-18(5)	-8(5)
ME5	95(6)	71(6)	95(7)	-18(5)	-26(5)	-37(5)
ME6	93(7)	121(8)	56(6)	-22(6)	-25(5)	49(6)
ME7	75(6)	51(5)	110(7)	-30(5)	-11(5)	7(4)
ME8	93(6)	106(7)	45(5)	-26(5)	-15(5)	-5(5)
ME9	74(6)	107(7)	99(7)	-15(6)	5(5)	-39(6)
ME10	82(7)	167(10)	128(9)	-79(8)	-52(6)	-11(6)
B	48(5)	37(5)	37(5)	-16(4)	-13(4)	0(4)
C(10)	42(4)	44(4)	33(4)	-12(3)	-9(3)	-1(3)
C(11)	49(4)	49(5)	41(5)	-20(4)	-6(4)	-3(4)
C(12)	67(5)	52(5)	73(6)	-36(5)	-24(5)	-2(4)
C(13)	93(6)	40(5)	74(7)	-12(5)	-29(5)	-7(4)
C(14)	84(6)	48(5)	50(6)	2(5)	-26(4)	-12(4)
C(15)	56(5)	48(5)	40(5)	-17(4)	-15(4)	-1(4)
C(20)	47(4)	42(4)	39(4)	-19(4)	-8(4)	-5(3)
C(21)	50(5)	41(4)	39(5)	-12(4)	-8(4)	-3(4)
C(22)	79(6)	45(5)	35(5)	-5(4)	-18(5)	-6(4)
C(23)	70(6)	45(5)	32(5)	-9(4)	7(4)	-18(4)
C(24)	47(5)	58(5)	42(5)	-25(4)	9(4)	-13(4)
C(25)	52(5)	51(5)	50(5)	-25(4)	-15(4)	-4(4)
C(30)	41(4)	32(4)	36(4)	-11(3)	-11(3)	-4(3)
C(31)	43(4)	40(4)	38(4)	-7(3)	-11(4)	-11(3)
C(32)	47(5)	49(4)	30(4)	-5(4)	-3(4)	-3(4)
C(33)	42(5)	67(5)	46(5)	-5(4)	-8(4)	-10(4)
C(34)	44(5)	65(5)	57(5)	-14(4)	-22(4)	-9(4)

C(35)	54(5)	49(4)	32(4)	-12(4)	-11(4)	-4(4)
C(40)	36(4)	58(5)	32(4)	-15(4)	4(3)	-13(4)
C(41)	41(4)	74(6)	36(4)	-22(4)	2(4)	-15(4)
C(42)	46(5)	101(7)	44(5)	-20(5)	-3(4)	-26(5)
C(43)	46(5)	121(9)	48(5)	-37(6)	9(4)	-47(6)
C(44)	58(5)	69(6)	59(5)	-38(5)	16(4)	-35(5)
C(45)	49(5)	50(5)	48(5)	-17(4)	1(4)	-9(4)
F(11)	90(3)	60(3)	42(3)	-21(2)	-9(2)	-14(2)
F(12)	118(4)	64(3)	89(4)	-42(3)	-23(3)	-16(3)
F(13)	152(5)	43(3)	111(4)	-9(3)	-40(4)	-27(3)
F(14)	154(5)	67(3)	61(3)	13(3)	-34(3)	-31(3)
F(15)	89(3)	59(3)	35(2)	-10(2)	-16(2)	-13(2)
F(21)	63(3)	58(3)	52(3)	-5(2)	-13(2)	10(2)
F(22)	99(3)	67(3)	50(3)	5(2)	-19(3)	-4(3)
F(23)	102(3)	87(3)	41(3)	-7(2)	9(2)	-28(3)
F(24)	63(3)	90(3)	71(3)	-26(3)	15(2)	-14(3)
F(25)	54(3)	68(3)	53(3)	-16(2)	-8(2)	9(2)
F(31)	51(2)	76(3)	45(2)	-35(2)	-5(2)	-14(2)
F(32)	58(3)	75(3)	44(3)	-22(2)	2(2)	-1(2)
F(33)	38(3)	116(4)	95(4)	-30(3)	-7(2)	-4(2)
F(34)	68(3)	128(4)	101(4)	-45(3)	-39(3)	-18(3)
F(35)	73(3)	82(3)	53(3)	-31(2)	-24(2)	-7(2)
F(41)	62(3)	71(3)	70(3)	-16(2)	-29(2)	0(2)
F(42)	60(3)	150(5)	74(3)	-20(3)	-30(3)	-26(3)
F(43)	93(4)	179(5)	100(4)	-59(4)	-9(3)	-81(4)
F(44)	98(4)	89(4)	103(4)	-56(3)	17(3)	-54(3)
F(45)	72(3)	46(2)	74(3)	-24(2)	-8(2)	-8(2)
N(1)	53(5)	56(5)	121(7)	-18(5)	-20(5)	2(4)
C(1)	92(9)	79(8)	112(9)	-40(7)	-21(7)	19(6)
O(1)	99(4)	74(4)	66(4)	-11(3)	-22(3)	34(3)
O(2)	149(7)	146(7)	192(8)	-56(6)	-46(6)	-76(6)

Table 20: Complete Distances and Angles for $Cp^*_2Ta(OH)(NCO)[B(C_6F_5)_4]$

Ta-O(1)	1.926(5)
Ta-N(1)	1.944(7)
Ta-CP10	2.420(6)
Ta-CP5	2.420(6)
Ta-CP1	2.445(6)
Ta-CP2	2.448(6)
Ta-CP8	2.456(7)
Ta-CP4	2.458(6)
Ta-CP9	2.465(7)
Ta-CP6	2.470(7)
Ta-CP3	2.470(7)
Ta-CP7	2.479(7)
CP1-CP5	1.412(9)
CP1-CP2	1.414(8)
CP1-ME1	1.508(9)
CP2-CP3	1.419(9)
CP2-ME2	1.508(8)
CP3-CP4	1.411(9)
CP3-ME3	1.499(9)
CP4-CP5	1.429(9)
CP4-ME4	1.495(9)
CP5-ME5	1.498(8)
CP6-CP7	1.408(9)
CP6-CP10	1.415(10)
CP6-ME6	1.495(9)
CP7-CP8	1.425(9)
CP7-ME7	1.489(9)
CP8-CP9	1.418(9)
CP8-ME8	1.491(9)
CP9-CP10	1.422(9)
CP9-ME9	1.497(9)
CP10-ME10	1.509(9)
ME1-H(1A)	0.95
ME1-H(1B)	0.95
ME1-H(1C)	0.95
ME2-H(2A)	0.95
ME2-H(2B)	0.95
ME2-H(2C)	0.95
ME3-H(3A)	0.95
ME3-H(3B)	0.95
ME3-H(3C)	0.95
ME4-H(4A)	0.95
ME4-H(4B)	0.95
ME4-H(4C)	0.95
ME5-H(5A)	0.95
ME5-H(5B)	0.95
ME5-H(5C)	0.95
ME6-H(6A)	0.95
ME6-H(6B)	0.95
ME6-H(6C)	0.95
ME7-H(7A)	0.95

ME7-H(7B)	0.95
ME7-H(7C)	0.95
ME8-H(8A)	0.95
ME8-H(8B)	0.95
ME8-H(8C)	0.95
ME9-H(9A)	0.95
ME9-H(9B)	0.95
ME9-H(9C)	0.95
ME10-H(10A)	0.95
ME10-H(10B)	0.95
ME10-H(10C)	0.95
B-C(40)	1.658(9)
B-C(30)	1.664(9)
B-C(10)	1.669(9)
B-C(20)	1.671(9)
C(10)-C(11)	1.380(8)
C(10)-C(15)	1.392(8)
C(11)-F(11)	1.345(7)
C(11)-C(12)	1.390(9)
C(12)-F(12)	1.337(7)
C(12)-C(13)	1.354(10)
C(13)-F(13)	1.344(8)
C(13)-C(14)	1.372(10)
C(14)-F(14)	1.343(8)
C(14)-C(15)	1.367(9)
C(15)-F(15)	1.350(7)
C(20)-C(21)	1.386(8)
C(20)-C(25)	1.392(8)
C(21)-F(21)	1.356(7)
C(21)-C(22)	1.371(9)
C(22)-C(23)	1.348(9)
C(22)-F(22)	1.352(7)
C(23)-F(23)	1.352(7)
C(23)-C(24)	1.357(9)
C(24)-F(24)	1.337(7)
C(24)-C(25)	1.378(9)
C(25)-F(25)	1.356(7)
C(30)-C(35)	1.385(8)
C(30)-C(31)	1.393(8)
C(31)-F(31)	1.352(7)
C(31)-C(32)	1.359(8)
C(32)-C(33)	1.348(9)
C(32)-F(32)	1.352(7)
C(33)-F(33)	1.349(7)
C(33)-C(34)	1.371(9)
C(34)-F(34)	1.346(7)
C(34)-C(35)	1.365(8)
C(35)-F(35)	1.349(7)
C(40)-C(45)	1.383(9)
C(40)-C(41)	1.393(9)
C(41)-F(41)	1.349(8)
C(41)-C(42)	1.364(9)
C(42)-C(43)	1.345(11)
C(42)-F(42)	1.356(8)

C(43)-F(43)	1.361(8)
C(43)-C(44)	1.369(10)
C(44)-F(44)	1.336(8)
C(44)-C(45)	1.364(9)
C(45)-F(45)	1.353(7)
N(1)-C(1)	1.076(11)
C(1)-O(2)	1.320(12)
O(1)-H(1)	0.77

O(1)-Ta-N(1)	99.4(3)
O(1)-Ta-CP10	84.9(2)
N(1)-Ta-CP10	130.1(3)
O(1)-Ta-CP5	102.5(2)
N(1)-Ta-CP5	131.7(3)
CP10-Ta-CP5	94.5(3)
O(1)-Ta-CP1	76.7(2)
N(1)-Ta-CP1	116.0(3)
CP10-Ta-CP1	113.3(2)
CP5-Ta-CP1	33.7(2)
O(1)-Ta-CP2	87.2(2)
N(1)-Ta-CP2	83.0(3)
CP10-Ta-CP2	146.7(2)
CP5-Ta-CP2	56.0(2)
CP1-Ta-CP2	33.6(2)
O(1)-Ta-CP8	129.3(2)
N(1)-Ta-CP8	85.9(3)
CP10-Ta-CP8	56.3(2)
CP5-Ta-CP8	111.0(2)
CP1-Ta-CP8	144.7(2)
CP2-Ta-CP8	143.2(2)
O(1)-Ta-CP4	132.5(2)
N(1)-Ta-CP4	103.5(3)
CP10-Ta-CP4	109.6(3)
CP5-Ta-CP4	34.1(2)
CP1-Ta-CP4	55.9(2)
CP2-Ta-CP4	55.6(2)
CP8-Ta-CP4	93.7(2)
O(1)-Ta-CP9	118.7(2)
N(1)-Ta-CP9	119.4(3)
CP10-Ta-CP9	33.8(2)
CP5-Ta-CP9	86.0(2)
CP1-Ta-CP9	117.4(2)
CP2-Ta-CP9	138.9(2)
CP8-Ta-CP9	33.5(2)
CP4-Ta-CP9	84.6(2)
O(1)-Ta-CP6	73.8(2)
N(1)-Ta-CP6	99.7(3)
CP10-Ta-CP6	33.6(2)
CP5-Ta-CP6	127.5(3)
CP1-Ta-CP6	136.6(2)
CP2-Ta-CP6	161.0(2)
CP8-Ta-CP6	55.7(2)
CP4-Ta-CP6	139.8(2)
CP9-Ta-CP6	55.4(2)

O(1)-Ta-CP3	120.6(2)
N(1)-Ta-CP3	75.8(3)
CP10-Ta-CP3	142.8(3)
CP5-Ta-CP3	56.0(2)
CP1-Ta-CP3	55.7(2)
CP2-Ta-CP3	33.5(2)
CP8-Ta-CP3	109.7(2)
CP4-Ta-CP3	33.3(2)
CP9-Ta-CP3	114.2(2)
CP6-Ta-CP3	165.3(2)
O(1)-Ta-CP7	99.1(2)
N(1)-Ta-CP7	74.8(3)
CP10-Ta-CP7	55.6(2)
CP5-Ta-CP7	141.1(2)
CP1-Ta-CP7	168.7(2)
CP2-Ta-CP7	157.6(2)
CP8-Ta-CP7	33.6(2)
CP4-Ta-CP7	126.9(2)
CP9-Ta-CP7	55.2(2)
CP6-Ta-CP7	33.1(2)
CP3-Ta-CP7	133.6(2)
CP5-CP1-CP2	107.9(6)
CP5-CP1-ME1	125.5(6)
CP2-CP1-ME1	126.3(7)
CP5-CP1-Ta	72.2(4)
CP2-CP1-Ta	73.3(4)
ME1-CP1-Ta	124.5(5)
CP1-CP2-CP3	108.4(6)
CP1-CP2-ME2	126.5(7)
CP3-CP2-ME2	124.9(7)
CP1-CP2-Ta	73.1(4)
CP3-CP2-Ta	74.1(4)
ME2-CP2-Ta	121.8(5)
CP4-CP3-CP2	107.8(6)
CP4-CP3-ME3	125.0(7)
CP2-CP3-ME3	126.7(7)
CP4-CP3-Ta	72.9(4)
CP2-CP3-Ta	72.4(4)
ME3-CP3-Ta	126.4(5)
CP3-CP4-CP5	107.9(6)
CP3-CP4-ME4	123.5(7)
CP5-CP4-ME4	127.4(7)
CP3-CP4-Ta	73.8(4)
CP5-CP4-Ta	71.5(4)
ME4-CP4-Ta	130.1(5)
CP1-CP5-CP4	107.9(6)
CP1-CP5-ME5	122.5(7)
CP4-CP5-ME5	127.6(7)
CP1-CP5-Ta	74.1(4)
CP4-CP5-Ta	74.4(4)
ME5-CP5-Ta	130.0(5)
CP7-CP6-CP10	108.1(7)
CP7-CP6-ME6	127.1(8)
CP10-CP6-ME6	124.8(8)

CP7-CP6-Ta	73.8(4)
CP10-CP6-Ta	71.3(4)
ME6-CP6-Ta	122.7(5)
CP6-CP7-CP8	108.5(6)
CP6-CP7-ME7	125.4(7)
CP8-CP7-ME7	125.8(7)
CP6-CP7-Ta	73.1(4)
CP8-CP7-Ta	72.4(4)
ME7-CP7-Ta	125.1(5)
CP9-CP8-CP7	107.2(6)
CP9-CP8-ME8	127.4(7)
CP7-CP8-ME8	124.7(7)
CP9-CP8-Ta	73.6(4)
CP7-CP8-Ta	74.1(4)
ME8-CP8-Ta	124.9(5)
CP8-CP9-CP10	108.1(6)
CP8-CP9-ME9	125.0(7)
CP10-CP9-ME9	124.5(7)
CP8-CP9-Ta	72.9(4)
CP10-CP9-Ta	71.4(4)
ME9-CP9-Ta	135.4(5)
CP6-CP10-CP9	107.9(7)
CP6-CP10-ME10	124.7(8)
CP9-CP10-ME10	126.7(8)
CP6-CP10-Ta	75.1(4)
CP9-CP10-Ta	74.8(4)
ME10-CP10-Ta	123.9(5)
CP1-ME1-H(1A)	106.4(4)
CP1-ME1-H(1B)	112.8(4)
H(1A)-ME1-H(1B)	109.5
CP1-ME1-H(1C)	109.1(4)
H(1A)-ME1-H(1C)	109.5
H(1B)-ME1-H(1C)	109.5
CP2-ME2-H(2A)	108.8(4)
CP2-ME2-H(2B)	107.6(4)
H(2A)-ME2-H(2B)	109.5
CP2-ME2-H(2C)	112.0(4)
H(2A)-ME2-H(2C)	109.5
H(2B)-ME2-H(2C)	109.5
CP3-ME3-H(3A)	109.0(4)
CP3-ME3-H(3B)	110.3(4)
H(3A)-ME3-H(3B)	109.5
CP3-ME3-H(3C)	109.0(4)
H(3A)-ME3-H(3C)	109.5
H(3B)-ME3-H(3C)	109.5
CP4-ME4-H(4A)	109.4(4)
CP4-ME4-H(4B)	111.1(4)
H(4A)-ME4-H(4B)	109.5
CP4-ME4-H(4C)	107.9(4)
H(4A)-ME4-H(4C)	109.5
H(4B)-ME4-H(4C)	109.5
CP5-ME5-H(5A)	110.2(4)
CP5-ME5-H(5B)	110.9(4)
H(5A)-ME5-H(5B)	109.5

CP5-ME5-H(5C)	107.3(4)
H(5A)-ME5-H(5C)	109.5
H(5B)-ME5-H(5C)	109.5
CP6-ME6-H(6A)	105.6(5)
CP6-ME6-H(6B)	113.2(4)
H(6A)-ME6-H(6B)	109.5
CP6-ME6-H(6C)	109.5(4)
H(6A)-ME6-H(6C)	109.5
H(6B)-ME6-H(6C)	109.5
CP7-ME7-H(7A)	109.7(5)
CP7-ME7-H(7B)	108.5(4)
H(7A)-ME7-H(7B)	109.5
CP7-ME7-H(7C)	110.1(4)
H(7A)-ME7-H(7C)	109.5
H(7B)-ME7-H(7C)	109.5
CP8-ME8-H(8A)	107.3(4)
CP8-ME8-H(8B)	111.0(4)
H(8A)-ME8-H(8B)	109.5
CP8-ME8-H(8C)	110.1(4)
H(8A)-ME8-H(8C)	109.5
H(8B)-ME8-H(8C)	109.5
CP9-ME9-H(9A)	109.5(5)
CP9-ME9-H(9B)	107.3(4)
H(9A)-ME9-H(9B)	109.5
CP9-ME9-H(9C)	111.6(4)
H(9A)-ME9-H(9C)	109.5
H(9B)-ME9-H(9C)	109.5
CP10-ME10-H(10A)	116.9(5)
CP10-ME10-H(10B)	106.5(4)
H(10A)-ME10-H(10B)	109.5
CP10-ME10-H(10C)	104.8(4)
H(10A)-ME10-H(10C)	109.5
H(10B)-ME10-H(10C)	109.5
C(40)-B-C(30)	114.1(5)
C(40)-B-C(10)	114.1(5)
C(30)-B-C(10)	100.2(5)
C(40)-B-C(20)	101.1(5)
C(30)-B-C(20)	114.0(5)
C(10)-B-C(20)	114.0(5)
C(11)-C(10)-C(15)	113.5(6)
C(11)-C(10)-B	127.3(6)
C(15)-C(10)-B	118.8(6)
F(11)-C(11)-C(10)	121.5(6)
F(11)-C(11)-C(12)	114.9(6)
C(10)-C(11)-C(12)	123.5(7)
F(12)-C(12)-C(13)	120.1(7)
F(12)-C(12)-C(11)	120.0(7)
C(13)-C(12)-C(11)	119.9(7)
F(13)-C(13)-C(12)	120.4(8)
F(13)-C(13)-C(14)	120.2(8)
C(12)-C(13)-C(14)	119.3(7)
F(14)-C(14)-C(15)	120.0(7)
F(14)-C(14)-C(13)	120.7(7)
C(15)-C(14)-C(13)	119.3(7)

F(15)-C(15)-C(14)	116.1(6)
F(15)-C(15)-C(10)	119.4(6)
C(14)-C(15)-C(10)	124.5(7)
C(21)-C(20)-C(25)	113.1(6)
C(21)-C(20)-B	127.1(6)
C(25)-C(20)-B	119.2(6)
F(21)-C(21)-C(22)	116.3(6)
F(21)-C(21)-C(20)	120.5(6)
C(22)-C(21)-C(20)	123.2(7)
C(23)-C(22)-F(22)	119.9(7)
C(23)-C(22)-C(21)	120.8(7)
F(22)-C(22)-C(21)	119.3(7)
C(22)-C(23)-F(23)	120.3(7)
C(22)-C(23)-C(24)	119.6(7)
F(23)-C(23)-C(24)	120.1(7)
F(24)-C(24)-C(23)	120.8(7)
F(24)-C(24)-C(25)	120.4(7)
C(23)-C(24)-C(25)	118.8(7)
F(25)-C(25)-C(24)	116.9(6)
F(25)-C(25)-C(20)	118.7(6)
C(24)-C(25)-C(20)	124.4(7)
C(35)-C(30)-C(31)	112.9(6)
C(35)-C(30)-B	119.9(5)
C(31)-C(30)-B	126.3(5)
F(31)-C(31)-C(32)	115.5(6)
F(31)-C(31)-C(30)	120.8(6)
C(32)-C(31)-C(30)	123.7(6)
C(33)-C(32)-F(32)	119.8(6)
C(33)-C(32)-C(31)	120.5(7)
F(32)-C(32)-C(31)	119.7(6)
C(32)-C(33)-F(33)	120.8(7)
C(32)-C(33)-C(34)	119.4(7)
F(33)-C(33)-C(34)	119.9(7)
F(34)-C(34)-C(35)	120.5(7)
F(34)-C(34)-C(33)	120.7(7)
C(35)-C(34)-C(33)	118.8(6)
F(35)-C(35)-C(34)	116.8(6)
F(35)-C(35)-C(30)	118.4(6)
C(34)-C(35)-C(30)	124.8(6)
C(45)-C(40)-C(41)	113.4(6)
C(45)-C(40)-B	119.8(6)
C(41)-C(40)-B	126.7(6)
F(41)-C(41)-C(42)	116.0(7)
F(41)-C(41)-C(40)	121.0(6)
C(42)-C(41)-C(40)	122.9(8)
C(43)-C(42)-F(42)	120.0(8)
C(43)-C(42)-C(41)	120.4(8)
F(42)-C(42)-C(41)	119.5(8)
C(42)-C(43)-F(43)	120.4(9)
C(42)-C(43)-C(44)	120.0(8)
F(43)-C(43)-C(44)	119.7(9)
F(44)-C(44)-C(45)	121.3(8)
F(44)-C(44)-C(43)	120.4(8)
C(45)-C(44)-C(43)	118.3(8)

F(45)-C(45)-C(44)	116.7(7)
F(45)-C(45)-C(40)	118.5(6)
C(44)-C(45)-C(40)	124.9(7)
C(1)-N(1)-Ta	163.8(10)
N(1)-C(1)-O(2)	177.5(12)
Ta-O(1)-H(1)	114.5(2)